

Cover Page



Universiteit Leiden



The handle <http://hdl.handle.net/1887/31432> holds various files of this Leiden University dissertation

Author: Khairoun, Meriem

Title: Microvascular alterations in transplantation

Issue Date: 2015-01-14

Microvascular Alterations in Transplantation



Meriem Khairoun

Microvascular alterations in transplantation

Meriem Khairoun

Cover design by: Pepijn Lampe
Printed by: Gildeprint - Enschede
Layout by: Gildeprint - Enschede
ISBN: 978-94-6108-868-0

Microvascular alterations in transplantation
Meriem Khairoun/Department of Nephrology of the Leiden University Medical Center, The Netherlands/Thesis.

© Meriem Khairoun 2015

All rights are reserved. No part of this publication may be reproduced, stored, or transmitted in any form or by any means, without permission of the author.

Printing of this thesis was financially supported by:

Microvascular alterations in transplantation

Proefschrift

ter verkrijging van
de graad van Doctor aan de Universiteit Leiden,
op gezag van Rector Magnificus prof.mr. C.J.J.M. Stolker,
volgens besluit van het College voor Promoties
te verdedigen op woensdag 14 januari 2015
klokke 13.45 uur

door

Meriem Khairoun

geboren te Tanger in 1982

Promotiecommissie

Promotores: Prof. dr. T.J. Rabelink
Prof. dr. A.J. van Zonneveld

Co-promotor: Dr. M.E.J. Reinders

Overige leden: Prof. dr. D. Briscoe (*Harvard Medical School*)
Prof. dr. J.J. Homan van der Heide (*Academisch Medisch Centrum*)
Prof. dr. V.W.M. van Hinsberg (*VU Medisch Centrum*)
Prof. dr. F.W. Dekker
Prof. dr. J.W. de Fijter
Prof. dr. C. van Kooten

Financial support by the Dutch Heart Foundation for the publication of this thesis is gratefully acknowledged.

For my parents, Safiye and Gürbey

Contents

Chapter 1:	General introduction	9
Chapter 2:	Renal ischemia-reperfusion induces a dysbalance of angiotensins, accompanied by proliferation of pericytes and fibrosis. <i>Am J Physiol Renal Physiol. 2013 Sep 15;305(6):F901-10</i>	25
Chapter 3:	Renal ischemia-reperfusion induces release of angiotensin-2 from human grafts of living and deceased donors. <i>Transplantation. 2013 Aug 15;96(3):282-9</i>	45
Chapter 4:	Early systemic microvascular damage in pigs with atherogenic diabetes mellitus coincides with renal angiotensin dysbalance. <i>Submitted</i>	65
Chapter 5:	Microvascular damage in type 1 diabetic patients is reversed in the first year after simultaneous pancreas-kidney transplantation. <i>Am J Transplant. 2013 May;13(5):1272-81</i>	87
Chapter 6:	Improvement of microvascular damage after living donor kidney-transplantation. <i>In preparation</i>	105
Chapter 7:	Acute rejection of kidney transplants is associated with a dysbalance in angiotensins and a sustained increase in systemic microvascular tortuosity. <i>Submitted</i>	119
Chapter 8:	General summary and future perspectives	135
Chapter 9:	Nederlandse samenvatting	143
	Acknowledgment	147
	Curriculum vitae	149
	Publication list	151

Chapter 1

Introduction, aims and thesis outline

1. Endothelial dysfunction in renal disease

1.1 General introduction

Endothelial cells (ECs) line the lumina of all blood vessels and form the interface between the blood and tissue (1). A well-functioning endothelium is critical for the delivery of oxygen and nutrients (2). The endothelium forms an important physical barrier and regulates vasomotor tone and the control of tissue inflammation and of thrombosis (3). This process is tightly regulated by both autocrine and paracrine factors that influence the microvascular integrity in the kidney and other organs (4;5). As a consequence of chemical and mechanical injuries, the endothelium is constantly undergoing injury and repair. Upon EC injury there is a switch from a quiescent phenotype toward responsive activated endothelium. Most cardiovascular risk factors, including diabetes mellitus (DM) and chronic kidney disease (CKD) activate the endothelial layer that consequently results in upregulation of chemokines, cytokines, and adhesion molecules designed to prevent further damage (2;6). Repetitive exposure to injury/activation of the endothelium can ultimately exhaust these protective anti-inflammatory mechanisms within ECs (6). As a consequence, the microvascular endothelium loses integrity and its ability to maintain homeostasis, which results in disturbed capillary blood flow and detachment of ECs into the circulation (6;7). Eventually, if damaged endothelium is not repaired by replication of adjacent mature ECs or circulating endothelial progenitor cells (EPCs), ECs become dysfunctional and irreversibly damaged, resulting in a disease state (6).

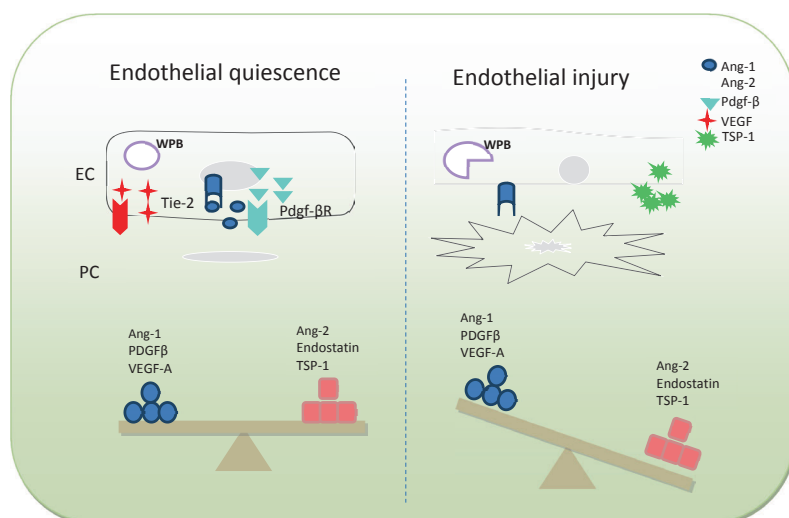


Figure 1: In healthy kidneys, there is a tightly controlled equilibrium between factors favoring (e.g. Angiopoietin-1 (Ang-1), Vascular Endothelial Growth Factors (VEGF), Platelet Derived Growth Factor (PDGF)) and inhibiting (e.g. Angiopoietin-2 (Ang-2), Thrombospondin-1 (TSP-1), Endostatin) EC proliferation and survival. When ECs become activated upon injury, a dysbalance in proangiogenic and antiangiogenic growth factors favors loss of renal microvascular ECs and loosening interaction with pericytes. EC: endothelial cells; PC: pericytes; WPB: Weibel Palade bodies.

1.2 Angiogenic factors play a central role in microvascular stability

The molecular mechanisms that lead to microvascular injury in organ failure are largely unknown. It has been suggested that several angioregulatory growth factors play a central role in the loss of vascular integrity (5;8). Under homeostatic conditions, there is a tightly controlled equilibrium between factors favoring (e.g. Angiopoietin-1 (Ang-1), Vascular endothelial growth factors (VEGF), Platelet derived growth factor (PDGF)) and inhibiting (e.g. Angiopoietin-2 (Ang-2), Hepatocyte Growth Factor (HGF), Endostatin) EC proliferation and survival in the kidney (5). A dysbalance in proangiogenic and antiangiogenic growth factors favors loss of renal microvascular ECs (Figure 1) (2;5). Recently, the angiopoietin/Tie2 system has been identified as playing a critical role in angiogenesis and inflammation of the renal microvasculature in progressive renal disease (5;9-12). Ang-1 and Ang-2 are growth factors that regulate endothelial function during angiogenesis and inflammation and are competitive ligands for the Tie-2 receptor. Ang-1 is produced by pericytes and has vasculoprotective effects by suppressing vessel leakage, inhibiting vascular inflammation, and preventing endothelial death. In addition, Ang-1 has a critical role in the crosstalk between ECs and perivascular stromal cells. In contrast, Ang-2 is released by ECs from Weibel Palade bodies (WPB) at sites of vascular remodeling and inflammation. Ang-2 has antagonistic effects and acts as a competitive inhibitor for Ang-1, with consequently vessel destabilization, inflammation and induction of the angiogenic response, with formation of abnormal tortuous capillary networks that lead to an abnormal blood flow and results in chronic hypoxia (8;12-15). Under pathological conditions, Ang-2 acts in concert with VEGF to induce inflammatory angiogenesis (16;17). By promoting pericyte dropout, Ang-2 will lead to loosening contacts between ECs and pericytes. In the presence of VEGF, Ang-2 can eventually lead to an active, sprouting state of ECs. Otherwise, when VEGF is absent, Ang-2 facilitates capillary regression (18).

1.3 Pericytes are the link between endothelial damage and renal fibrosis

Pericytes are contractile cells that wrap around ECs and have important roles in supporting the growth and maintenance of capillaries (19). In the microvasculature, communication between ECs and pericytes has been shown to stabilize capillaries and protect them from regression and rarefaction (20;21). Pericytes signal to the endothelium through secreted factors such as PDGF- β , TGF- β and Ang-1, as well as by direct endothelial/pericyte crosstalk which involves notch-3 signaling (22). Similarly, the endothelium signals to surrounding stromal cells using similar growth factors such as Ang-2 and VEGF as well as the notch ligand jagged-1. Bidirectional signaling between pericytes and ECs in disease states may result in pericyte detachment from capillary ECs, resulting in an angiogenic response and formation of unstable tortuous ECs, capillary rarefaction and exacerbation of tissue hypoxia and fibrosis (Figure 2) (8;12-15;23-25). The group of Duffield et al showed migration of pericytes from capillaries into the renal interstitium, already 9 hr after induction of unilateral ureter obstruction (UUO).

After loosening contact from the capillaries, pericytes became activated and proliferated into collagen producing myfibroblasts contributing to fibrosis (20;23;24). Using a transgenic mouse model of UUO, expressing green fluorescent protein in cells producing the collagen type I, the same group confirmed that pericytes are the main source for interstitial myofibroblasts during renal fibrosis (23). Transformation of pericytes into myofibroblasts also induced a switch in VEGF isomers from proangiogenic to antiangiogenic isoforms, which counted for ECs loss (25). The process of pericyte detachment has been suggested to be reversible. For example, blockade of PDGFR- β on pericytes attenuated recruitment of inflammatory cells and detachment of pericytes from ECs in mice subjected to renal I/R injury and unilateral ureter model. Conversely, inhibition of VEGF on ECs abolished pericyte detachment and attenuated both EC loss and development of fibrosis during kidney injury induced by UUO or renal I/R injury (20). These data suggest that targeting interaction between ECs and pericytes may provide a novel therapeutic targets to improve microvasculature and treat acute and chronic kidney injuries.

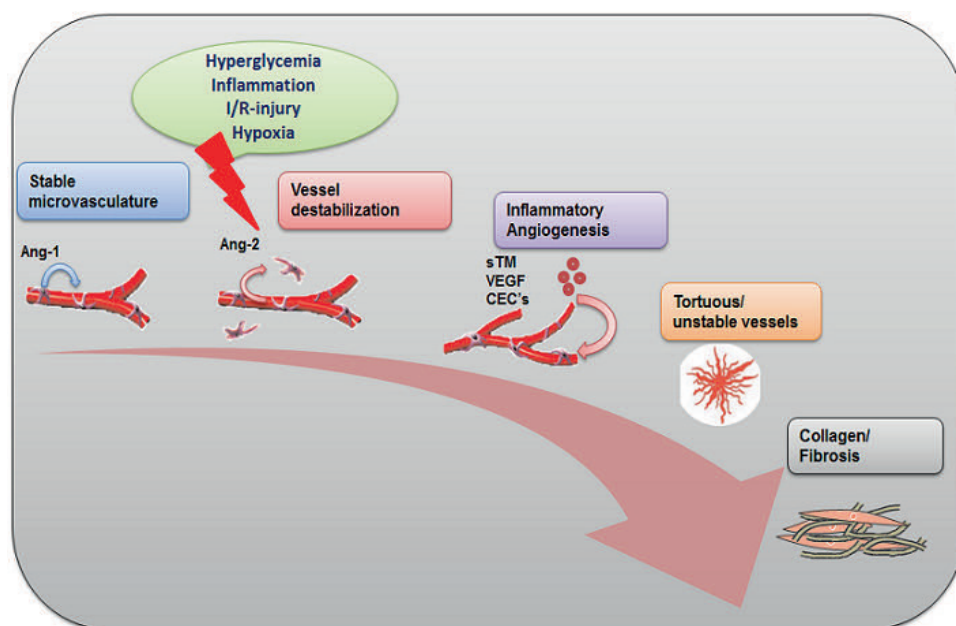


Figure 2: Angiopoietin-1 (Ang-1) produced by pericytes regulates vascular assembly and endothelial quiescence. Endothelial injury induced by different insults (e.g. diabetes mellitus, renal ischemia reperfusion (I/R) injury) leads to activation of endothelial cells (ECs) and release of Ang-2. Consequently, pericytes will detach from the capillary wall which results in vessel destabilization and induction of angiogenesis, partly in concert with other cytokines such as VEGF. When inflammation is sustained, formation of unstable tortuous capillaries occurs and finally microvascular rarefaction. This exacerbates tissue hypoxia and leads to transformation of pericytes into collagen producing myofibroblasts and ultimately scar formation with loss of renal function. sTM: soluble thrombomodulin; VEGF: Vascular Endothelial Growth Factor; CECs: Circulating Endothelial Cells.

2 Assessment of endothelial function

2.1 Circulating markers of endothelial function

The endothelium is relatively inaccessible to direct examination; therefore investigators have concentrated on various surrogate markers of endothelial function which include the measurement of specific plasma markers including the angiopoietins and sTM and measurement of circulating ECs and EPC's in peripheral blood (9;11;26-30). Elevated circulating levels of Ang-2 are reported to be associated with progression of renal disease and with systemic markers of micro-inflammation in chronic kidney disease (CKD) patients (9;26). Furthermore, elevated Ang-2 levels are shown to be strong predictors of long term mortality in CKD patients, independent of vascular stiffness and calcifications (31). Accordingly, renal angiopoietin dysbalance, in favor of Ang-2, has been found in different animal and human models of renal disease (both diabetic and non-diabetic) (13;32;33). In line, trombosmodulin levels are studied in detail in different vascular disease including CKD (29;34). Indeed, increased levels of sTM are demonstrated in CKD patients with and without diabetes and normalization after KTx is reported (29). In patients undergoing long-term hemodialysis treatment increased number of circulating ECs, as marker for systemic endothelial dysfunction, were found compared to healthy controls. EPCs in renal disease have been suggested to be useful for regenerating and maintaining the integrity of vascular structures. In patients with chronic renal disease, EPC numbers and function were decreased compared with healthy subjects, which may prevent physiological vascular repair and contribute to the increased risk for cardiovascular diseases observed in CKD patients (30;35;36).

2.2 Noninvasive visualization of human microcirculation

An additional method for the assessment of endothelial function in CKD includes the non-invasive monitoring of the microvasculature. Capillary nailfold videomicroscopy in advanced CKD patients showed an impaired functional and structural capillary density in the skin (37). These abnormalities may represent manifestations of ongoing systemic microvascular damage and underlie much of the organ dysfunction associated with cardiovascular disease in CKD patients (38). Another study has found a significant association between retinal microvascular abnormalities, using retinal fundus photographs, and renal function deterioration (39). Recently, sidestream dark field (SDF) imaging has been used to visualize the human microcirculation. Compared to conventional capillaroscopy, this method has been used to assess the microvasculature in vivo without injecting fluorescent dyes (40;41). The SDF imaging has opened a way to study the human microcirculation in more detail than previously. In this technique, the tissue is illuminated by light with a wavelength corresponding to the hemoglobin spectrum. Part of the light will be absorbed by the hemoglobin and the rest will be reflected from the background. Specific optical filtration allows the elimination of the light reflected at the surface of the tissue to produce high-contrast reflected light images of the

microcirculation. Hence, red blood cells will appear dark and white blood cells and platelets may be visible as refrinent bodies. Vessel walls are not visible and therefore, vessels will be visible only if they contain red blood cells (Figure 3). The SDF imaging device is particularly convenient for studying tissues protected by a thin epithelial layer such as mucosal surfaces (40). By using SDF imaging, capillary tortuosity and density can be measured to assess microvascular damage. In addition, this technique also enables measurement of the Endothelial Surface Layer (ESL) dimensions, calculated as the difference in Red Blood Cell (RBC) column width before (functionally perfused capillary diameter) and after (anatomical capillary diameter) leukocyte passage (42;43).

We previously used this validated technique to compare the labial mucosal tortuosity, as markers for microvascular damage, in DM patients and controls. We found increased capillary tortuosity in DM patients compared with healthy controls (41). However, there are no studies which have used SDF imaging for assessment of systemic microvascular alterations in CKD patients (including patients with diabetic nephropathy) before and after (pancreas) kidney transplantation.

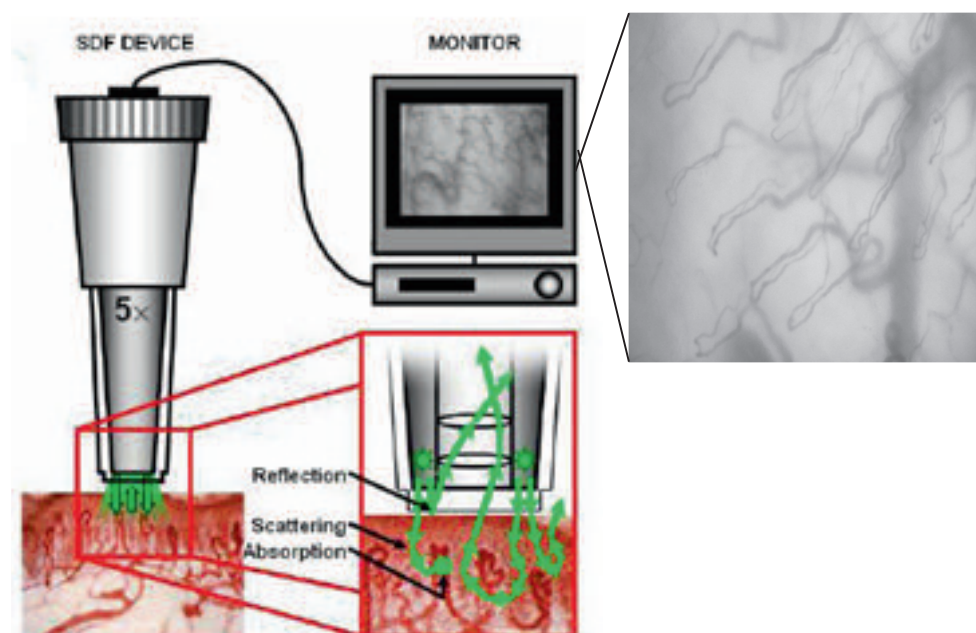


Figure 3: Visualization of the microcirculation using SDF imaging. The tissue is illuminated by light with a wavelength corresponding to the haemoglobin spectrum (548nm). Part of the light will be absorbed by the haemoglobin containing red blood cells and the rest will be reflected from the background. Specific optical filtration allows the elimination of the light reflected at the surface of the tissue to produce high-contrast reflected light images of the microcirculation. Vessels will be visible only if they contain red blood cells. Adapted from Goedhart et al 2007.

3. The microvasculature in disease

3.1 Endothelial injury in renal disease

Injury of microvascular ECs contributes to the impairment of renal perfusion and continued renal hypoxia/ischemia (44). Chronic hypoxia is an important trigger for profibrotic and inflammatory changes, from the early stages of chronic kidney disease (CKD), and finally scar formation and progression to end stage renal disease (5). A dysfunctional endothelium loses its ability to protect the microvasculature by reducing its anti-inflammatory and anti-coagulation effects (45). With decreasing renal function, the endothelium is exposed to pro-inflammatory cytokines which lead to upregulation of cell-surface adhesion molecules and impairs endothelium-dependent vascular relaxation, with further loss of ECs and development of fibrosis (5). In both experimental animal models and in humans, it has been shown that there is significant loss of peritubular capillaries and reduction in the capacity of EC proliferation as well as defective capillary repair in association with the development of renal interstitial fibrosis (2). Interestingly, there is intriguing evidence that stimulation of capillary repair may stabilize renal function and slow progression and that this benefit occurs independently of effects on blood pressure or proteinuria (4;5). Indeed, in patients with chronic renal failure, autopsy material revealed not only diffuse media calcifications and thickening of the arteries, but above all changes in the myocardial microcirculation including rarefaction of the intramyocardial capillaries (46).

3.2 Microvascular disease in diabetes mellitus

Diabetes mellitus is strongly associated with the development of macrovascular and microvascular disease, including retinopathy, neuropathy and nephropathy (DN), which is the leading cause of CKD (47;48). The development of these complications have been correlated with glucose mediated endothelial damage, oxidative stress due to accumulation of toxic intracellular products such as sorbitol or advanced glycation end products (AGEs) (49). As a response to hyperglycemia, microvascular ECs undergo several metabolic derangements, which cause activation of ECs, increased expression of different growth factors, altered blood flow and permeability of the endothelium and coagulation resulting in structural and functional alterations in microvascular integrity (50;51). Endothelial dysfunction and increased oxidative stress are reported in patients with prediabetes and in the early course of DM as well, indicating a prominent role of microvascular EC damage in the onset of early microangiopathy (52). Different angiogenic growth factors have been shown to be increased in DM including VEGF and Ang-2 (53). Several studies suggest that Ang-2 and VEGF act together inducing sprouting angiogenesis and ultimately leading to vascular destabilization and dysfunction (17). In diabetic retinopathy, loss of pericytes is reported to be one of the first morphological changes that occurs in the capillaries with concomitant endothelial alterations, such as ECs loss, irregular shaping of capillaries and local areas of hypoxia (19;54).

3.3 Transplantation and microvasculature

Kidney transplantation has improved survival and quality of life for patients with end-stage renal failure. Despite dramatic improvements in short-term survival, long-term survival of renal allografts has changed little during the past decade (55). Most late renal allograft loss has been attributed to progressive renal dysfunction, histological characterized by interstitial fibrosis and renal atrophy (IFTA) (56). The fibrosis in the transplanted kidney represents cumulative and incremental damage to nephrons from various immunological (antibody-mediated and T cell-mediated rejection, sensitization, HLA mismatch) and non-immunological (nephrotoxicity of calcineurin inhibitors, ischemia-reperfusion (I/R) injury, donor age, hypertension, infections) insults (57). Among these factors, acute rejection and I/R injury primarily target the endothelium and disrupt microvascular homeostasis. Activation of pro-inflammatory and pro-coagulant pathways lead to irreversible injury of the endothelium with ensuing renal fibrosis and loss of allograft function (2;58).

3.3.1 Ischemia-reperfusion injury

Renal I/R injury is an inevitable consequence of organ transplantation, and a major determinant of patient and graft survival (59). The pathophysiology of I/R injury is complex and incompletely understood (60). Although the role of tubular cell injury in post-transplantation graft dysfunction is widely acknowledged, damage to microvascular endothelial cells is emerging as increasingly important (61). Inflammation after reperfusion is considered to be the most crucial initiator of EC injury in kidneys subjected to I/R. This will lead to production and release of pro-inflammatory and pro-angiogenic factors by ECs (e.g. tumor necrosis factor, VEGF, Ang-2) and upregulation of different adhesion molecules, that facilitate leukocyte-endothelial cell interactions with consequently ECs dysfunction and peritubular capillary loss (62;63). If early capacity of EC repair and protection is limited, ongoing local ischemic injury will result in persistent cell death and chronic allograft injury (2). Indeed, it is demonstrated that early loss of peritubular capillaries predicts the development of tubulointerstitial fibrosis and rejection after transplantation and can be predictive of long-term graft survival (64). Therapeutic interventions aiming at enhancement of the microvasculature and promoting repair early after transplantation may be beneficial for graft health and prevent chronic injury and rejection.

3.3.2 Allograft rejection

In the pathogenesis of rejection, ECs respond to cytokines and growth factors produced in association with alloimmune responses (64;65). Activated microvascular ECs express adhesion molecules, cytokines, chemokines and growth factors that mediate the recruitment of recipient leukocytes (2;64;65). In addition, activated ECs express MHC class I and II molecules which are critical for the presentation of alloantigen to infiltrating lymphocytes (64). It is proposed that repetitive insults target the microvasculature and induce loss of the microvasculature, which

may result in impaired delivery of oxygen and nutrients to renal tubular epithelial cells, chronic ischemia and cell death (58). In vascularized solid organ allografts, such as the kidney, the degree of injury and microvascular EC loss has been reported to predict the development of IFTA and later chronic rejection and strategies which can protect the endothelium have potential to improve long-term graft survival (58;66;67).

4. Restoration of the renal microvasculature

The concept that injury to the endothelium may precede renal fibrosis strongly suggests that interventions to maintain vascular integrity are of major importance in the treatment of renal disease (5). On the beneficial effects of preservation of the microvasculature in renal disease several studies have been reported using different therapeutic strategies. Promising results about the administration of different growth factors have been shown in experimental animal models to enhance angiogenic sprouting and subsequently repair the injured kidney microvasculature. The use of recombinant COMP-Ang-1 (a soluble, stable and more potent form of Ang-1) and VEGF-A in kidney models of progressive renal failure, improved renal function, preserved renal microvasculature and decreased inflammation and fibrosis. Another important factor for angiogenic therapy to be successful is the stage of disease. Indeed, initial stages of DN are associated with upregulation of VEGF and increased number of vessels, implicating that at this stage antiangiogenic therapy may be beneficial. In contrast, advanced stage of DN is associated with loss of peritubular capillaries, and proangiogenic therapies have shown promising results at this stage (5;10;68;69). An alternative strategy is the use of EPCs. In different animal models of CKD, transplantation of EPCs resulted in preservation of peritubular capillaries, improvement in renal function and reduction glomerulosclerosis and development of fibrosis, by homing to areas of injury and inflammation in the kidney. Furthermore, there is also evidence that resident stem/progenitor cells in the kidney might contribute to the maintenance and repair of renal endothelium and interstitium (2;5;35;36;70). Finally, mesenchymal stromal cells (MSCs) have been reported to have potent immunomodulatory and reparative effects. In different experimental animal models of renal disease, infusion of MSCs decreased fibrosis and promoted angiogenesis. For example, in renal ischemia, the process of microvascular loss was hampered in postischemic kidneys after injection of MSCs (71;72).

5. Aims and outline of this thesis

The growing literature indicates that endothelial injury and repair are most important concepts for our understanding of renal disease and that manipulation of the response might have major consequences for therapeutics in the future. The use of SDF imaging to measure

microvascular damage and the measurement of endothelial dysfunction markers may be useful diagnostic tool for monitoring the microvasculature before and after transplantation. This could ultimately lead to a better understanding of the pathogenesis, earlier diagnosis and effective treatment of microvascular damage in CKD and renal (pancreas) transplant recipients. This thesis focuses on the mechanisms involved in the process of endothelial damage and repair in CKD, (early) DM, renal I/R injury and after transplantation

The aims of this thesis are:

1. Study in detail the effect of renal I/R injury on angiotensin expression and its association with pericytes and fibrosis development, using a rat I/R injury model (**chapter 2**).
2. Study damage to the microvasculature and the role of angiotensins in human renal I/R injury and compare living-donor (LD) and deceased-donor (DD) kidney transplantation (**chapter 3**).
3. Investigate the early effects of atherogenic diabetes on systemic microvasculature and its association with renal damage using a streptozotocin -induced model of diabetes and atherogenesis in pigs (**chapter 4**).
4. Assess effect of simultaneous pancreas kidney transplantation in DN patients on microvascular alterations using SDF imaging and endothelial dysfunction markers (**chapter 5**).
5. Investigate systemic microvascular alterations in CKD patients before and after living kidney transplantation, using SDF imaging and endothelial dysfunction markers (**chapter 6**).
6. Investigate whether acute rejection after kidney transplantation is associated with systemic microvascular damage (**chapter 7**).

Reference List

- (1) Dora KA. Cell-cell communication in the vessel wall. *Vasc Med* 2001;6(1):43-50.
- (2) Reinders ME, Rabelink TJ, Briscoe DM. Angiogenesis and endothelial cell repair in renal disease and allograft rejection. *J Am Soc Nephrol* 2006 April;17(4):932-42.
- (3) Rajendran P, Rengarajan T, Thangavel J, Nishigaki Y, Sakthisekaran D, Sethi G et al. The vascular endothelium and human diseases. *Int J Biol Sci* 2013;9(10):1057-69.
- (4) Kang DH, Kanellis J, Hugo C, Truong L, Anderson S, Kerjaschki D et al. Role of the microvascular endothelium in progressive renal disease. *J Am Soc Nephrol* 2002 March;13(3):806-16.
- (5) Long DA, Norman JT, Fine LG. Restoring the renal microvasculature to treat chronic kidney disease. *Nat Rev Nephrol* 2012 April;8(4):244-50.
- (6) Deanfield JE, Halcox JP, Rabelink TJ. Endothelial function and dysfunction: testing and clinical relevance. *Circulation* 2007 March 13;115(10):1285-95.
- (7) Chiu JJ, Chien S. Effects of disturbed flow on vascular endothelium: pathophysiological basis and clinical perspectives. *Physiol Rev* 2011 January;91(1):327-87.
- (8) Fiedler U, Augustin HG. Angiopoietins: a link between angiogenesis and inflammation. *Trends Immunol* 2006 December;27(12):552-8.
- (9) David S, Kumpers P, Lukasz A, Fliser D, Martens-Lobenhoffer J, Bode-Boger SM et al. Circulating angiopoietin-2 levels increase with progress of chronic kidney disease. *Nephrol Dial Transplant* 2010 August;25(8):2571-6.
- (10) Kim W, Moon SO, Lee SY, Jang KY, Cho CH, Koh GY et al. COMP-angiopoietin-1 ameliorates renal fibrosis in a unilateral ureteral obstruction model. *J Am Soc Nephrol* 2006 September;17(9):2474-83.
- (11) Kumpers P, Hellpap J, David S, Horn R, Leitolf H, Haller H et al. Circulating angiopoietin-2 is a marker and potential mediator of endothelial cell detachment in ANCA-associated vasculitis with renal involvement. *Nephrol Dial Transplant* 2009 June;24(6):1845-50.
- (12) Moss A. The angiopoietin:Tie 2 interaction: a potential target for future therapies in human vascular disease. *Cytokine Growth Factor Rev* 2013 December;24(6):579-92.
- (13) Woolf AS, Gnudi L, Long DA. Roles of angiopoietins in kidney development and disease. *J Am Soc Nephrol* 2009 February;20(2):239-44.
- (14) Falcon BL, Hashizume H, Koumoutsakos P, Chou J, Bready JV, Coxon A et al. Contrasting actions of selective inhibitors of angiopoietin-1 and angiopoietin-2 on the normalization of tumor blood vessels. *Am J Pathol* 2009 November;175(5):2159-70.
- (15) Dvorak HF, Nagy JA, Dvorak JT, Dvorak AM. Identification and characterization of the blood vessels of solid tumors that are leaky to circulating macromolecules. *Am J Pathol* 1988 October;133(1):95-109.
- (16) Kim KL, Shin IS, Kim JM, Choi JH, Byun J, Jeon ES et al. Interaction between Tie receptors modulates angiogenic activity of angiopoietin2 in endothelial progenitor cells. *Cardiovasc Res* 2006 December 1;72(3):394-402.
- (17) Lobov IB, Brooks PC, Lang RA. Angiopoietin-2 displays VEGF-dependent modulation of capillary structure and endothelial cell survival in vivo. *Proc Natl Acad Sci U S A* 2002 August 20;99(17):11205-10.
- (18) Jain RK. Molecular regulation of vessel maturation. *Nat Med* 2003 June;9(6):685-93.
- (19) Bergers G, Song S. The role of pericytes in blood-vessel formation and maintenance. *Neuro Oncol* 2005 October;7(4):452-64.
- (20) Lin SL, Chang FC, Schrimpf C, Chen YT, Wu CF, Wu VC et al. Targeting endothelium-pericyte cross talk by inhibiting VEGF receptor signaling attenuates kidney microvascular rarefaction and fibrosis. *Am J Pathol* 2011 February;178(2):911-23.

- (21) Pan SY, Chang YT, Lin SL. Microvascular pericytes in healthy and diseased kidneys. *Int J Nephrol Renovasc Dis* 2014 January 17;7:39-48.
- (22) Gaengel K, Genove G, Armulik A, Betsholtz C. Endothelial-mural cell signaling in vascular development and angiogenesis. *Arterioscler Thromb Vasc Biol* 2009 May;29(5):630-8.
- (23) Lin SL, Kisseleva T, Brenner DA, Duffield JS. Pericytes and perivascular fibroblasts are the primary source of collagen-producing cells in obstructive fibrosis of the kidney. *Am J Pathol* 2008 December;173(6):1617-27.
- (24) Basile DP, Sutton TA. Activated pericytes and the inhibition of renal vascular stability: obstacles for kidney repair. *J Am Soc Nephrol* 2012 May;23(5):767-9.
- (25) Schrimpf C, Xin C, Campanholle G, Gill SE, Stallcup W, Lin SL et al. Pericyte TIMP3 and ADAMTS1 modulate vascular stability after kidney injury. *J Am Soc Nephrol* 2012 May;23(5):868-83.
- (26) Chang FC, Lai TS, Chiang CK, Chen YM, Wu MS, Chu TS et al. Angiopoietin-2 is associated with albuminuria and microinflammation in chronic kidney disease. *PLoS One* 2013;8(3):e54668.
- (27) David S, Kumpers P, Lukasz A, Kielstein JT, Haller H, Fliser D. Circulating angiopoietin-2 in essential hypertension: relation to atherosclerosis, vascular inflammation, and treatment with olmesartan/pravastatin. *J Hypertens* 2009 August;27(8):1641-7.
- (28) David S, Kumpers P, Hellpap J, Horn R, Leitolf H, Haller H et al. Angiopoietin 2 and cardiovascular disease in dialysis and kidney transplantation. *Am J Kidney Dis* 2009 May;53(5):770-8.
- (29) Keven K, Elmaci S, Sengul S, Akar N, Egin Y, Genc V et al. Soluble endothelial cell protein C receptor and thrombomodulin levels after renal transplantation. *Int Urol Nephrol* 2010 December;42(4):1093-8.
- (30) Chen YT, Cheng BC, Ko SF, Chen CH, Tsai TH, Leu S et al. Value and level of circulating endothelial progenitor cells, angiogenesis factors and mononuclear cell apoptosis in patients with chronic kidney disease. *Clin Exp Nephrol* 2013 February;17(1):83-91.
- (31) David S, John SG, Jefferies HJ, Sigrist MK, Kumpers P, Kielstein JT et al. Angiopoietin-2 levels predict mortality in CKD patients. *Nephrol Dial Transplant* 2012 May;27(5):1867-72.
- (32) Reed BY, Masoumi A, Elhassan E, McFann K, Cadnapaphornchai MA, Maahs DM et al. Angiogenic growth factors correlate with disease severity in young patients with autosomal dominant polycystic kidney disease. *Kidney Int* 2011 January;79(1):128-34.
- (33) Rizkalla B, Forbes JM, Cao Z, Boner G, Cooper ME. Temporal renal expression of angiogenic growth factors and their receptors in experimental diabetes: role of the renin-angiotensin system. *J Hypertens* 2005 January;23(1):153-64.
- (34) Chao TH, Li YH, Tsai WC, Chen JH, Liu PY, Tsai LM. Elevation of the soluble thrombomodulin levels is associated with inflammation after percutaneous coronary interventions. *Clin Cardiol* 2004 July;27(7):407-10.
- (35) Chade AR, Zhu X, Lavi R, Krier JD, Pislaru S, Simari RD et al. Endothelial progenitor cells restore renal function in chronic experimental renovascular disease. *Circulation* 2009 February 3;119(4):547-57.
- (36) Hohenstein B, Kuo MC, Addabbo F, Yasuda K, Ratliff B, Schwarzenberger C et al. Enhanced progenitor cell recruitment and endothelial repair after selective endothelial injury of the mouse kidney. *Am J Physiol Renal Physiol* 2010 June;298(6):F1504-F1514.
- (37) Thang OH, Serne EH, Grooteman MP, Smulders YM, ter Wee PM, Tangelder GJ et al. Capillary rarefaction in advanced chronic kidney disease is associated with high phosphorus and bicarbonate levels. *Nephrol Dial Transplant* 2011 November;26(11):3529-36.
- (38) Edwards MS, Wilson DB, Craven TE, Stafford J, Fried LF, Wong TY et al. Associations between retinal microvascular abnormalities and declining renal function in the elderly population: the Cardiovascular Health Study. *Am J Kidney Dis* 2005 August;46(2):214-24.

- (39) Lim LS, Cheung CY, Sabanayagam C, Lim SC, Tai ES, Huang L et al. Structural changes in the retinal microvasculature and renal function. *Invest Ophthalmol Vis Sci* 2013 April;54(4):2970-6.
- (40) Goedhart PT, Khalilzada M, Bezemer R, Merza J, Ince C. Sidestream Dark Field (SDF) imaging: a novel stroboscopic LED ring-based imaging modality for clinical assessment of the microcirculation. *Opt Express* 2007 November 12;15(23):15101-14.
- (41) Djaberi R, Schuijff JD, de Koning EJ, Wijewickrama DC, Pereira AM, Smit JW et al. Non-invasive assessment of microcirculation by sidestream dark field imaging as a marker of coronary artery disease in diabetes. *Diab Vasc Dis Res* 2013 March;10(2):123-34.
- (42) Martens RJ, Vink H, van Oostenbrugge RJ, Staals J. Sublingual microvascular glycocalyx dimensions in lacunar stroke patients. *Cerebrovasc Dis* 2013;35(5):451-4.
- (43) Nieuwdorp M, Meuwese MC, Mooij HL, Ince C, Broekhuizen LN, Kastelein JJ et al. Measuring endothelial glycocalyx dimensions in humans: a potential novel tool to monitor vascular vulnerability. *J Appl Physiol* (1985) 2008 March;104(3):845-52.
- (44) Molitoris BA, Sutton TA. Endothelial injury and dysfunction: role in the extension phase of acute renal failure. *Kidney Int* 2004 August;66(2):496-9.
- (45) Xu J, Zou MH. Molecular insights and therapeutic targets for diabetic endothelial dysfunction. *Circulation* 2009 September 29;120(13):1266-86.
- (46) Amann K, Tyralla K. Cardiovascular changes in chronic renal failure--pathogenesis and therapy. *Clin Nephrol* 2002 July;58 Suppl 1:S62-S72.
- (47) Cade WT. Diabetes-related microvascular and macrovascular diseases in the physical therapy setting. *Phys Ther* 2008 November;88(11):1322-35.
- (48) Sampanis C. Management of hyperglycemia in patients with diabetes mellitus and chronic renal failure. *Hippokratia* 2008 January;12(1):22-7.
- (49) Giacco F, Brownlee M. Oxidative stress and diabetic complications. *Circ Res* 2010 October 29;107(9):1058-70.
- (50) Basta G, Schmidt AM, De CR. Advanced glycation end products and vascular inflammation: implications for accelerated atherosclerosis in diabetes. *Cardiovasc Res* 2004 September 1;63(4):582-92.
- (51) Hsueh WA, Anderson PW. Hypertension, the endothelial cell, and the vascular complications of diabetes mellitus. *Hypertension* 1992 August;20(2):253-63.
- (52) Grundy SM. Pre-diabetes, metabolic syndrome, and cardiovascular risk. *J Am Coll Cardiol* 2012 February 14;59(7):635-43.
- (53) Lim HS, Blann AD, Chong AY, Freestone B, Lip GY. Plasma vascular endothelial growth factor, angiotensin-1, and angiotensin-2 in diabetes: implications for cardiovascular risk and effects of multifactorial intervention. *Diabetes Care* 2004 December;27(12):2918-24.
- (54) Hammes HP, Lin J, Wagner P, Feng Y, Vom HF, Krzizok T et al. Angiotensin-2 causes pericyte dropout in the normal retina: evidence for involvement in diabetic retinopathy. *Diabetes* 2004 April;53(4):1104-10.
- (55) Lodhi SA, Meier-Kriesche HU. Kidney allograft survival: the long and short of it. *Nephrol Dial Transplant* 2011 January;26(1):15-7.
- (56) Jevnikar AM, Mannon RB. Late kidney allograft loss: what we know about it, and what we can do about it. *Clin J Am Soc Nephrol* 2008 March;3 Suppl 2:S56-S67.
- (57) Nankivell BJ, Borrows RJ, Fung CL, O'Connell PJ, Allen RD, Chapman JR. The natural history of chronic allograft nephropathy. *N Engl J Med* 2003 December 11;349(24):2326-33.
- (58) Contreras AG, Briscoe DM. Every allograft needs a silver lining. *J Clin Invest* 2007 December;117(12):3645-8.
- (59) de Vries DK, Schaapherder AF, Reinders ME. Mesenchymal stromal cells in renal ischemia/reperfusion injury. *Front Immunol* 2012;3:162.

- (60) de Vries DK, Lindeman JH, Tsikas D, de HE, Roos A, de Fijter JW et al. Early renal ischemia-reperfusion injury in humans is dominated by IL-6 release from the allograft. *Am J Transplant* 2009 July;9(7):1574-84.
- (61) Basile DP. The endothelial cell in ischemic acute kidney injury: implications for acute and chronic function. *Kidney Int* 2007 July;72(2):151-6.
- (62) Eltzschig HK, Collard CD. Vascular ischaemia and reperfusion injury. *Br Med Bull* 2004;70:71-86.
- (63) Park P, Haas M, Cunningham PN, Alexander JJ, Bao L, Guthridge JM et al. Inhibiting the complement system does not reduce injury in renal ischemia reperfusion. *J Am Soc Nephrol* 2001 July;12(7):1383-90.
- (64) Bruneau S, Woda CB, Daly KP, Boneschansker L, Jain NG, Kochupurakkal N et al. Key Features of the Intragraft Microenvironment that Determine Long-Term Survival Following Transplantation. *Front Immunol* 2012;3:54.
- (65) Daly KP, Seifert ME, Chandraker A, Zurakowski D, Nohria A, Givertz MM et al. VEGF-C, VEGF-A and related angiogenesis factors as biomarkers of allograft vasculopathy in cardiac transplant recipients. *J Heart Lung Transplant* 2013 January;32(1):120-8.
- (66) Rabelink TJ, Wijewickrama DC, de Koning EJ. Peritubular endothelium: the Achilles heel of the kidney? *Kidney Int* 2007 October;72(8):926-30.
- (67) Steegh FM, Gelens MA, Nieman FH, van Hooff JP, Cleutjens JP, van Suylen RJ et al. Early loss of peritubular capillaries after kidney transplantation. *J Am Soc Nephrol* 2011 June;22(6):1024-9.
- (68) Chade AR. VEGF: Potential therapy for renal regeneration. *F1000 Med Rep* 2012;4:1.
- (69) Jung YJ, Kim DH, Lee AS, Lee S, Kang KP, Lee SY et al. Peritubular capillary preservation with COMP-angiopoietin-1 decreases ischemia-reperfusion-induced acute kidney injury. *Am J Physiol Renal Physiol* 2009 October;297(4):F952-F960.
- (70) Chen B, Bo CJ, Jia RP, Liu H, Wu R, Wu J et al. The renoprotective effect of bone marrow-derived endothelial progenitor cell transplantation on acute ischemia-reperfusion injury in rats. *Transplant Proc* 2013 June;45(5):2034-9.
- (71) Reinders ME, Fibbe WE, Rabelink TJ. Multipotent mesenchymal stromal cell therapy in renal disease and kidney transplantation. *Nephrol Dial Transplant* 2010 January;25(1):17-24.
- (72) Semedo P, Wang PM, Andreucci TH, Cenedeze MA, Teixeira VP, Reis MA et al. Mesenchymal stem cells ameliorate tissue damages triggered by renal ischemia and reperfusion injury. *Transplant Proc* 2007 March;39(2):421-3.

Chapter 2

Renal ischemia/reperfusion induces a dysbalance of angiotensins, accompanied by proliferation of pericytes and fibrosis

Meriem Khairoun, Pieter van der Pol, Dorottya K. de Vries, Ellen Lievers,
Nicole Schlagwein, Hetty C. de Boer, Ingeborg M. Bajema, Joris I. Rotmans,
Anton Jan van Zonneveld, Ton J. Rabelink, Cees van Kooten, Marlies E.J. Reinders

Am J Physiol Renal Physiol. 305, F901-F910, 2013

Abstract

Introduction: Endothelial cells (ECs) are highly susceptible to hypoxia and easily affected upon ischemia/reperfusion (I/R) during renal transplantation. Pericytes and angiopoietins play important role in modulating EC function. In the present study, we investigate the effect of renal I/R on dynamics of angiopoietin expression and its association with pericytes and fibrosis development.

Methods: Male Lewis rats were subjected to unilateral renal ischemia for 45 minutes followed by removal of the contralateral kidney. Rats were sacrificed at different time points after reperfusion. Endothelial integrity (RECA-1), pericytes (PDGFR β), Angiopoietin-2 (Ang-2)/Angiopoietin-1 (Ang-1) expression and interstitial collagen deposition (Sirius Red and α -SMA) were assessed using immunohistochemistry and RT-PCR.

Results: Our study shows an increase in protein expression of Ang-2 starting at 5 hours and remaining elevated up to 72 hours, with consequently higher Ang-2/Ang-1 ratio after renal I/R ($p < 0.05$ at 48 hours). This was accompanied by an increase in protein expression of the pericytic marker PDGFR β and a loss of ECs (both at 72 hours after I/R, $p < 0.05$). Nine weeks after I/R, when renal function was restored, we observed normalization of the Ang-2/Ang-1 ratio and PDGFR β expression and increase in cortical ECs, which was accompanied by fibrosis.

Conclusions: Renal I/R induces a dysbalance of Ang-2/Ang-1 accompanied by proliferation of pericytes, EC loss and development of fibrosis. The Ang-2/Ang-1 balance was reversed to baseline at 9 weeks after renal I/R, which coincided with restoration of cortical ECs and pericytes. Our findings suggest that angiopoietins and pericytes play an important role in renal microvascular remodeling and development of fibrosis.

Introduction

Renal I/R is an inevitable consequence of renal transplantation causing significant graft injury (5;16;29). Renal I/R impairs the integrity of ECs and leads to loss of peritubular capillaries (6;9;17;19;25;32;36). Loss of integrity and function of the endothelial monolayer lead to renal hypoxia, which is suggested to be a major initiator of profibrotic changes and interstitial scar formation in the kidney (2;24). These microvascular changes and renal scarring eventually lead to a deteriorating of renal function and graft loss (26).

Pericytes play a critical role in the stabilization and proliferation of peritubular capillaries via interaction with ECs (1;20;30). This process is mediated by several angioregulatory factors, including Ang-1, produced by pericytes and Ang-2 produced by activated ECs (7;30;35). Angiopoietins are a group of vascular regulatory molecules that bind to the receptor tyrosine kinase Tie-2, which is predominantly expressed by vascular ECs. Ang-1 is a strong vascular protective agonist of the Tie-2 receptor responsible for suppressing vascular leakage, maintaining EC survival and inhibiting vascular inflammation. Ang-2 acts as an antagonist of Ang-1 and promotes, in a dose dependent manner, destabilization, vessel leakage and inflammation. By promoting pericyte dropout, Ang-2 will lead to loosening contacts between ECs and perivascular cells, with subsequent vessel destabilization and abnormal microvascular remodeling (7;14;15;35). Recent studies have shown that pericytes detach from the endothelium and migrate to the interstitium to become activated and differentiate into myofibroblasts contributing to renal fibrosis (10;12). Interestingly, treatment with cartilage oligomeric matrix protein (COMP)-Ang-1 in a mice model of renal I/R injury resulted in protection against peritubular capillary damage and decrease in inflammatory cells and renal interstitial fibrosis (19).

However, dynamics and the time course of angiopoietin expression, its relation with EC and pericyte expression and development of fibrosis in the repair phase after renal I/R injury are unknown. Using an established rat model of renal I/R injury, we assessed the impact of I/R on Ang-2/Ang-1 balance and its effect on microvascular remodeling, pericytes and the formation of fibrosis up to 9 weeks after renal I/R injury. We hypothesize that I/R injury leads to activation of ECs with consequent elevation of Ang-2 levels, which may lead to proliferation of pericytes and loss of ECs, but may also induce fibrosis in the long term.

Materials and Methods

Rat model of renal I/R injury

Renal I/R injury was induced as previously described (34). The Animal Care and Use Committee of the Leiden University Medical Center approved all experiments. Eight-week-

old male Lewis rats (200–250 g) purchased from Harlan (Horst, The Netherlands) were housed in standard laboratory cages and allowed free access to food and water throughout the experiments. Unilateral ischemia was induced by clamping of the left renal pedicle for 45 min using a bulldog clamp (Fine Science Tools, Heidelberg, Germany). During clamping the contra-lateral kidney was removed. Sham-treated rats had identical surgical procedures except for clamping of the left kidney. Tail blood samples were taken before and at indicated time points after reperfusion and were kept on ice. Rats were sacrificed at 2, 5, 24, 48 or 72 hours (hr) and 1, 6 and 9 weeks (wk) after reperfusion and kidneys were harvested for histological examination and immunohistochemical staining. Renal function was assessed by measuring creatinine and urea (BUN) in serum samples using standard auto analyzer methods by our hospital research services.

Immunohistochemistry and immunofluorescent staining

Rat kidney sections (4 μ m) of snap-frozen kidneys were air dried and acetone fixed. Slides were incubated overnight with goat polyclonal IgG against Ang-1 (N18) or Ang-2 (F18; both Santa Cruz Biotechnology), mouse monoclonal IgG against endothelial cells (RECA-1; Hycult Biotechnology, Uden Netherlands and CD31; Abcam, Cambridge, England), myofibroblasts (α -SMA, Progen, Heidelberg, Germany), inflammatory cells (OX42* for monocytes, dendritic cells and granulocytes (kindly provided by Dr. P. Kuppen, LUMC Leiden, the Netherlands)) and CD45 for leukocytes (BD Pharmingen, Breda Netherlands) or rabbit polyclonal IgG against pericytes (PDGFR β ; Abcam, Cambridge, England). Antibody binding was detected with horseradish peroxidase (HRP)-labeled rabbit anti-goat IgG (DAKO, Glostrum, Germany), goat anti-mouse IgG (Jackson, Suffolk, England) or goat anti-rabbit IgG (DAKO), respectively. After washing, sections were incubated with tyramide-fluorescein isothiocyanate in tyramide buffer (NENTM Life Science Products, Boston, MA, USA), washed and incubated with HRP-labeled rabbit anti-fluorescein isothiocyanate (DAKO, Glostrum, Germany) and developed with 3,3'-Diaminobenzidine (DAB) (Sigma, St Louis, MO, USA). Sections were counterstained with haematoxylin (Merck, Darmstadt, Germany) and mounted with imsol (Klinipath, Duiven, the Netherlands). Quantification of immunohistochemistry was performed in a blinded manner by assessing consecutive high power fields (magnification, \times 100) on each section from the cortex, outer and inner medulla. Using Image J software, the percentage of positivity per specific region of the kidney was determined, with exception of Ang-1 and Ang-2, which was only analyzed for the cortex. For cortical RECA-1 expression, the ratio of mean percentage of positivity of I/R injured and sham operated rats was calculated. Glomeruli were excluded from all analyses of the cortex. Since the Ang-2/Ang-1 ratio, rather than the absolute expression of either angiopoietin is generally used to determine the functional status of the microvasculature (26), this ratio was calculated using the Ang-2 and Ang-1 quantification. Immunofluorescent double stainings were performed for ki-67 (cell proliferation marker) using

polyclonal rabbit IgG (Abcam, Cambridge, England) and RECA-1 and Ang-2/RECA-1. Due to technical reasons double stainings with Ang-1/ PDGFR β and RECA-1/ PDGFR β could not be performed, therefore the pericyte marker NG2 (rabbit polyclonal IgG; BD Pharmingen, Breda, Netherlands) was used for these double stainings. Antibody binding was visualized using AlexaTM 488-labeled goat anti-rabbit IgG, AlexaTM 568-labeled goat anti-mouse IgG (both Life science) and donkey anti-goat IgG (Jackson, Suffolk, England). Nuclei were stained using Hoechst (Molecular Probes, Leiden, the Netherlands). Micrographs were made using a fluorescence microscope (Leica, DMI6000, Rijswijk, the Netherlands).

Histologic evaluation

Renal fibrosis was evaluated histologically by Sirius Red staining as described previously (27) on 4 μ m paraffin slides of renal rat tissue. From each part of the kidney (cortex, outer and inner medulla) five random images were obtained. Image analyses was performed using Image J software. The amount of collagen deposition was measured and expressed as percentage of positivity per region of the kidney. In addition, all tissue specimens were scored for severity of fibrosis on a semi-quantitative scale (0-3) in a blinded manner by an experienced pathologist.

RNA isolation and Real-Time PCR

RT-PCR was performed as described previously (34). Total RNA was extracted from snap frozen cross-section kidney slices using the RNeasy Mini isolation Kit according to the manufacturer's instructions (QIAGEN, Hilden, Germany). cDNA was synthesized from 1 μ g total RNA, using an oligo dT primer, RNase-OUT, M-MLV reverse transcriptase, 0.1 M-DTT and buffers in a volume of 20 μ L (all purchased from Invitrogen, Breda, The Netherlands). Quantitative real-time PCR was performed in duplicate by using iQ SYBR Green Supermix on iCycler Real-Time Detection System (BioRad). The amplification reaction volume was 20 μ L, consisting of 10 μ L iQ SYBR Green PCR mastermix, 1 μ L primers, 1 μ L cDNA, and 8 μ L water. Data were analyzed using Gene Expression Analysis for iCycler Real-Time PCR Detection System (Biorad). Expression of each gene was normalized against mRNA expression of the housekeeping gene Rsp-15. RT PCRs were performed in duplicate. The primer sequences are shown in Table 1.

Table 1: Primer sequences used for quantitative real-time polymerase chain reaction

Gene	Forward primer 5'→3'	Reverse primer 5'→3'	Supplier
RSP-15	CGTCACCCGTAATCCACC	CAGCTTCGCGTATGCCAC	Biolegio
ANG-1	TCTCTTCCCAGAAACTTCA	TTTGATTTAGTACCTGGGTCTC	Biolegio
ANG-2	TGCATCTGCAAGTGTTCCTC	GCCTTGAGCGAGTAACCG	Biolegio
TIE-2	GTCCTATGGTGTATTGCTCTG	TCTCTCATAAGGCTTCTCCC	Biolegio

Statistical analyses

Data are reported as mean \pm standard error of the mean (SEM). Statistical comparisons were performed using one-way ANOVA or Mann–Whitney test with GraphPad Prism software (GraphPad Software Inc., San Diego, CA, U.S.A.). A value of $p < 0.05$ was considered statistically significant.

Results

Renal I/R induces transient deterioration of renal function, influx of inflammatory cells and interstitial fibrosis

In the current study we used a rat model of renal I/R resulting in extensive renal dysfunction, as shown by increased serum creatinine and BUN levels, but characterized by normalized renal function after 1 week following I/R ($p < 0.05$, compared to 72 hr) (Fig. 1A, B). Renal dysfunction was accompanied by significant infiltration of OX42⁺ inflammatory cells in the cortex, outer and inner medulla at 72 hr ($p < 0.05$), which peaked at 1 week compared to sham-operated rats (Fig. 1E, F, G). A decrease in OX42⁺ inflammatory cells was observed at 6 and 9 weeks in the different parts of the kidney compared to 1 week following I/R ($p < 0.05$). In the outer and inner medulla, the influx of OX42⁺ cells remained significantly increased up to 6 and 9 weeks ($p < 0.05$), respectively, after renal I/R injury compared with sham-operated rats (Fig. 1G). Consistently, CD45 expression in the cortex showed a similar pattern as OX42⁺ staining (Fig. 1C, D).

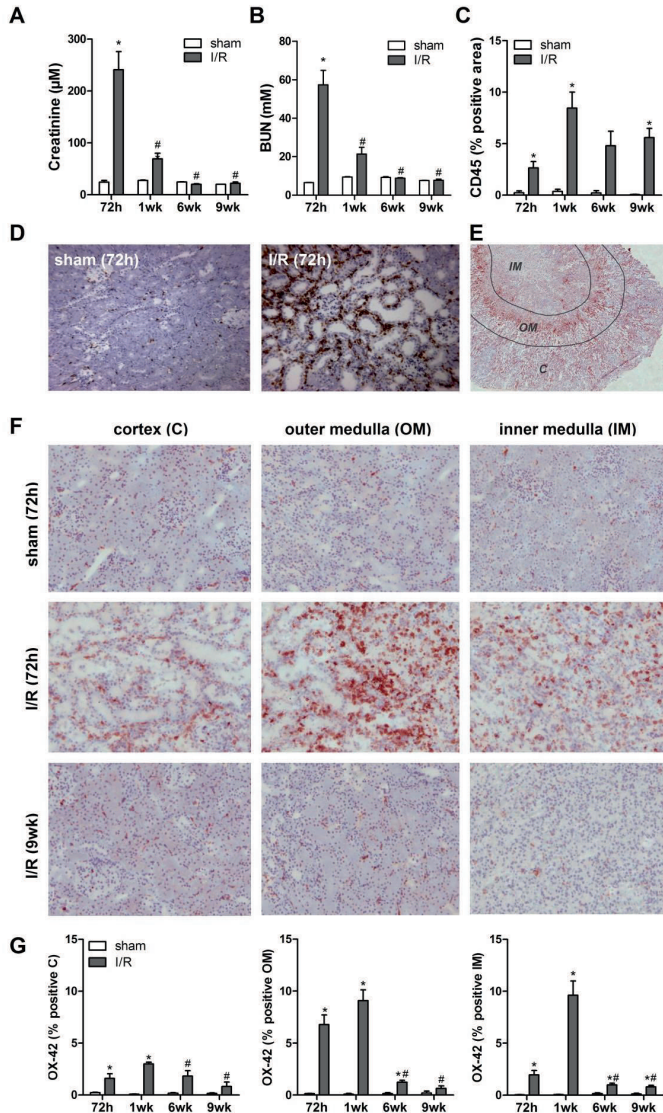


Figure 1. Renal I/R induces deterioration of renal function and influx of inflammatory cells

Serum creatinine levels (A) and BUN (B) were measured at consecutive time points after reperfusion. CD45 positive leukocyte infiltrate was quantified using digital image analysis (C). Representative photomicrographs of kidney sections stained with CD45 (D) from a sham-operated rat and a rat subjected to I/R and sacrificed at 72 hr after reperfusion. An overview of the division of the different regions (cortex, outer medulla and inner medulla) in a kidney section stained with OX42 (E). Representative photomicrographs of kidney sections stained with OX42⁺ from a sham-operated rat and rats subjected to I/R and sacrificed at 72 hr or 9 weeks after reperfusion (F). OX42⁺ infiltrate of sham-operated rats and rats subjected to I/R was quantified in the different areas using digital image analysis (G) and demonstrated as % of the depicted area. Data are shown as mean \pm SEM (n = 5 rats per group). *P < 0.05 compared to corresponding sham controls. #P < 0.05 compared to 72 hr or 1 wk rats. Original magnification of D, E and F, x200. C=cortex; OM=outer medulla; IM=inner medulla.

One week after reperfusion, significant diffuse interstitial collagen deposition was observed in the cortex, outer and inner medulla compared to sham-operated rats ($p < 0.05$) (Fig. 2A, B). After 9 weeks collagen deposition was significantly decreased in different regions of the kidney compared to 1 week following renal I/R injury ($p < 0.05$), although kidneys were still characterized by focal areas of intense Sirius Red staining. The semi-quantitative analyses showed that fibrosis scores at 9 weeks were not statistically different from 1 week after I/R (data not shown), which is probably due to the focal areas of fibrosis. Consistently, the α -SMA immunohistochemical staining revealed a significant increase of fibrosis in cortex and outer medulla at 72 hr ($p < 0.05$) and at all parts of the kidney at 1 week ($p < 0.05$) following I/R injury compared with sham-operated rats (Fig. 2C, D). At 9 weeks, α -SMA staining was significantly decreased in the cortex, outer and inner medulla compared with 1 week after I/R injury (Fig. 2C).

Restoration of peritubular capillaries in the cortex 9 weeks after renal I/R

Since endothelial damage is an important hallmark of I/R injury, we assessed peritubular capillaries over time by staining for RECA-1. A significant reduction in RECA-1 expression was observed at 72 hr post I/R ($p < 0.05$) in the cortex and outer medulla and at 1 week in the inner medulla ($p < 0.05$) compared with sham-operated rats (Fig. 3A-C). Interestingly, we found a significant increase of RECA-1 staining at 6 and 9 weeks in the cortex ($p < 0.05$) following I/R compared to rats that were sacrificed at 72 hr (Fig. 3B). Calculation of the ratio IR injured/sham operated rats for RECA-1 expression confirmed the observed increase at 6 and 9 weeks after injury (Fig. 3B). RECA-1 staining co localized with the proliferation marker Ki-67, suggesting EC proliferation in peritubular capillaries within the renal cortex at 9 weeks after I/R (Fig. 3D, E). No proliferation of ECs was found in the glomeruli following renal I/R. In the outer and inner medulla a different pattern was found. Here a significant reduction in RECA-1 expression was observed at 72 hr post I/R in the outer medulla ($p < 0.05$) and at 1 week in the inner medulla ($p < 0.05$) compared with sham-operated rats (Fig. 3C). In contrast to the cortex, RECA-1 staining in these areas showed a further decrease up to 9 weeks after ischemic injury ($p < 0.05$) (Fig. 3C). CD31 staining demonstrated a pattern comparable to the RECA-staining (Fig. 3F).

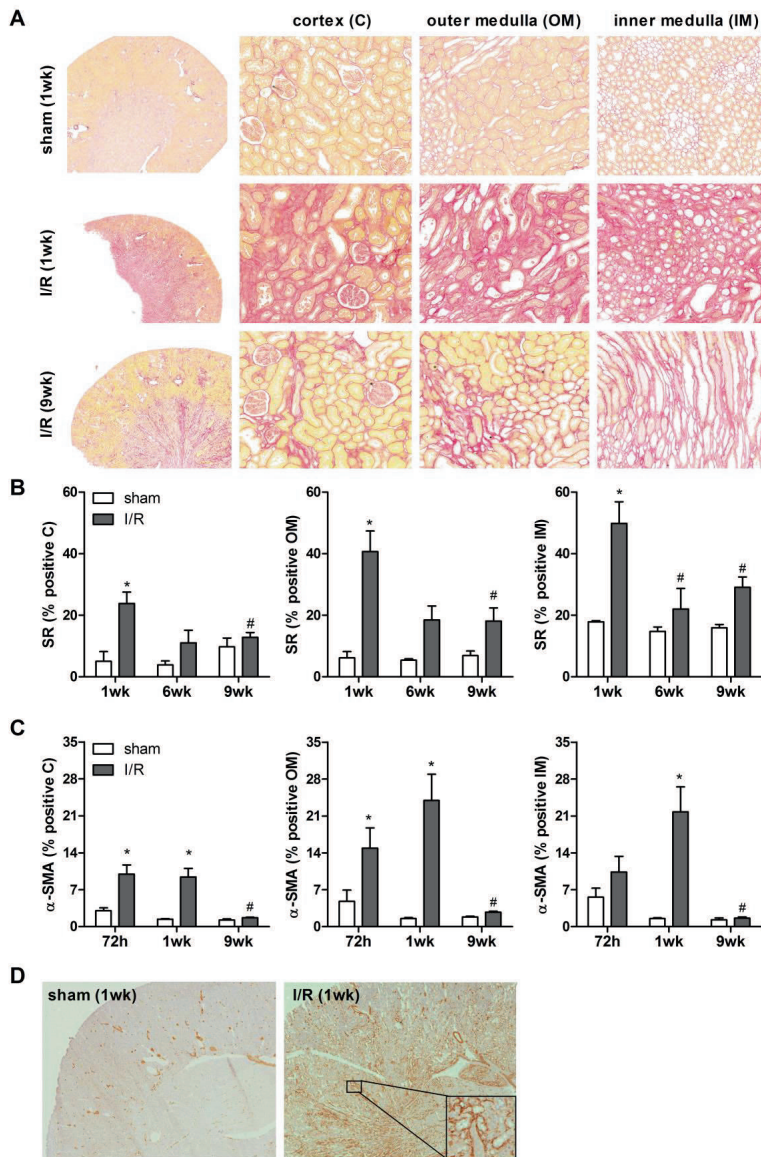


Figure 2. Renal I/R induces interstitial fibrosis

Representative photomicrographs of Sirius Red stained kidney sections (A) of the cortex, outer medulla and inner medulla obtained from a sham-operated rat (sacrificed at 1 week), and rats subjected to I/R and sacrificed at 1 or 9 weeks after reperfusion as indicated. Quantitative analysis of Sirius Red staining (B) and α -SMA staining (C) at different time points after reperfusion in sham-operated rats and rats subjected to I/R in the different regions as indicated. Quantification was performed by digital image analysis and is demonstrated as % of the depicted area. Representative images of whole kidney sections stained with α -SMA (D) of sham operated rat (sacrificed at 1 week) and rat subjected to 1 week I/R injury with insert showing α -SMA staining in the outer medulla. Data are shown as mean \pm SEM (n= 5 rats per group). *P<0.05 compared to corresponding sham controls. #P<0.05 compared to 72 hr or 1 wk rats. Original magnification of A, x200; D, x100; insert at 1 week, x200. C=cortex; OM=outer medulla; IM=inner medulla.

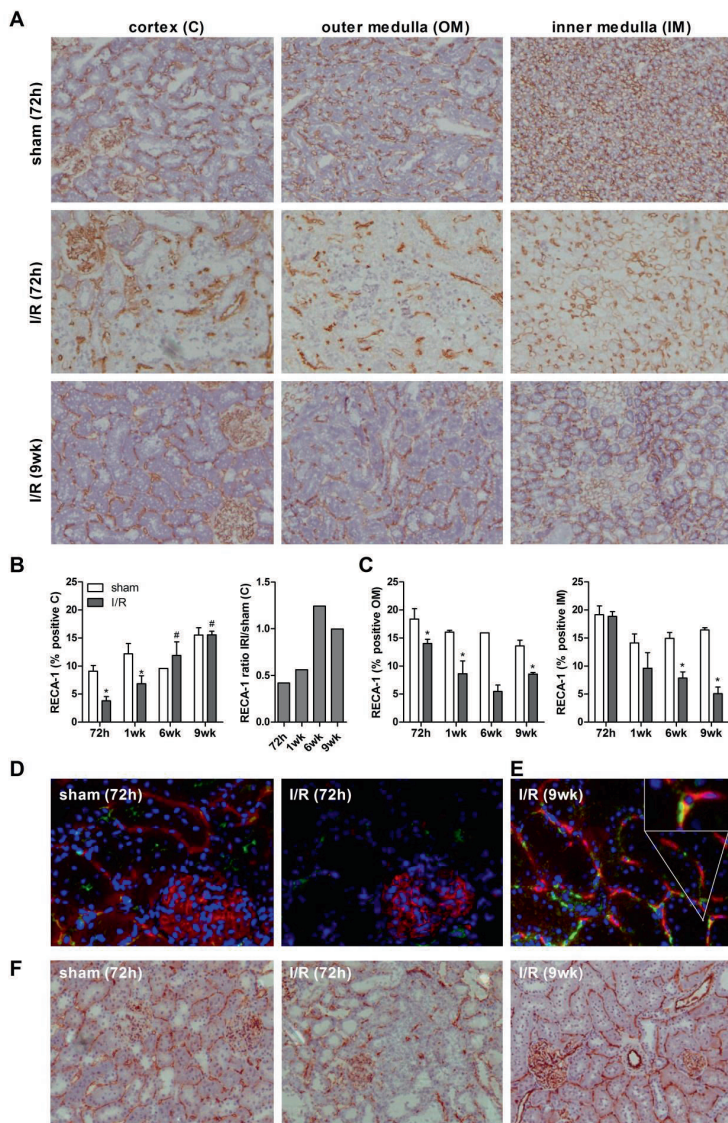


Figure 3. Restoration of I/R-induced peritubular capillary loss in the cortex late after reperfusion
 Representative images of kidney sections of the cortex, outer medulla and inner medulla stained for RECA-1 (A) obtained from a sham-operated rat and rats subjected to I/R and sacrificed at 72 hr and 9 weeks after reperfusion. Quantitative analysis of cortical (B), outer medullary and inner medullary (C) RECA-1 expression. Immunofluorescent double staining for RECA-1 (red) and Ki-67 (green) of representative kidney sections of a sham-operated rat and rats sacrificed at 72 hr (D) or 9 weeks (E) after reperfusion. Insert is showing double positivity of RECA-1 and Ki-67 staining in yellow in kidney sections at 9 weeks after reperfusion. Representative images of kidney sections of the cortex stained for CD31 (F) obtained from a sham-operated rat and rats subjected to I/R and sacrificed at 72 hr or 9 weeks after reperfusion. Data are shown as mean \pm SEM (n= 5 rats in grouper group). *P<0.05 compared to corresponding sham controls. #P<0.05 compared to 72hr. Original magnification of A, D, E and F, x200; insert at 9 weeks, x400.

Renal I/R induces a dysbalance in Ang-2/Ang-1 ratio at early time points and return to baseline after 6 weeks

In control kidneys of sham-operated rats, Ang-1 staining was observed in the glomeruli and in a capillary like pattern between the tubuli (Fig. 4A). Double staining of Ang-1 and the pericyte marker NG2 revealed co localization, suggesting that Ang-1 is expressed by pericytes (Fig. 4C). Starting at 24 hr after renal I/R, a significant decrease in Ang-1 expression was observed (data not shown), reaching a maximal decrease at 72 hr ($p < 0.05$) (Fig. 4A, F). Ang-1 expression increased significantly at 9 weeks after renal I/R compared to 72 hr ($p < 0.05$) (Fig. 4A, F). Additionally, RT-PCR analyses revealed a decrease in Ang-1 mRNA levels which reached significance at 1 week compared the sham-operated rats ($p < 0.05$; Fig. 4I).

In control rats, low levels of Ang-2 protein were observed in glomeruli, interstitial vessels and on brushborders of tubuli (Fig. 4B, G). Due to the apical and brush border expression on tubuli of Ang-2 in the medulla, it was technically not possible to distinguish between interstitial and tubular presence of Ang-2 (Fig. 4E). Therefore quantification of angiopoietins was only performed in the cortex. Additional double staining of Ang-2 and RECA-1 confirmed the expression of Ang-2 by ECs (Fig. 4D). Compared to sham-operated rats, Ang-2 expression increased at 5 hr (data not shown) and remained elevated up to 72 hr ($p < 0.05$) after I/R (Fig. 4G). Consequently higher Ang-2/Ang-1 ratios were observed after 48 hr and 72 hr ($p < 0.05$) (Fig. 4H). After 1 week, Ang-2 levels and Ang-2/Ang-1 ratio started to decrease, reaching significance at 6 and 9 weeks compared to 72 hr after renal I/R (Fig. 4B, G and H). Ang-2 mRNA levels did not confirm the observed changes at protein levels (Fig. 4J). Tie-2 mRNA expression showed a significant decrease at 1 week compared with sham-operated group and reversal to baseline levels at 9 weeks after I/R (Fig. 4K).

Renal I/R leads to proliferation of pericytes

Immunohistochemical staining revealed the presence of PDGFR β positive cells in the mesangium, Bowman's capsule, large vessels and peritubular capillaries (Fig. 5A). A significant increase of pericytes was observed at 48 hr upon I/R in all parts of the kidney compared with sham-operated rats, which persisted up to 72 hr in the cortex and up to 9 weeks in both the outer and inner medulla ($p < 0.05$) (Fig. 5A, B). PDGFR β expression showed normalization at the protein level in all regions of the kidney ($p < 0.05$) at 9 weeks after renal I/R injury (Fig. 5A, B). To investigate the anatomical relation of ECs and pericytes double staining with RECA-1 and the pericyte marker NG2 were performed, which revealed expression of both markers in the glomeruli and peritubular space (Fig. 5C).

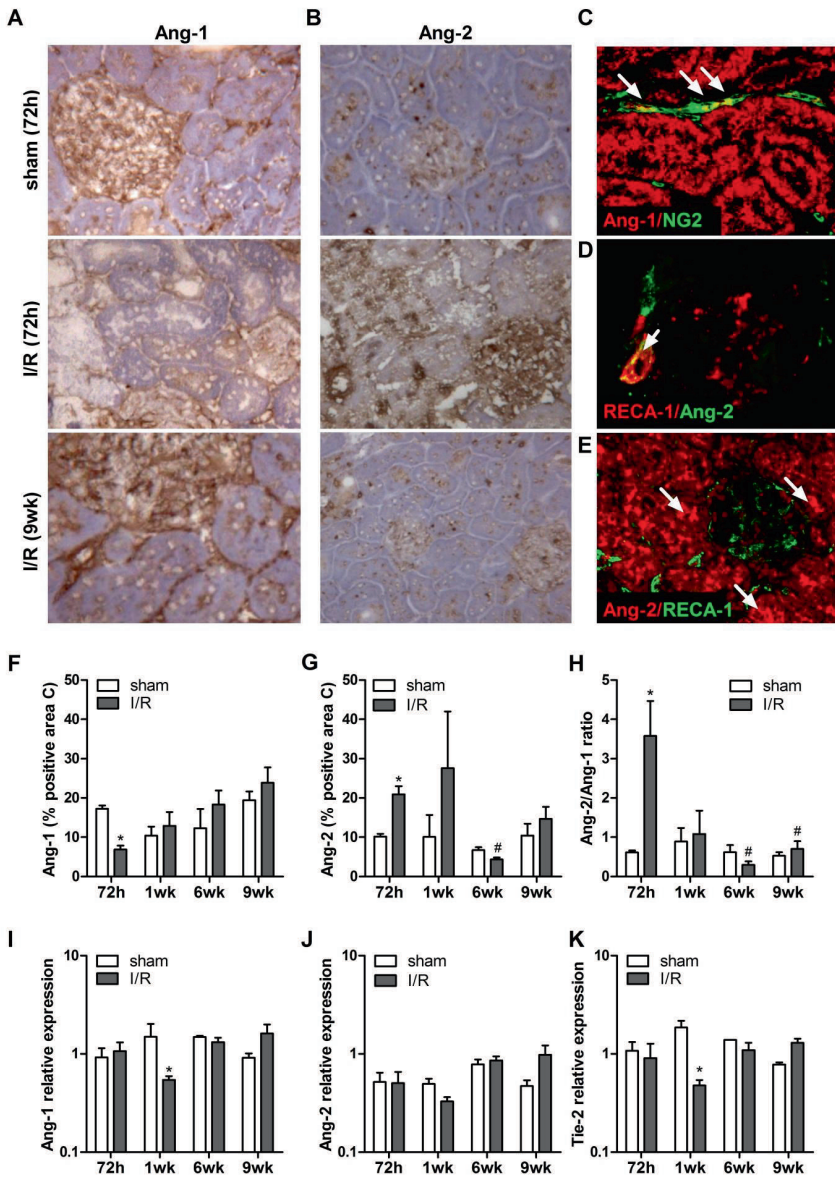


Figure 4. Renal I/R induces a dysbalance in the Ang-2/Ang-1 ratio early after reperfusion

Representative cortical photomicrographs of kidney sections stained with Ang-1 (A) or Ang-2 (B) in a sham-operated rat and rats subjected to I/R and sacrificed at 72 hr or 9 weeks after reperfusion. Immunofluorescent double staining for Ang-1/NG2 (C), RECA-1/Ang-2 (D) and Ang-2/RECA-1 (E) of representative kidney sections in a sham-operated rat. Arrows indicate double staining in yellow (C,D) and apical expression of Ang-2 (E). Quantitative analysis of cortical protein expression of Ang-1 (F), Ang-2 (G), and Ang-2/Ang-1 ratio (H) at consecutive time points after reperfusion. Quantitative analysis of RNA expression of Ang-1 (I), Ang-2 (J) and Tie-2 (K) at consecutive time points after reperfusion. Data are shown as mean \pm SEM (n = 5 rats per group). *P<0.05 compared to corresponding sham controls. #P<0.05 compared to 72 hr. Magnification of A-E, x400.

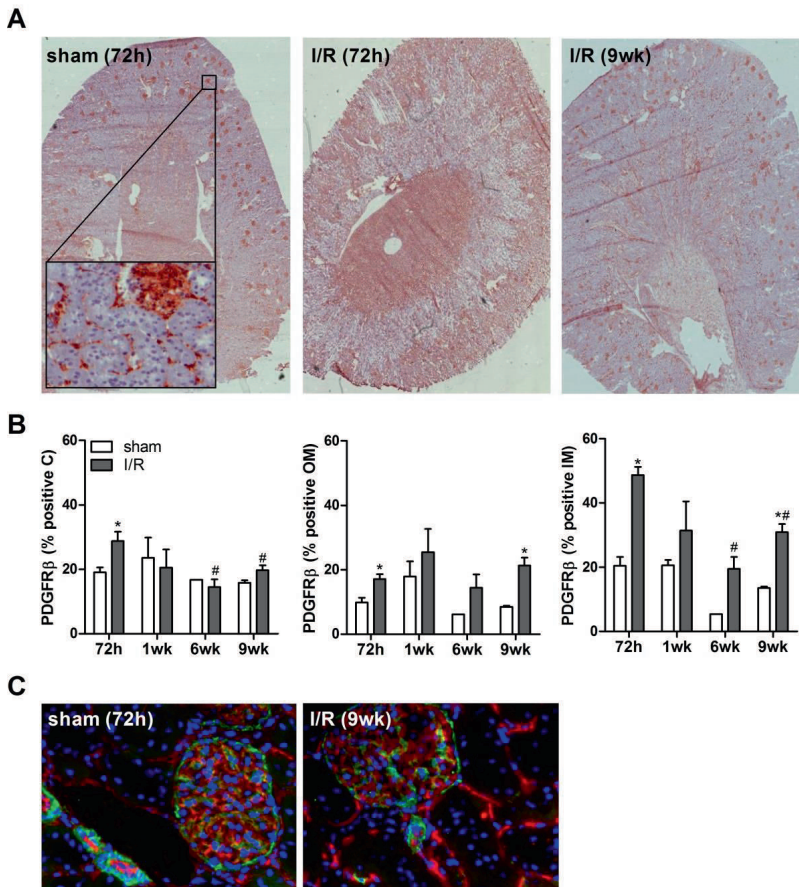


Figure 5. Renal I/R induces proliferation of pericytes

Representative photomicrographs of whole kidney sections stained for PDGFR β (A) in a sham-operated rat and rats subjected to I/R and sacrificed at 72 hr or 9 weeks after reperfusion. Insert is showing peritubular and glomerular expression of PDGFR β in sham-operated rats. Quantitative analysis of PDGFR β protein expression (B) at consecutive time points after reperfusion. Immunofluorescent double staining for RECA-1 (red) and NG2 (green) of representative kidney sections (C) in a sham-operated rat and rat subjected to I/R and sacrificed at 9 weeks after reperfusion. Data are shown as mean \pm SEM (n= 5 rats per group). *P<0.05 compared to corresponding sham controls. #P<0.05 compared to 72hr. Original magnification of A, x100; insert at 72hr and C, x200.

Discussion

We performed a detailed kinetic analysis of angiopoietin and pericyte expression after renal I/R injury. We demonstrate that renal I/R induces a dysbalance in Ang-2/Ang-1 which is accompanied by a loss of ECs, proliferation of pericytes and development of fibrosis. At 9 weeks post I/R, we show reversal to baseline in Ang-2/Ang-1 balance, an increase in ECs and

normalization of PDGFR β expression in the cortex. Whereas renal function is fully restored at this time point, the renal tissue does still show signs of fibrosis.

It is postulated that loss of ECs is a central common pathway involved in organ failure that precedes and drives the profibrotic changes of the kidney parenchyma (2;3;24). Different reports using animal models have been published which demonstrate chronic deleterious effects of ischemic injury on long-term renal function and microvascular structure (2;6;16;17;29;36). Basile et al have shown that renal I/R in a rat model results in permanent damage to peritubular capillaries with development of tubulointerstitial fibrosis and decline in long-term renal function (2). In the present study, we also observed loss of peritubular capillaries and development of tubulointerstitial fibrosis following renal I/R, which were more severe and extensive in the outer and inner medulla than the cortex. The observed fibrosis at early time points after renal I/R injury in our study coincided with the influx of inflammatory cells. At later time points, we observed a different pattern of fibrosis, which was more dense and unrelated to the areas of inflammation. This 'inflammatory fibrosis' observed at early times has been reported to be important for restoration of the original tissue morphology and function (13). It is, however, also suggested that if repair is not efficient at early times, fibrosis at the repair phase cannot be prevented (9). In our study, at 9 weeks after reperfusion, restoration and proliferation of ECs was found in the cortex, but not in the outer and inner medulla. This could be caused by the anatomical relationship of capillaries and tubules in the outer and inner medulla, with consequently a greater impact of hypoxia- and leucocyte-induced EC damage than in the cortical peritubular capillaries (5).

In contrast to the study of Basile et al, we found restoration and proliferation of ECs in the cortex in the repair phase (9 weeks after I/R). Possible explanations for this discrepancy between our study and the studies of Basile could be differences in clamping time (45-versus 60-minutes, respectively) and the removal of the healthy contralateral kidney in our study. In the study of Basile, additional experiments in which rats were subjected to 30 and 45 minutes of bilateral ischemia were performed, to assess whether the duration of ischemic injury affects damage to the renal microvasculature and function. Both renal function and capillary density were more disturbed in the 45 minutes group compared to the 30 minutes rats, which might implicate a "critical ischemia time" for endothelial repair (2).

The molecular mechanisms that lead to microvascular injury in organ failure are largely unknown. It has been suggested that several angioregulatory growth factors, including the angiopoietins, play a central role in the loss of vascular integrity (18;36). In this regard, a study has shown that treatment with COMP-Ang-1 (soluble, stable and potent form of Ang-1) in a mice model of renal I/R resulted in protection against peritubular capillary damage,

decrease in interstitial inflammatory cells and renal interstitial fibrosis (5). Other investigators have demonstrated stabilization of peritubular capillaries along with increased fibrosis and inflammation after adenoviral Ang-1 treatment in a mouse model of folic acid-induced nephrotoxicity (37). These studies suggest that differences in efficacy of Ang-1 in the kidney may be due to variation in potency of Ang-1 and COMP-Ang-1 or difference in kidney disease models (5;12;37). Ang-2 acts as an antagonist of Ang-1 and increases vessel leakage, inflammation and destabilization by promoting pericyte loss, therefore loosening contacts between ECs and pericytes (18;36).

An interesting observation in this study is that we found a relation in time between Ang-2/Ang-1 balance and microvascular integrity and pericytes in the cortex after I/R. Activation of ECs, reflected by increase in Ang-2 expression and consequently higher Ang-2/Ang-1 ratio, was accompanied by proliferation of pericytes, EC loss and development of fibrosis. This relation between EC loss and dysbalance in angiopoietins has also been demonstrated in a mouse model of anti-glomerular basement membrane glomerulonephritis, where glomerular capillary loss was associated with reduced Ang-1 and increased Ang-2 expression (38). In addition, in an animal model of diabetic retinopathy, Ang-1 was shown to have a profound effect in repairing integrity of the retinal EC permeability barrier (39). Moreover, injection of Ang-2 into the eyes of normal rats has been shown to induce a dose-dependent pericyte loss (28). These findings suggest an important role for the angiopoietins in generating a proangiogenic environment that is necessary for capillary repair.

Several studies have pointed at the critical importance of the interaction between pericytes and ECs in maintenance of the capillary network (1;30). Surprisingly, hardly any data are available on the relation between pericytes and loss of ECs in renal I/R. Only one study has shown an association between damage to peritubular capillaries and decreased number of pericytes in cadaveric renal allografts after I/R (21). Peritubular capillary integrity was better preserved and pericytes were more pronounced in patients who had a better recovery of their graft function compared to patients with sustained postischemic acute kidney injury (21). However, this study investigated the expression of pericytes at only one time-point early after renal I/R and did not investigate the relation to angiopoietins and development of fibrosis in a time course.

To investigate the role of pericytes in renal I/R injury, we used PDGFR β as pericyte marker. PDGFR β is a single-spanning transmembrane glycoprotein that binds to its dimeric ligand PDGF and a crucial receptor for recruitment and survival of pericytes by paracrine secretion of PDGFB by ECs (4;23;33). PDGFR β has been shown in studies of obstructive and post-ischemic kidney injury to be expressed by pericytes and fibroblasts (8;22;23). Compared with

other pericyte markers, PDGFR β continued to be expressed after proliferation of pericytes and after transformation into myofibroblasts upon injury. Recently, Duffield et al provided evidence for the contribution of pericytes to the development of renal fibrosis (11;18;23;30). Using a transgenic mouse model of unilateral ureter obstruction (UUO), expressing green fluorescent protein in cells producing the collagen type I, they demonstrated that pericytes are the main source for interstitial myofibroblasts during renal fibrosis (23). The same investigators showed migration of perivascular stromal cells from capillaries into the renal interstitium, within 9 hr after induction of ureter obstruction. After loosening contact from the capillaries, pericytes became activated and proliferated into collagen producing myofibroblasts contributing to fibrosis (23). PDGFR β signaling has been reported to play an important role in the development of fibrosis. Blockade of PDGFR β attenuated recruitment of inflammatory cells, loss of ECs and fibrosis in mice subjected to renal I/R injury and UUO (22). Also in our study we demonstrated proliferation of pericytes and loss of ECs which was accompanied by development of fibrosis. The pericytes may have responded to injury by detaching from the capillaries and becoming pathologic matrix depositing cells, that contribute to the population of α -SMA–positive cells in the fibrotic interstitial space observed in this study (8;31). The process of pericyte detachment has been suggested to be reversible, which could explain the observed decrease in PDGFR β expression and the restoration of ECs in the cortex (22). However, in both the inner and outer medulla an increase of PDGFR β cells was observed up to 9 weeks after renal I/R. Interestingly, these areas had no increase in EC staining and demonstrated a more profound fibrosis reaction compared to the less damaged cortex area.

An important discussion point remains whether the decrease in RECA-1 in the cortex observed in our study is explained by EC loss or by interstitial edema and compression of peritubular capillaries. However, previous studies utilizing microfilm analyses and EC staining with CD31 confirmed the loss of ECs after I/R (2;3;17;19;32). Additional CD31 staining in this study, revealed a similar pattern as observed with RECA-1. Although, our study clearly suggests that angiopoietins are essential in renal microvascular remodeling in the cortex, we were not able to analyze the outer and inner medulla of Ang-2 staining. Ang-2 showed brush border and apical expression on tubules in the medulla, making it difficult to distinguish between interstitial and tubular presence of Ang-2. Therefore, we focused only on the cortex for angiopoietins staining. Furthermore, we observed a discrepancy in Ang-2 protein and mRNA expression, which could be explained by the use of whole kidney RNA extractions instead of a specific region as for immunohistochemistry or contribution of earlier produced Ang-2 by infiltrating cells, while lacking the detectable transcript (28). A therapeutic intervention would be required to prove a causal relationship between the functions of angiopoietins and pericytes and its role in EC stabilization and repair.

In conclusion, our study demonstrates that renal I/R induces a dysbalance in angiopoietins, accompanied by proliferation of pericytes and development of fibrosis. These findings support the hypothesis that angiopoietins and pericytes play an important role in renal microvascular remodeling. Since angiopoietins and pericytes are considered as important hallmarks of microvascular integrity, strategies to counteract microvascular destabilization after I/R may well improve long term graft function.

Grants

This work was supported by a Veni grant from ZonMW (01086089) to M.E.J. Reinders and Dutch Kidney Foundation grants to P. van der Pol (NSN KSTP 11.005) and T.J. Rabelink (C 09.2329)

Reference List

- (1) **Armulik A, Abramsson A, Betsholtz C.** Endothelial/pericyte interactions. *Circ Res* 97: 512-523, 2005.
- (2) **Basile DP, Donohoe D, Roethe K, Osborn JL.** Renal ischemic injury results in permanent damage to peritubular capillaries and influences long-term function. *Am J Physiol Renal Physiol* 281: F887-F899, 2001.
- (3) **Basile DP, Friedrich JL, Spahic J, Knipe N, Mang H, Leonard EC, et al.** Impaired endothelial proliferation and mesenchymal transition contribute to vascular rarefaction following acute kidney injury. *Am J Physiol Renal Physiol* 300: F721-F733, 2011.
- (4) **Bergers G, Song S.** The role of pericytes in blood-vessel formation and maintenance. *Neuro Oncol* 7: 452-464, 2005.
- (5) **Bonventre JV, Yang L.** Cellular pathophysiology of ischemic acute kidney injury. *J Clin Invest* 121: 4210-4221, 2011.
- (6) **Brodsky SV, Yamamoto T, Tada T, Kim B, Chen J, Kajiya F, et al.** Endothelial dysfunction in ischemic acute renal failure: rescue by transplanted endothelial cells. *Am J Physiol Renal Physiol* 282: F1140-F1149, 2002.
- (7) **Cai J, Kehoe O, Smith GM, Hykin P, Boulton ME.** The angiotensin/Tie-2 system regulates pericyte survival and recruitment in diabetic retinopathy. *Invest Ophthalmol Vis Sci* 49: 2163-2171, 2008.
- (8) **Chen YT, Chang FC, Wu CF, Chou YH, Hsu HL, Chiang WC, et al.** Platelet-derived growth factor receptor signaling activates pericyte-myofibroblast transition in obstructive and post-ischemic kidney fibrosis. *Kidney Int* 80: 1170-1181, 2011.
- (9) **Contreras AG, Briscoe DM.** Every allograft needs a silver lining. *J Clin Invest* 117: 3645-3648, 2007.
- (10) **Duffield JS.** The elusive source of myofibroblasts: problem solved? *Nat Med* 18: 1178-1180, 2012.
- (11) **Duffield JS, Humphreys BD.** Origin of new cells in the adult kidney: results from genetic labeling techniques. *Kidney Int* 79: 494-501, 2011.
- (12) **Dulauroy S, Di Carlo SE, Langa F, Eberl G, Peduto L.** Lineage tracing and genetic ablation of ADAM12(+) perivascular cells identify a major source of profibrotic cells during acute tissue injury. *Nat Med* 2012.
- (13) **Farris AB, Colvin RB.** Renal interstitial fibrosis: mechanisms and evaluation. *Curr Opin Nephrol Hypertens* 21: 289-300, 2012.
- (14) **Feng Y, vom HF, Pfister F, Djokic S, Hoffmann S, Back W, et al.** Impaired pericyte recruitment and abnormal retinal angiogenesis as a result of angiotensin-2 overexpression. *Thromb Haemost* 97: 99-108, 2007.
- (15) **Hammes HP, Lin J, Renner O, Shani M, Lundqvist A, Betsholtz C, et al.** Pericytes and the pathogenesis of diabetic retinopathy. *Diabetes* 51: 3107-3112, 2002.
- (16) **Hattori R, Ono Y, Kato M, Komatsu T, Matsukawa Y, Yamamoto T.** Direct visualization of cortical peritubular capillary of transplanted human kidney with reperfusion injury using a magnifying endoscopy. *Transplantation* 79: 1190-1194, 2005.
- (17) **Horbelt M, Lee SY, Mang HE, Knipe NL, Sado Y, Kribben A, et al.** Acute and chronic microvascular alterations in a mouse model of ischemic acute kidney injury. *Am J Physiol Renal Physiol* 293: F688-F695, 2007.
- (18) **Humphreys BD, Lin SL, Kobayashi A, Hudson TE, Nowlin BT, Bonventre JV, et al.** Fate tracing reveals the pericyte and not epithelial origin of myofibroblasts in kidney fibrosis. *Am J Pathol* 176: 85-97, 2010.

- (19) **Jung YJ, Kim DH, Lee AS, Lee S, Kang KP, Lee SY, et al.** Peritubular capillary preservation with COMP-angiopoietin-1 decreases ischemia-reperfusion-induced acute kidney injury. *Am J Physiol Renal Physiol* 297: F952-F960, 2009.
- (20) **Kida Y, Duffield JS.** Pivotal role of pericytes in kidney fibrosis. *Clin Exp Pharmacol Physiol* 38: 417-423, 2011.
- (21) **Kwon O, Hong SM, Sutton TA, Temm CJ.** Preservation of peritubular capillary endothelial integrity and increasing pericytes may be critical to recovery from postischemic acute kidney injury. *Am J Physiol Renal Physiol* 295: F351-F359, 2008.
- (22) **Lin SL, Chang FC, Schrimpf C, Chen YT, Wu CF, Wu VC, et al.** Targeting endothelium-pericyte cross talk by inhibiting VEGF receptor signaling attenuates kidney microvascular rarefaction and fibrosis. *Am J Pathol* 178: 911-923, 2011.
- (23) **Lin SL, Kisseleva T, Brenner DA, Duffield JS.** Pericytes and perivascular fibroblasts are the primary source of collagen-producing cells in obstructive fibrosis of the kidney. *Am J Pathol* 173: 1617-1627, 2008.
- (24) **Long DA, Norman JT, Fine LG.** Restoring the renal microvasculature to treat chronic kidney disease. *Nat Rev Nephrol* 8: 244-250, 2012.
- (25) **Molitoris BA, Sutton TA.** Endothelial injury and dysfunction: role in the extension phase of acute renal failure. *Kidney Int* 66: 496-499, 2004.
- (26) **Reinders ME, Rabelink TJ, Briscoe DM.** Angiogenesis and endothelial cell repair in renal disease and allograft rejection. *J Am Soc Nephrol* 17: 932-942, 2006.
- (27) **Roos-van Groningen MC, Scholten EM, Lelieveld PM, Rowshani AT, Baelde HJ, Bajema IM, et al.** Molecular comparison of calcineurin inhibitor-induced fibrogenic responses in protocol renal transplant biopsies. *J Am Soc Nephrol* 17: 881-888, 2006.
- (28) **Sandhu R, Teichert-Kuliszewska K, Nag S, Proteau G, Robb MJ, Campbell AI, et al.** Reciprocal regulation of angiopoietin-1 and angiopoietin-2 following myocardial infarction in the rat. *Cardiovasc Res* 64: 115-124, 2004.
- (29) **Schmitz V, Schaser KD, Olschewski P, Neuhaus P, Puhl G.** In vivo visualization of early microcirculatory changes following ischemia/reperfusion injury in human kidney transplantation. *Eur Surg Res* 40: 19-25, 2008.
- (30) **Schrimpf C, Xin C, Campanholle G, Gill SE, Stallcup W, Lin SL, et al.** Pericyte TIMP3 and ADAMTS1 Modulate Vascular Stability after Kidney Injury. *J Am Soc Nephrol* 23: 868-883, 2012.
- (31) **Strutz F, Zeisberg M.** Renal fibroblasts and myofibroblasts in chronic kidney disease. *J Am Soc Nephrol* 17: 2992-2998, 2006.
- (32) **Sutton TA, Mang HE, Campos SB, Sandoval RM, Yoder MC, Molitoris BA.** Injury of the renal microvascular endothelium alters barrier function after ischemia. *Am J Physiol Renal Physiol* 285: F191-F198, 2003.
- (33) **Toffalini F, Hellberg C, Demoulin JB.** Critical role of the platelet-derived growth factor receptor (PDGFR) beta transmembrane domain in the TEL-PDGFRbeta cytosolic oncoprotein. *J Biol Chem* 285: 12268-12278, 2010.
- (34) **van der Pol P, Schlagwein N, van Gijlswijk DJ, Berger SP, Roos A, Bajema IM, et al.** Mannan-binding lectin mediates renal ischemia/reperfusion injury independent of complement activation. *Am J Transplant* 12: 877-887, 2012.
- (35) **Woolf AS, Gnudi L, Long DA.** Roles of angiopoietins in kidney development and disease. *J Am Soc Nephrol* 20: 239-244, 2009.
- (36) **Yamamoto T, Tada T, Brodsky SV, Tanaka H, Noiri E, Kajijiya F, et al.** Intravital videomicroscopy of peritubular capillaries in renal ischemia. *Am J Physiol Renal Physiol* 282: F1150-F1155, 2002.

Chapter 3

Renal ischemia/reperfusion induces release of angiotensin-2 from human grafts of living and deceased donors

Dorottya K. de Vries, Meriem Khairoun, Jan H.N. Lindeman, Ingeborg M. Bajema,
Emile de Heer, Mark Roest, Anton J. van Zonneveld, Cees van Kooten, Ton J. Rabelink,
Alexander F. Schaapherder, Marlies E.J. Reinders

Transplantation. 96; 282-289, 2013

Abstract

Background: Recent insights suggest that endothelial cell (EC) activation plays a major role in renal ischemia/reperfusion (I/R) injury. Interactions between ECs and pericytes via signaling molecules, including angiopoietins, are involved in maintenance of the vascular integrity. Experimental data have shown that enhancement of Angiopoietin (Ang)-1 signaling might be beneficial in renal I/R injury. However, little is known about the role of angiopoietins in human renal I/R injury.

Methods: In this study, EC activation and changes in angiopoietins are assessed in human living and deceased donor kidney transplantation. Local release of angiopoietins was measured by unique, dynamic arteriovenous measurements over the reperfused kidney.

Results: Renal I/R is associated with acute EC activation shown by a vast Ang-2 release from both living and deceased donors shortly after reperfusion. Its counterpart Ang-1 was not released. Histological analysis of kidney biopsies showed EC loss after reperfusion. Baseline protein and mRNA Ang-1 expression was significantly reduced in deceased compared to living donors and declined further after reperfusion.

Conclusions: Human renal I/R injury induces EC activation after reperfusion reflected by Ang-2 release from the kidney. Interventions aimed at maintenance of vascular integrity by modulating angiopoietin signaling may be promising in human clinical kidney transplantation.

Introduction

Ischemia reperfusion (I/R) injury is an inevitable consequence of organ transplantation and a major determinant of patient and graft survival (1,2). The pathophysiology of renal I/R injury is complex and incompletely understood. Although the role of tubular cell injury in post-transplantation graft dysfunction is widely acknowledged, microvascular endothelial cell (EC) damage is considered increasingly important (3). ECs line the lumen of all blood vessels within the kidney graft and in this unique position they form the interface between the recipient blood and the allograft tissue. ECs are very susceptible to damage, including I/R injury (4). The repetitive insults during transplantation may induce loss of the microvasculature, on the long term resulting in impaired delivery of oxygen and nutrients to renal tubular epithelial cells, chronic ischemia and cell death (4-8).

The molecular mechanisms that lead to microvascular graft injury are largely unknown. Endothelial homeostasis is regulated by the angiotensin system and pericytes (9). Pericytes are the basic supportive cells of the endothelium, connected to the vessel's basement membrane (10). Angiotensin-1 (Ang-1) and -2 (Ang-2) are both ligands for the Tie2 receptor, but have opposite effects. Ang-1 is produced by pericytes and is responsible for suppressing vascular leakage, maintaining EC survival and inhibiting vascular inflammation. Ang-2 acts as an antagonist of Ang-1 and thereby destabilizes quiescent endothelium (11-14). Ang-2 promotes pericyte loss, leading to loosening contacts between ECs and pericytes, subsequent vessel destabilization and abnormal microvascular remodeling (15-18). ECs store Ang-2 in Weibel-Palade bodies from where it can be released quickly following stimulation, and Ang-2 expression can be upregulated manifold following endothelial activation (19). A few experimental studies have focused on the functional role of angiotensins in endothelial damage in the kidney. The relation between a disbalance in angiotensins and EC loss was demonstrated in a mouse model of anti-glomerular basement membrane glomerulonephritis, where glomerular capillary loss was associated with reduced Ang-1 and increased Ang-2 expression (20). Similarly, Ang-1 expression decreased after renal I/R injury in mice (21). Moreover, Ang-1 overexpression even significantly improved renal function and renal tissue blood flow after renal I/R in mice and decreases inflammatory cells and renal interstitial fibrosis (22).

Although these experimental data suggest a functional role of angiotensins in renal I/R injury, their involvement in human renal I/R injury had not been investigated yet. In addition, their involvement in living and deceased donor kidney transplantation had not been compared. In our recent studies on renal I/R, we exploited selective arteriovenous measurements over the kidney as a reliable method to study inflammatory processes after reperfusion (23,24). In this study, local renal angiotensin expression and release during renal I/R is systematically assessed in human living and deceased donor kidney transplantation.

Results

Integrity of the renal microvasculature is disturbed after reperfusion

To assess endothelial structure and viability, staining for ECs was quantified in both living and deceased donor kidney tissue. Both CD34 and vWf staining showed a characteristic positive pattern of peritubular and glomerular ECs. Pre-reperfusion biopsies did not show a difference between living and deceased donor kidneys in either CD34 ($p=0.76$) or vWf ($p=0.07$; Figure 1). Next, pre- and post-reperfusion biopsies of LD kidneys were compared. There was a trend towards a decrease in CD34 positive cells after reperfusion ($p=0.08$, data not shown), whereas vWf staining of ECs showed a significant decrease in expression after reperfusion ($p<0.001$; Figure 1).

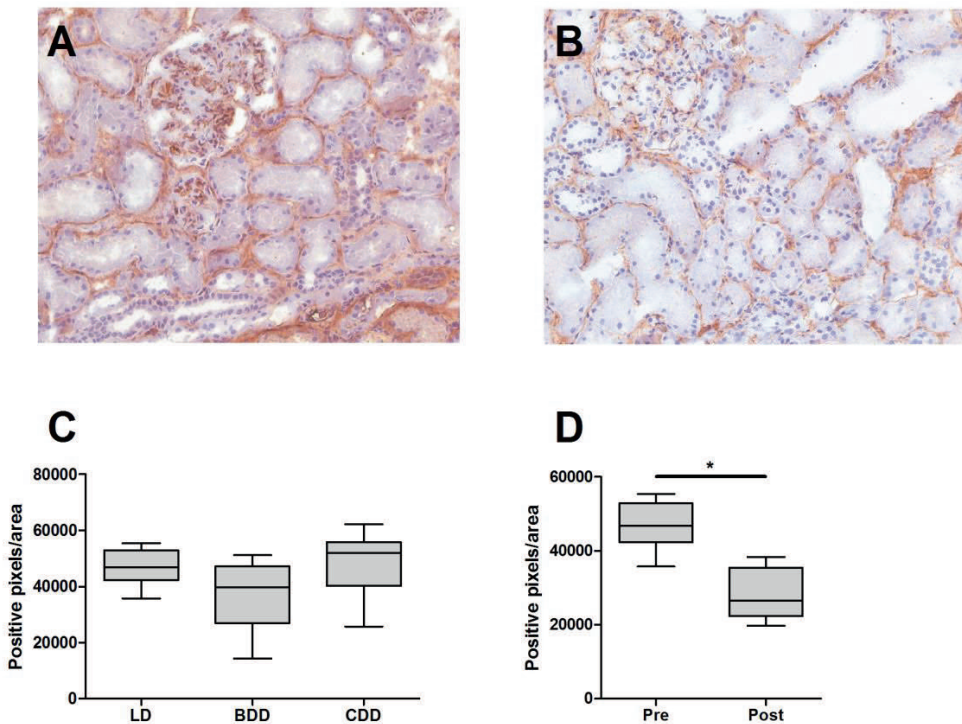


Figure 1: vWf staining decreased after reperfusion. Staining for vWf showed a characteristic positive endothelial pattern. Typical example of vWf staining in **A** a pre-reperfusion biopsy, **B** a post-reperfusion biopsy of a LD kidney. **C** Quantification of vWf staining showed no differences in intensity between groups before transplantation ($p=0.07$). **D** After reperfusion, vWf signal showed a vast decrease ($p<0.005$) in LD kidneys. The boxes run from the lower to upper quartile, the whiskers indicate the 5 to 95 percentile, while the horizontal line is set at the median.

Ang-2 is released from the reperfused kidney

Arteriovenous differences for Ang-1 and Ang-2 were assessed over the kidney during reperfusion. Ang-1 levels did not change significantly over the reperfused kidney in LD, BDD and CDD kidney transplantation, making it unlikely that anti-inflammatory Ang-1 is released from the kidney after reperfusion (Figure 2A-C). In contrast Ang-2, a marker for endothelial activation, was released from the kidney both early and late after reperfusion (Figure 2D-F). Ang-2 release was statistically significant in LD kidneys early after reperfusion (3 min., $p=0.005$; 30 min. $p=0.064$), in BDD kidneys only late after reperfusion (3 min. $p=0.15$; 30 min., $p=0.036$) and in CDD kidneys both early and late after reperfusion (3 min., $p<0.001$; 30 min., $p=0.017$). In the total group of deceased donor kidney transplantations, both early and late Ang-2 release was statistically significant (3 min., $p=0.024$; 30 min., $p=0.001$). The Ang-1/Ang-2 ratio was consistently higher in the arterial compared to renal venous samples at both time points for all donor types, although this trend was statistically not significant (data not shown). There was no early or late release of vWf or its more dynamic propeptide (Supplemental figure 1).

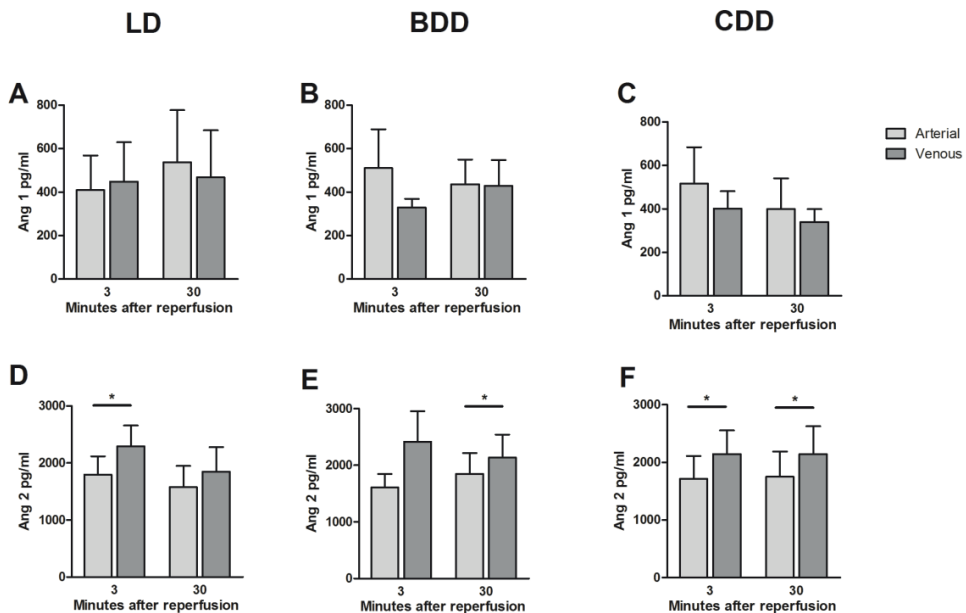


Figure 2: Ang-2 is released from the kidney during reperfusion. Ang-1 was not released from the kidney either 3 or 30 minutes after reperfusion in **A** LD (3 min. $p=0.18$; 30 min. $p=0.59$); **B** BDD (3 min. $p=0.29$, 30 min. $p=1.0$); **C** CDD (3 min. $p=0.47$; 30 min. $p=1.0$). Ang-2 was significantly released from the kidney in **D** LD kidneys early after reperfusion (3 min. $p=0.005$; 30 min. $p=0.064$), **E** in BDD kidneys only later after reperfusion (3 min. $p=0.15$; 30 min. $p=0.036$) and **F** in CDD kidneys both early and late after reperfusion (3 min. $p<0.001$; 30 min. $p=0.017$). $N=6$ in each group. Bars represent mean and error bars represent SEM.

Ang-1 protein and mRNA expression are significantly higher in LD kidneys and are reduced after reperfusion

Protein and mRNA expression of angiopoietins was assessed in the three donor groups. Ang-1 protein was expressed in glomeruli and capillary walls (Figure 3A, B). The protein expression was already reduced before transplantation in CDD kidneys ($p=0.003$), not BDD kidneys ($p=0.17$) compared to LD kidneys (Figure 3C, D). Consistently, Ang-1 mRNA expression before transplantation was significantly higher in LD kidneys compared to CDD kidneys ($p=0.006$) (Figure 3E). In LD kidney biopsies collected before and 45 minutes after reperfusion, there was a significant reduction in both Ang-1 mRNA ($p=0.007$) and protein expression after reperfusion ($p=0.001$; Figure 3D, F).

Ang-2 protein and RNA expression levels are similar between LD and deceased donors

Ang-2 immunostaining of kidney sections revealed expression in interstitial vessels and negative staining in the glomeruli (Figure 4A, B). There were no differences in Ang-2 protein and mRNA expression between LD, BDD and CDD kidneys ($p=0.69$, $p=0.73$, respectively; Figure 4C, E). Quantification of Ang-2 staining showed a decrease of protein expression after reperfusion in LD kidneys ($p=0.006$, Figure 4D). However, mRNA expression of Ang-2 did not change after reperfusion in LD kidney transplantation ($p=0.72$, Figure 4F). The mRNA expression of the angiopoietin receptor Tie-2 was similar between the different donor types ($p=0.48$) and not upregulated after reperfusion in LD grafts ($p=0.32$) (data not shown).

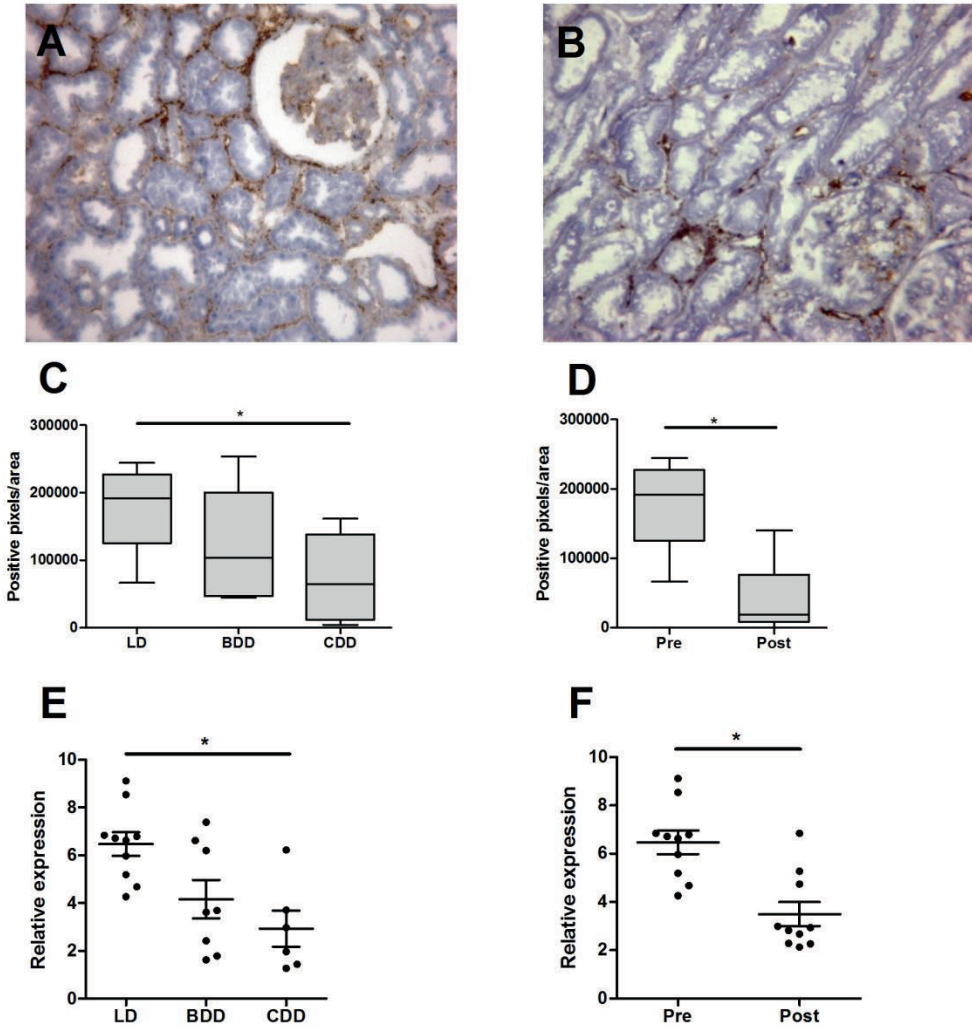


Figure 3: Ang-1 protein and mRNA expression decreased after reperfusion. Ang-1 staining was positive in glomeruli and peritubular capillaries. Typical example of Ang-1 staining in **A** a pre-reperfusion biopsy and **B** a post reperfusion biopsy of a LD kidney. **C** Quantification of Ang-1 in pre-transplantation kidney biopsies showed a significantly decrease in CDD ($p=0.003$) compared to LD grafts. **D** Ang-1 in LD kidney biopsies taken before (pre) and after (post) reperfusion showed a significant decrease in Ang-1 protein expression ($p=0.001$). The boxes run from the lower to upper quartile, the whiskers indicate the 5 to 95 percentile, while the horizontal line is set at the median. In kidney biopsies mRNA expression of Ang-1 was assessed. **E** pre-transplantation Ang-1 mRNA expression was significantly reduced in CDD kidneys compared to LD kidneys ($p=0.006$). **F** when comparing biopsies collected before (pre) and after (post) reperfusion, in LD kidneys there was a significant reduction in Ang-1 mRNA expression after reperfusion ($p=0.007$).

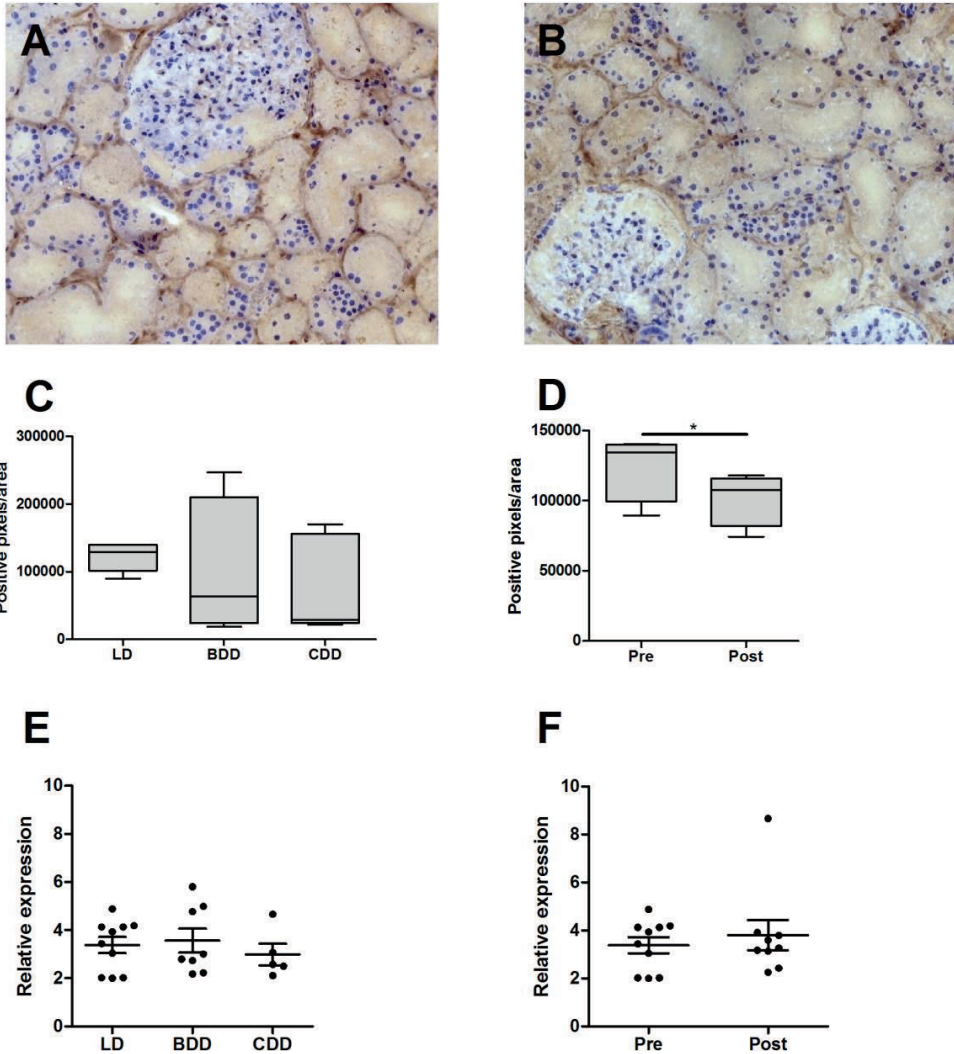


Figure 4: Ang-2 protein and mRNA levels are similar between living and deceased donors.

Ang-2 staining was positive in interstitial vessels and peritubular capillaries. Typical example of Ang-2 staining in **A** a pre-reperfusion biopsy and **B** a post-reperfusion biopsy of a LD kidney. **C** There were no differences in Ang-2 protein expression between groups before transplantation ($p=0.69$). **D** After reperfusion, there was a decrease in Ang-2 protein expression ($p=0.006$), consistent with degranulation of ECs and loss of Ang-2. The boxes run from the lower to upper quartile, the whiskers indicate the 5 to 95 percentile, while the horizontal line is set at the median. mRNA expression of Ang-2 was assessed in kidney biopsies. **E** Ang-2 expression was similar before reperfusion in all groups ($p=0.73$). **F** In LD kidney biopsies collected before (pre) and after (post) reperfusion, Ang-2 expression did not change ($p=0.721$).

Discussion

Previous studies, primarily exploiting animal models, have revealed that EC activation plays a major role in I/R injury and that the angiopoietin balance may be critical in maintaining vascular integrity. Enhancement of Ang-1 signaling has been demonstrated to be beneficial in renal I/R injury (25). However, thus far, no study has reported on the role of angiopoietins in human renal I/R injury or local release of angiopoietins from the kidney. In this study, the local response of the reperfused kidney was assessed by arteriovenous concentration differences of angiopoietins during the first 30 minutes after reperfusion in living and deceased donor kidney transplantation. Results demonstrate that renal I/R is associated with acute EC activation shown by a vast Ang-2 release from both living and deceased donor kidneys shortly after reperfusion.

In the present study, a reduction in CD34 and vWf protein expression was observed in tissue biopsies after reperfusion, consistent with either EC death or endothelial injury that induces loss of their characteristic epitopes. These findings are consistent with experimental models of acute ischemic renal endothelial injury after reperfusion (7,26,27), and recently observed in humans as well (28-31). EC activation represents a switch from a quiescent phenotype toward one that is involved in the host defense response. This process will result in expression of chemokines, cytokines, angiogenic factors and adhesion molecules designed to interact with leukocytes and platelets and target inflammation. In our previous study in human living donor kidney transplantation no evidence for EC activation was found by absence of local release of ICAM-1, P-selectin and vWf (23). However, the angiopoietins and endothelial/pericyte interactions were not studied.

Angiopoietins have been shown to play a critical role in the maintenance of the microvasculature (15). This study focused on the release of these factors from both living and deceased donor kidneys. Results show that Ang-1 was not released from the kidney during reperfusion in any of the three groups, consistent with the theory that Ang-1 is constitutively expressed and dynamic changes in Tie-2 signaling are mediated via Ang-2. Consistent with previous reports, Ang-1 protein was found in glomeruli and capillary walls (32). Interestingly, we show that Ang-1 mRNA and protein expression decreased after reperfusion in human renal I/R injury. In contrast, in rodents Ang-1 expression has been shown to increase after chemical or ischemic kidney injury (33,34). However, these observations in experimental animals were done days after the injury, in contrast to the immediate changes observed in our patients. The loss of Ang-1 signal may indicate loss of vital pericytes, since pericytes are the main Ang-1 producing cells. However, decreased Ang-1 protein in renal tissue may also be related to the decrease in Ang-2 signal. Since Ang-1 and Ang-2 share a 60% amino acid identity, the storage

and release of Ang-1 may have the same mechanism as that of Ang-2 (35). Loss of Ang-1 signaling appears important in many disease processes, and enhancement of Ang-1 signaling was beneficial in sepsis and renal I/R injury (25,36).

High Ang-2 levels have repeatedly been shown in pathological conditions, such as in diabetes mellitus, renal failure and in myocardial I/R injury (37-39). Ang-2 triggers an inflammatory response by inducing permeability of the vascular lining (40), possibly mediated by the Ang-2 induced loss of pericytes (41). Results of this study show a vast Ang-2 release from both living and deceased donor kidneys shortly after reperfusion. This indicates injury to ECs, which can release Ang-2 from Weibel-Palade bodies upon activation (42). Since expression of Ang-2 did not change upon reperfusion, the arteriovenous difference may reflect Ang-2 release from Weibel-Palade bodies upon stress. This was confirmed by decreased endothelial Ang-2 tissue biopsy staining after reperfusion, consistent with exocytosis of Ang-2 containing granulae. In contrast to Ang-1, there was no expression of Ang-2 in the glomeruli, and positive signal was mainly seen on peritubular capillaries (32). The Ang-2 release from the kidney may induce continuing endothelial damage, ultimately leading to pericyte dropout, loosening contacts between endothelial and perivascular cells, with subsequent vessel destabilization and fibrosis.

In our arteriovenous measurements directly over the reperfused graft no release of vWf itself or its propeptide was observed, while Ang-2, another constituent of Weibel-Palade bodies was released. Possible explanations include that Ang-2 may be more easily detectable by arteriovenous measurements due to a shorter half-life, or that Ang-2 release from Weibel-Palade bodies is regulated independent from vWf release (43). Moreover, when vWf multimers are secreted from stimulated ECs they may remain anchored to the endothelial surface (44). This early retention of vWf to endothelium may provide a further explanation for the lack of a detectable release of vWf into the renal vein.

A limitation of our study was the fact that sampling time was restricted to maximally 45 minutes following reperfusion. Although endothelial damage is considered to be initiated during cold ischemia and expected to be vast around reperfusion, we cannot exclude continuing damage after 45 minutes. Another limitation is that we had to include different patient cohorts for arteriovenous measurements and collection of biopsies. Since for ethical reasons from every patient only one biopsy could be obtained, either DNA isolation or immunohistochemistry was done. Although one cohort for all sampling may have been preferable, our sampling is not expected to have influenced the conclusions from this study, since no correlations with patient characteristics are made. The aim of this study was to explore the endothelium-pericyte interactions in the pathophysiology of renal I/R injury. In future studies correlations between patient characteristics and angiotensin release will be made.

In conclusion, human renal I/R injury induces EC activation after reperfusion which leads to Ang-2 release from the kidney in both living and deceased donor kidney transplantation. This is accompanied by loss of ECs and diminished Ang-1 protein and mRNA expression. Moreover, compared to living donors expression of Ang-1 was significantly reduced in deceased donors. Interventions aimed at maintenance of vascular integrity by modulation of angiopoietin signaling may provide new therapeutical insights for I/R injury in human clinical kidney transplantation.

Materials and methods

Patient population

Eighteen patients undergoing renal allograft transplantation were included for arteriovenous sampling, 6 living donor (LD), 6 brain dead donor (BDD), and 6 cardiac dead donor (CDD) kidney recipients. BDD and CDD together are referred to as deceased donors (DD). Twenty-three other patients receiving a kidney from a LD (n=10), a BDD (n=7) or a CDD (n=6) were included for mRNA isolation from renal biopsies. Immunohistochemical analyses were performed on biopsies of 10 LD, BDD and CDD kidney graft recipients. Patient characteristics are shown in Supplemental Table 1. All kidneys were still functioning at 1 year after transplantation, except for one patient in the arteriovenous sampling cohort who received a kidney from a CDD (the recipient was not compliant with immunosuppressive medication) and one patient in the PCR cohort, that received a BDD kidney transplant and died 6 months after transplantation (because of veno-occlusive disease ultimately causing hepatic failure). For technical reasons (renal vein sampling) only patients receiving a left kidney were included in the arteriovenous group. The reason for including different cohorts was to minimize patient burden by collecting one type of material per patient, i.e. either blood or a single renal biopsy. The study protocol was approved by the local ethics committee, and informed consent was obtained from each patient.

Operation and materials

Kidney transplantations were performed according to local standardized protocol. In LD minimally invasive nephrectomy was performed. For cold perfusion and storage of the kidney, Custodiol® Histidine–tryptophan–ketoglutarate solution (HTK) solution (Tramedico, Weesp, The Netherlands) was used. DD kidneys were perfused and stored with University of Wisconsin solution (UW) or HTK. The immunosuppressive regimen was based on induction therapy with an interleukin-2 receptor blocker (basiliximab, day 0 and day 4) and maintenance treatment with tacrolimus or cyclosporine A, in addition to mycophenolate mofetil and steroids in all groups.

Arterial and renal venous blood samples were obtained as described before in detail (23). In short, via a small catheter placed in the renal vein, blood aliquots were sampled at 3, and 30 minutes after reperfusion. Paired arterial blood samples were obtained simultaneously. All samples were collected in tubes containing EDTA and immediately placed on ice. Blood samples were centrifuged (1,550 g, 20 min, 4°C) and the derived plasma was subsequently centrifuged to deplete it from leukocytes and platelets (1,550 g, 20 min, 4°C). Plasma was aliquotted and stored at -70°C until assayed.

Immunohistochemical analysis

A renal cortical biopsy was obtained after cold storage from LD, BDD and CDD kidney graft recipients. For logistical reasons, only in the LD group a second biopsy 45 minutes after reperfusion was collected as well. Immunohistochemical analyses were performed on 4 µm cryostat kidney tissue sections fixed in acetone. Slides were washed and incubated with peroxidase blocking solution and blocked with PBS containing 5% normal human serum (NHS) and 1% BSA. Then slides were incubated with the following primary antibodies: Ang-1 mouse monoclonal IgG, 1:800 (R&D systems), Ang-2 mouse monoclonal IgG, 1:100 (Novus Biologicals), ECs (CD34) mouse polyclonal IgG, 1:3200 (Dako), vWf, rabbit polyclonal, 1:2500 (Dako). Next, the following peroxidase-conjugated secondary antibodies were applied: goat anti-rabbit IgG, 1:200 (Dako); goat anti-mouse IgG, 1:200 (Dako); or rabbit anti-goat IgG, 1:200 (Dako), followed by sequential fluorescein isothiocyanate (FITC, amplification reagent) and anti-fluorescein-HRP. Staining was completed by incubation with 3,3' diaminobenzidine tetrahydrochloride (DAB)/ hydrogen peroxide and counterstained with Mayer's Hematoxylin Solution (Merck, Darmstadt, Germany). At 100 × magnification, 10 microscopic fields of each kidney section were quantified using computerized image analysis (ImageJ).

Plasma measurements of endothelial cell activation

Activation of the endothelium was assessed by measuring the local release of endothelial activation markers from the kidney. Release of Ang-1 and Ang-2 from the kidney was assessed by ELISA (R&D Systems, Minneapolis, MN, USA) according to the manufacturer's protocol. The paired arteriovenous samples were also analyzed on more classical markers of endothelial activation; von Willebrand factor (vWf) and vWf propeptide. The propeptide has a shorter circulating half-time (2–3 h), compared with vWf itself (>12 h), and may therefore be a more sensitive marker of acute endothelial activation. Plasma levels of vWf and vWf propeptide were determined using a semi-automated ELISA. Plates were coated overnight with coating buffer, consisting of sodium carbonate, sodium bicarbonate and NaN₃. Commercial antibody duo sets, optimized for ELISA, were used (rabbit anti-human vWf and peroxidase-conjugated rabbit anti-human vWf, A00082 and P0226, Dako, Glostrup, Denmark). vWf propeptide, rabbit-anti-propeptide, and rabbit-anti-propeptide-biotine were used for the analysis of vWf propeptide as described previously (45).

mRNA expression in human kidney biopsies

A renal cortical biopsy was obtained after cold storage from LD, BDD and CDD kidneys, and a second biopsy was collected 45 minutes after reperfusion from LD kidneys. Biopsies were immediately snap frozen in liquid nitrogen and stored at -70°C. Total RNA was extracted from renal tissues using RNazol (Campro Scientific, Veenendaal, The Netherlands) and glass beads (46). The integrity of each RNA sample was examined by Agilent Lab-on-a-chip technology using the RNA 6000 Nano LabChip kit and a bioanalyzer 2100 (Agilent Technologies, Amstelveen, The Netherlands). RNA preparations were considered suitable for further processing if samples showed intact 18S and 28S rRNA bands, and displayed no chromosomal peaks or RNA degradation products (RNA Integrity Number >8.0) (47). cDNA was synthesized from 1 µg total RNA, using an oligo dT primer, RNase-OUT, M-MLV reverse transcriptase, 0.1 M-DTT and buffers in a volume of 20 µL (all purchased from Invitrogen, Breda, The Netherlands). Quantitative real-time PCR was performed in duplicate by using iQ SYBR Green Supermix on iCycler Real-Time Detection System (BioRad). The amplification reaction volume was 20 µL, consisting of 10 µL iQ SYBR Green PCR mastermix, 1 µL primers, 1 µL cDNA, and 8 µL water. Data were analyzed using Gene Expression Analysis for iCycler Real-Time PCR Detection System (BioRad). Expression of each gene was normalized against mRNA expression of the housekeeping gene GAPDH. The primer sequences are shown in Supplemental Table 2.

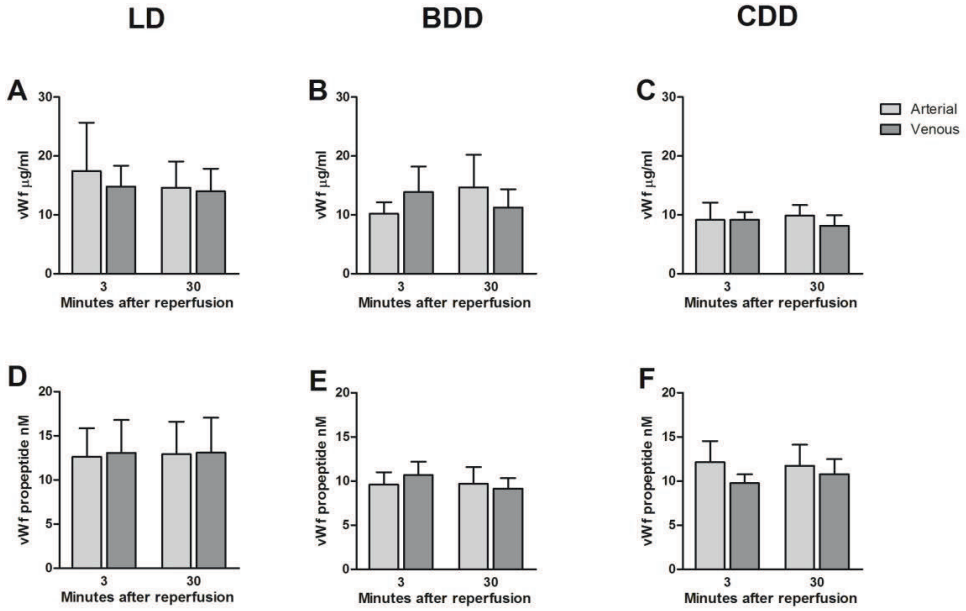
Analysis

Clinical donor data were retrieved from Eurotransplant Foundation (Leiden, The Netherlands). Delayed graft function (DGF) was defined as the need for dialysis within one week after transplantation. Acute rejection was defined as biopsy proven rejection within 60 days after transplantation. Statistical analysis was performed using SPSS 17.0 statistical analysis software (SPSS Inc, Chicago, Ill). Paired, non-parametric test (Wilcoxon) was applied to assess differences between arterial and venous concentration, and between pre- and post-reperfusion samples. Graph error bars represent the standard error of the mean (SEM), unless otherwise stated. A *P*-value of less than 0.05 was considered significant.

Acknowledgements

We thank The Netherlands Organization for Health Research and Development for the financial support: project AGIKO 92003525 (D.K. de Vries) and Veni grant (M.E.J. Reinders). Ellen Lievers is thanked for technical assistance.

Supplemental material



Supplemental figure 1: No vWf or vWf propeptide release from the reperfused kidney. vWf was not released from the reperfused graft both early (3 min.) and later (30 min.) after reperfusion in kidney transplantation with **A** LD ($p=0.89$, $p=0.78$), **B** BDD ($p=0.89$, $p=0.33$) and **C** CDD ($p=0.40$, $p=0.18$) respectively. The shorter lived and more dynamic vWf propeptide, was not released either from the kidney in **D** LD ($p=0.78$, $p=0.62$), **E** BDD ($p=0.19$, $p=0.89$) and **F** CDD ($p=0.35$, $p=0.74$) kidney transplantation. Bars represent mean and error bars represent SEM.

Supplemental table 1: Transplantation and outcome characteristics of the three different patient cohorts that were included. In each cohort material was collected from living donor (LD), brain dead donor (BDD) and cardiac dead donor (CDD) grafts during kidney transplantation.

	AV			IHC			PCR		
	LD	BDD	CDD	LD	BDD	CDD	LD	BDD	CDD
N	6	6	6	10	10	10	10	7	6
Donor age: mean (SD)	42(11)	51(21)	52(16)	57(10)	48(16)	41(10)	52(8)	45(21)	41(13)
Donor gender (M:F)	5:1	2:4	3:3	5:5	5:5	6:4	2:8	3:4	4:2
WIT1 in min. (SD)	N/A	N/A	23(8)	N/A	N/A	18(5)	N/A	N/A	18(6)
CIT in h. (SD)	2.9(0.3)	21.3(7.1)	17.1(2.9)	2.8(0.5)	18.6(9.6)	17.8(3.4)	3.0(0.4)	17.4(7.6)	15.6(3.9)
WIT2 in min. (SD)	33(7)	31(6)	34(7)	29(8)	28(4)	28(8)	29(7)	34(3)	28(5)
Recipient age: mean (SD)	41(11)	57(13)	52(10)	54(16)	51(13)	45(15)	49(16)	53(14)	54(9)
Recipient gender (M:F)	3:3	2:4	5:1	4:6	7:3	7:3	6:4	4:3	3:3
Creatinine clearance day 30 (ml/min)	73(19)	64(13)	35(12)	45(11)	63(30)	48(21)	56(17)	47(14)	50(8)
DGF	0/6	3/6	5/6	0/10	3/10	7/10	0/10	3/7	4/6
DGF: dialysis after transplantation in days (SD)	0	5(6)	13(10)	0	5(2)	13(6)	0	3(4)	7(6)
Acute rejection n (%)	1(17%)	0(0%)	1(17%)	0(0%)	2(20%)	1(10%)	1(10%)	0(0%)	0(0%)

AV: cohort of patients included for arteriovenous sampling over the kidney; IHC: cohort of patients in which renal biopsies were used for immunohistochemical analysis; PCR: cohort of patients from which renal biopsies were used for PCR analysis; WIT1: first warm ischemia time; CIT: cold ischemia time; WIT2: second warm ischemia time; DGF: delayed graft function.

Supplemental table 2: Primer sequences used for quantitative real-time polymerase chain reaction.

Gene	Forward primer 5'->3'	Reverse primer 5'->3'	Supplier
GAPDH	TTCCAGGAGCGAGATCCCT	CACCCATGACGAACATGGG	Biolegio
Ang-1	GCAACTGGAGCTGATGGACACA	CATCTGCACAGTCTCTAAATGGT	Biolegio
Ang-2	TGGGATTTGGTAACCCTTCA	GTAAGCCTCATTCCCTTCCC	Biolegio
Tie-2	GTATGGA CTCTTAGCCGGCTT	TTCGCCCATCTCTGGTCAC	Biolegio

References

1. Dragun D, Hoff U, Park JK et al. Ischemia-reperfusion injury in renal transplantation is independent of the immunologic background. *Kidney Int* 2000;58: 2166-2177.
2. Ojo AO, Wolfe RA, Held PJ, Port FK, Schmouder RL. Delayed graft function: risk factors and implications for renal allograft survival. *Transplantation* 1997;63: 968-974.
3. Contreras AG, Briscoe DM. Every allograft needs a silver lining. *J Clin Invest* 2007;117: 3645-3648.
4. Reinders ME, Rabelink TJ, Briscoe DM. Angiogenesis and endothelial cell repair in renal disease and allograft rejection. *J Am Soc Nephrol* 2006;17: 932-942.
5. Basile DP, Donohoe D, Roethe K, Osborn JL. Renal ischemic injury results in permanent damage to peritubular capillaries and influences long-term function. *Am J Physiol Renal Physiol* 2001;281: F887-F899.
6. Basile DP, Friedrich JL, Spahic J et al. Impaired endothelial proliferation and mesenchymal transition contribute to vascular rarefaction following acute kidney injury. *Am J Physiol Renal Physiol* 2011;300: F721-F733.
7. Sutton TA, Mang HE, Campos SB, Sandoval RM, Yoder MC, Molitoris BA. Injury of the renal microvascular endothelium alters barrier function after ischemia. *Am J Physiol Renal Physiol* 2003;285: F191-F198.
8. Horbelt M, Lee SY, Mang HE et al. Acute and chronic microvascular alterations in a mouse model of ischemic acute kidney injury. *Am J Physiol Renal Physiol* 2007;293: F688-F695.
9. Fiedler U, Augustin HG. Angiopoietins: a link between angiogenesis and inflammation. *Trends Immunol* 2006;27: 552-558.
10. Smith SW, Chand S, Savage CO. Biology of the renal pericyte. *Nephrol Dial Transplant* 2012;27: 2149-2155.
11. Thurston G, Suri C, Smith K et al. Leakage-resistant blood vessels in mice transgenically overexpressing angiopoietin-1. *Science* 1999;286: 2511-2514.
12. Maisonpierre PC, Suri C, Jones PF et al. Angiopoietin-2, a natural antagonist for Tie2 that disrupts in vivo angiogenesis. *Science* 1997;277: 55-60.
13. Roviezzo F, Tsigkos S, Kotanidou A et al. Angiopoietin-2 causes inflammation in vivo by promoting vascular leakage. *J Pharmacol Exp Ther* 2005;314: 738-744.
14. Scharpfenecker M, Fiedler U, Reiss Y, Augustin HG. The Tie-2 ligand angiopoietin-2 destabilizes quiescent endothelium through an internal autocrine loop mechanism. *J Cell Sci* 2005;118: 771-780.
15. Woolf AS, Gnudi L, Long DA. Roles of angiopoietins in kidney development and disease. *J Am Soc Nephrol* 2009;20: 239-244.
16. Hammes HP, Lin J, Renner O et al. Pericytes and the pathogenesis of diabetic retinopathy. *Diabetes* 2002;51: 3107-3112.
17. Feng Y, vom HF, Pfister F et al. Impaired pericyte recruitment and abnormal retinal angiogenesis as a result of angiopoietin-2 overexpression. *Thromb Haemost* 2007;97: 99-108.
18. Cai J, Kehoe O, Smith GM, Hykin P, Boulton ME. The angiopoietin/Tie-2 system regulates pericyte survival and recruitment in diabetic retinopathy. *Invest Ophthalmol Vis Sci* 2008;49: 2163-2171.
19. Oh H, Takagi H, Suzuma K, Otani A, Matsumura M, Honda Y. Hypoxia and vascular endothelial growth factor selectively up-regulate angiopoietin-2 in bovine microvascular endothelial cells. *J Biol Chem* 1999;274: 15732-15739.

20. Yuan HT, Tipping PG, Li XZ, Long DA, Woolf AS. Angiotensin II correlates with glomerular capillary loss in anti-glomerular basement membrane glomerulonephritis. *Kidney Int* 2002;61: 2078-2089.
21. Tasanarong A, Khositseth S, Thitiarchakul S. The mechanism of increased vascular permeability in renal ischemic reperfusion injury: potential role of angiotensin-1 and hyaluronan. *J Med Assoc Thai* 2009;92: 1150-1158.
22. Jung YJ, Kim DH, Lee AS et al. Peritubular capillary preservation with COMP-angiotensin-1 decreases ischemia-reperfusion-induced acute kidney injury. *Am J Physiol Renal Physiol* 2009;297: F952-F960.
23. de Vries DK, Lindeman JH, Tsikas D et al. Early renal ischemia-reperfusion injury in humans is dominated by IL-6 release from the allograft. *Am J Transplant* 2009;9: 1574-1584.
24. de Vries DK, Lindeman JH, Ringers J, Reinders ME, Rabelink TJ, Schaapherder AF. Donor brain death predisposes human kidney grafts to a proinflammatory reaction after transplantation. *Am J Transplant* 2011;11: 1064-1070.
25. Jung YJ, Kim DH, Lee AS et al. Peritubular capillary preservation with COMP-angiotensin-1 decreases ischemia-reperfusion-induced acute kidney injury. *Am J Physiol Renal Physiol* 2009;297: F952-F960.
26. Yamamoto T, Tada T, Brodsky SV et al. Intravital videomicroscopy of peritubular capillaries in renal ischemia. *Am J Physiol Renal Physiol* 2002;282: F1150-F1155.
27. Brodsky SV, Yamamoto T, Tada T et al. Endothelial dysfunction in ischemic acute renal failure: rescue by transplanted endothelial cells. *Am J Physiol Renal Physiol* 2002;282: F1140-F1149.
28. Kwon O, Hong SM, Sutton TA, Temm CJ. Preservation of peritubular capillary endothelial integrity and increasing pericytes may be critical to recovery from postischemic acute kidney injury. *Am J Physiol Renal Physiol* 2008;295: F351-F359.
29. Hattori R, Ono Y, Kato M, Komatsu T, Matsukawa Y, Yamamoto T. Direct visualization of cortical peritubular capillary of transplanted human kidney with reperfusion injury using a magnifying endoscopy. *Transplantation* 2005;79: 1190-1194.
30. Schmitz V, Schaser KD, Olschewski P, Neuhaus P, Puhl G. In vivo visualization of early microcirculatory changes following ischemia/reperfusion injury in human kidney transplantation. *Eur Surg Res* 2008;40: 19-25.
31. Snoeijis MG, Vink H, Voesten N et al. Acute ischemic injury to the renal microvasculature in human kidney transplantation. *Am J Physiol Renal Physiol* 2010;299: F1134-F1140.
32. Satchell SC, Harper SJ, Tooke JE, Kerjaschki D, Saleem MA, Mathieson PW. Human podocytes express angiotensin 1, a potential regulator of glomerular vascular endothelial growth factor. *J Am Soc Nephrol* 2002;13: 544-550.
33. Horbelt M, Lee SY, Mang HE et al. Acute and chronic microvascular alterations in a mouse model of ischemic acute kidney injury. *Am J Physiol Renal Physiol* 2007;293: F688-F695.
34. Long DA, Woolf AS, Suda T, Yuan HT. Increased renal angiotensin-1 expression in folic acid-induced nephrotoxicity in mice. *J Am Soc Nephrol* 2001;12: 2721-2731.
35. Xu J, Lan D, Li T, Yang G, Liu L. Angiotensins regulate vascular reactivity after haemorrhagic shock in rats through the Tie2-nitric oxide pathway. *Cardiovasc Res* 2012;96: 308-319.
36. Witznitchler B, Westermann D, Kneuppel S, Schultheiss HP, Tschope C. Protective role of angiotensin-1 in endotoxic shock. *Circulation* 2005;111: 97-105.
37. Lee KW, Lip GY, Blann AD. Plasma angiotensin-1, angiotensin-2, angiotensin receptor tie-2, and vascular endothelial growth factor levels in acute coronary syndromes. *Circulation* 2004;110: 2355-2360.
38. David S, Kumpers P, Hellpap J et al. Angiotensin 2 and cardiovascular disease in dialysis and kidney transplantation. *Am J Kidney Dis* 2009;53: 770-778.

39. Lim HS, Lip GY, Blann AD. Angiopoietin-1 and angiopoietin-2 in diabetes mellitus: relationship to VEGF, glycaemic control, endothelial damage/dysfunction and atherosclerosis. *Atherosclerosis* 2005;180: 113-118.
40. Parikh SM, Mammoto T, Schultz A et al. Excess circulating angiopoietin-2 may contribute to pulmonary vascular leak in sepsis in humans. *PLoS Med* 2006;3: e46.
41. Hammes HP, Lin J, Wagner P et al. Angiopoietin-2 causes pericyte dropout in the normal retina: evidence for involvement in diabetic retinopathy. *Diabetes* 2004;53: 1104-1110.
42. Goligorsky MS, Patschan D, Kuo MC. Weibel-Palade bodies--sentinels of acute stress. *Nat Rev Nephrol* 2009;5: 423-426.
43. Babich V, Meli A, Knipe L et al. Selective release of molecules from Weibel-Palade bodies during a lingering kiss. *Blood* 2008;111: 5282-5290.
44. Dong JF, Moake JL, Nolasco L et al. ADAMTS-13 rapidly cleaves newly secreted ultralarge von Willebrand factor multimers on the endothelial surface under flowing conditions. *Blood* 2002;100: 4033-4039.
45. Borchiellini A, Fijnvandraat K, ten Cate JW et al. Quantitative analysis of von Willebrand factor propeptide release in vivo: effect of experimental endotoxemia and administration of 1-deamino-8-D-arginine vasopressin in humans. *Blood* 1996;88: 2951-2958.
46. Haslinger B, Kleemann R, Toet KH, Kooistra T. Simvastatin suppresses tissue factor expression and increases fibrinolytic activity in tumor necrosis factor-alpha-activated human peritoneal mesothelial cells. *Kidney Int* 2003;63: 2065-2074.
47. Kleemann R, Verschuren L, van Erk MJ et al. Atherosclerosis and liver inflammation induced by increased dietary cholesterol intake: a combined transcriptomics and metabolomics analysis. *Genome Biol* 2007;8: R200.

Chapter 4

Early systemic microvascular damage in pigs with atherogenic diabetes mellitus coincides with renal angiotensin dysbalance

Meriem Khairoun, Mieke van den Heuvel, Bernard M. van den Berg, Oana Sorop,
Rients de Boer, Nienke S. van Ditzhuijzen, Ingeborg M. Bajema, Dirk J. Duncker,
Ton J. Rabelink, Marlies E.J Reinders, Wim J van der Giessen, Joris I. Rotmans

Submitted

Abstract

Background: Diabetes mellitus (DM) is associated with a range of microvascular complications including diabetic nephropathy (DN). Microvascular abnormalities in the kidneys are common histopathologic findings in DN, which represent one manifestation of ongoing systemic microvascular damage. Recently, sidestream dark-field (SDF) imaging has emerged as a noninvasive tool that enables one to visualize the microcirculation. In this study, we investigated whether changes in the systemic microvasculature induced by DM and an atherogenic diet correlated spatiotemporally with renal damage.

Methods: Atherosclerotic lesion development was triggered in streptozotocin-induced DM pigs (140 mg/kg body weight) by administering an atherogenic diet for approximately 11 months. Fifteen months following induction of DM, microvascular morphology was visualized in control pigs (n=7), non-diabetic pigs fed an atherogenic diet (ATH, n=5), and DM pigs fed an atherogenic diet (DM+ATH, n=5) using SDF imaging of oral mucosal tissue. Subsequently, kidneys were harvested from anesthetized pigs and the expression levels of well-established markers for microvascular integrity, such as Angiopoietin-1 (Angpt1) and Angiopoietin-2 (Angpt2) were determined immunohistochemically, while endothelial cell (EC) abundance was determined by immunostaining for von Willebrand factor (vWF).

Results: Our study revealed an increase in the capillary tortuosity index in DM+ATH pigs (2.31 ± 0.17) as compared to the control groups (Controls 0.89 ± 0.08 and ATH 1.55 ± 0.11 ; $p < 0.05$). Kidney biopsies showed marked glomerular lesions consisting of mesangial expansion and podocyte lesions. Furthermore, we observed a disturbed Angpt2/ Angpt1 balance in the cortex of the kidney, as evidenced by increased expression of Angpt2 in DM+ATH pigs as compared to Control pigs ($p < 0.05$).

Conclusion: In the setting of DM, atherogenesis leads to the augmentation of mucosal capillary tortuosity, indicative of systemic microvascular damage. Concomitantly, a dysbalance in renal angiopoietins was correlated with the development of diabetic nephropathy. As such, our studies strongly suggest that defects in the systemic microvasculature mirror the accumulation of microvascular damage in the kidney.

Introduction

Diabetes mellitus (DM) is associated with macrovascular and microvascular complications that lead to retinopathy, neuropathy and nephropathy. Diabetic nephropathy is the leading cause of chronic kidney disease (CKD) worldwide [1,2]. In this disease setting, the combination of endothelial dysfunction and an imbalanced angiogenic response play an important role in the development of microvascular complications. Recently, the angiopoietins have gained much attention as critical regulators of diverse pathological angiogenic conditions, including vascular complications associated with diabetes. The tight control of Angiopoietin-1 (Angpt1) and Angiopoietin-2 (Angpt2) levels is critical in minimizing microvascular derangements that are the direct result of negative interference of Angpt2 with Angpt1-mediated Tie-2 signaling. This in turn disturbs the expression levels of key angiogenic factors such as von Willebrand factor (vWF) and vascular endothelial growth factor (VEGF). The ensuing loss of EC-pericyte interactions is responsible for destabilization of the capillary network and the loss of microvascular integrity. [3,4]-[5,6].

Histopathological findings in patients with diabetic nephropathy (DN) include mesangial expansion, mesangial sclerosis and vascular lesions such as hyalinosis [7]. These renal abnormalities could potentially be indicative of the systemic microvascular damage [8]. However, the detection of such pathophysiologies in DN is complex, as it is asymptomatic in early stages, while at later stages the direct demonstration of renal injury requires renal biopsy material, which is an unattractive tool for screening purposes due to the invasive nature of the procedure. Therefore, methods geared towards the non-invasive monitoring for early signs of microvascular changes is of clinical importance in patients with DM. However, at present these tools do not exist. Sidestream dark-field (SDF) imaging is a relatively new, non-invasive tool that enables one to visualize the microcirculation without the use of fluorescent dyes [9]. Recently, we used this apparatus to assess labial mucosal capillary tortuosity and density in diabetic patients compared with healthy non-diabetic controls, studies that revealed increased capillary density and tortuosity in diabetic patients [10]. These studies focused on the effects of prolonged diabetes in patients (24 ± 14 years). However, at present there is limited data regarding how disturbance of the microvasculature in early diabetes correlates with renal damage.

In light of these considerations, we sought to investigate whether an atherogenic diet in the early stages of DM could accelerate microvascular disease, and could serve as a diagnostic tool for DM-induced renal damage. Using SDF imaging, we show that an atherogenic diet during the early stages of DM leads to microvascular abnormalities, and immunohistochemically confirm that these systemic effects are associated with renal endothelial dysfunction, as evidenced by a disturbed Angpt2/Angpt1 balance and microalbuminuria.

Material and Methods

Animal experiments

The experimental protocol was performed in compliance with the ARRIVE guidelines on animal research [11]. Protocols describing the management, surgical procedures, and animal care were reviewed and approved by the ASG-Lelystad Animal Care and Use Committee (Lelystad, The Netherlands) and by the Institutional Review Board for animal experimentation of the Erasmus University Medical Center (Rotterdam, The Netherlands). Ten neutered male domestic pigs (Landrace x Yorkshire, T-line) with an age ~11 weeks and a body weight of ~30 kg entered the study. After one week of acclimatization, DM was induced in a subgroup of 5 pigs by slow intravenous injection of streptozotocin (STZ 140 mg/kg; Enzo Life Sciences, Raamsdonkveer, The Netherlands) as described previously [12–15]. Five non-diabetic pigs received placebo treatment. Three weeks after DM induction, all of the pigs were gradually introduced to an atherogenic diet (ATH), containing 25% of saturated fats and 1% of cholesterol (16). The 5 diabetic pigs (DM+ATH) and 5 non-diabetic pigs (ATH) were subsequently followed for up to 15 months, during which similar growth patterns were observed in both groups by adjusting individual caloric intake. In the diabetic pigs, glucose and ketone levels in plasma and urine were regularly checked in the 15-month follow-up period. Insulin therapy was started only in instances where plasma ketones were detected. Following 12 months, 24h urine samples were obtained from all pigs, while microcirculatory imaging and plasma samples were obtained from anesthetized pigs (20mg/kg ketamine + 1 mg/kg midazolam+ 1 mg atropine, i.m. and 12mg/kg thiopental, i.v.) at 14 and 15 months of follow up, respectively. At 15 months, the pigs were sacrificed by intravenous injection of an overdose of pentobarbital via the jugular vein catheter at 15 months, at which point plasma samples were obtained and the kidneys were harvested for histological examination. Invasive imaging analyses prompted us to choose this time frame as after 12 months of follow up more complex atherosclerotic lesions were present in the coronary arteries of the studied pigs (23).

In addition, we also studied a separate control group (Controls) of 7 female domestic pigs (Landrace) at the age of 5 months with a body weight of ~78 kg, who were fed a standard diet for growing pigs.

Microcirculatory imaging and analysis of SDF measurements

SDF microscanning (MicroVision Medical Inc., Wallingford, PA, U.S.A) and analysis of images was performed as described earlier with minor modifications [10,16]. Anaesthetized pigs were imaged at 14 months of study duration. All pigs were studied during standardized conditions of general anesthesia by a trained observer.

Laboratory assessment

Serum Angpt1 and Angpt2 concentrations were measured after 12 months by enzyme-linked immunosorbent assay (ELISA) (Bioconnect, Huissen, The Netherlands and Antibodies-online, Atlanta, USA). At 12 months, protein and creatinine levels were measured in 24h urine samples. To calculate the urinary albumin-creatinine ratio, we measured albumin excretion by ELISA (ITK diagnostics, Uithoorn, The Netherlands), and urinary creatinine concentration was measured by standard laboratory methods. Both the plasma and urinary creatinine levels were measured as previously described. Plasma samples collected at 15 months were used to measure concentrations of glucose, total cholesterol, triglycerides and low and high-density lipoproteins (LDL and HDL) and creatinine by standardized methods at the clinical chemical laboratory of the Erasmus Medical Center (Rotterdam, The Netherlands). In the absence of an established mathematical formula to estimate creatinine clearance in pigs, we expressed creatinine levels in $\mu\text{mol/L/kg}$ to adjust for body weight. Blood collection tubes were centrifuged for 10 minutes at 3000 rpm after which serum was stored in microcentrifuge tubes at -20°C until required for analysis.

Histological analysis of the kidney

Immunohistochemical analyses of snap-frozen porcine kidney cortex sections (4 μm) were air-dried and acetone fixed as previously described [17]. Monoclonal antibodies utilized were directed against mouse anti-human Angpt1 (clone 171718; R&D Systems, Abingdon, UK), mouse anti-human VEGF (sc-7269 Santa Cruz Biotechnology, Huissen, the Netherlands) and mouse anti-human plasminogen activator inhibitor-1 (clone HD-PAI-1 14.1) (American Diagnostica, Pfungstadt, Germany). Polyclonal antibodies were used directed against goat anti-mouse Angpt2 (clone F18; sc-7017; Santa Cruz Biotechnology, Huissen, the Netherlands) and rabbit anti-human vWF (Codonr A0082; Dako, Glostrup, Germany). Primary antibody binding was detected using the following isotype-matching secondary horseradish peroxidase (HRP)-labeled antibodies; goat anti-mouse IgG (Angpt1), rabbit anti-goat IgG (Angpt2), anti-mouse Envision K4007 (VEGF) or goat anti-rabbit IgG (vWF) (all purchased from Dako, Glostrup, Germany). Quantification of immunohistochemistry was performed in a blinded manner by assessing 10 consecutive high power fields (magnification, $\times 200$) using Image J software. Glomerular and large vessels were excluded from analysis. Data are presented in terms of the Angpt2/Angpt1 ratio as previously described [18,19]. Immunofluorescent double stainings were performed for desmin (pericyte marker; mouse anti-pig clone DE-B-5; Millipore, Amsterdam, the Netherlands)/Angpt1 (goat anti-human; clone N-18; sc-6319; Santa Cruz Biotechnology, Huissen, the Netherlands) and vWF/Angpt2. Secondary antibodies were Alexa-488 labeled donkey anti-rabbit (vWF) and alexa-546 labelled rabbit anti-mouse (desmin). Furthermore, HRP labelled rabbit anti-goat (Angpt1) and donkey anti-goat (Angpt2) were used. Nuclei were visualized using Hoechst (Molecular Probes, Leiden, the Netherlands). Photomicrographs were made using a fluorescence microscope (DM5500B; Leica, Rijswijk, the Netherlands).

Next, we performed periodic acid-Schiff (PAS) staining on paraffin sections of renal cortex for the evaluation of histopathological changes and morphometric analysis of the glomeruli. In a blinded fashion, 25 consecutive glomeruli were selected from both superficial and deep cortex and the mesangial expansion index was scored. Subsequently, we determined the extent of increase in mesangial matrix (defined as mesangial area) by quantitating PAS-positive and nuclei-free areas in the mesangium using Image J [20,21]. Evaluation of histopathological lesions was performed by a pathologist who was blinded to the code of the sections.

Electron microscopy

Kidney tissues for electron microscopy were processed as described previously [22]. In typical cases from the ATH and DM+ATH groups, the glomerular basement membrane (GBM) width was measured.

RNA isolation and Real-Time PCR

To analyze renal Angpt1 and Angpt2 mRNA levels, RT-PCR was performed as described previously [23]. Expression was normalized against β -actin mRNA levels. RT-PCR analysis for biological replicates was performed in duplicate. The primer sequences were as follows: β -actin (forward 5'-ATCGTGCGGGACATCAAGGA-3' and reverse 5'-AGGAAGGAGGGCTGGAAGAG-3'), Angpt1 (forward 5'-AGGAGCAAGTTTTGCGAGAG-3' and reverse 5'-CTCAGAGCGTTTGTGTTGT-3') and Angpt2 (forward 5'-AAAGTTGCTGCAGGGAA-AGA-3' and reverse 5'-TCACAGCTCAGAGCGAAGAA-3').

Statistical analysis

All data are presented as mean \pm standard error of the mean (SEM). Differences between experimental groups were analyzed using one way-analysis of variance followed by post-hoc testing with an unpaired Student's t-test. Analyses were performed with GraphPad software (GraphPad Software Inc., San Diego, CA, U.S.A.). P-values less than 0.05 (two-tailed) were considered statistically significant.

Results

Model characteristics

Initial plasma profiling of DM+ATH and ATH pigs revealed that DM significantly influenced glucose levels (17.64 ± 4.54 mmol/L vs. 5.12 ± 0.42 mmol/L; $p < 0.05$) (Table 1) at 15 months. Total cholesterol, triglycerides, HDL and LDL were not significantly affected by the induction of DM in pigs. Two pigs were administered insulin during the study period due to elevated plasma ketone levels. The mean body weight at the time of microvascular imaging was comparable between DM+ATH (96 ± 2.8 kg) and ATH group (93 ± 0.4 kg, $p > 0.05$). At the time of sacrifice, substantial coronary lesions as well as generalised atherosclerosis for example in the aorta were observed in both DM+ATH and ATH groups, as described previously [24].

Table 1: Model characteristics at 15 months of follow up

	Controls (N=7)	ATH (N=5)	DM+ATH (N=5)
Glucose (mmol/l)	4.26±0.29	5.12±0.42	17.64±4.54 [#]
Triglycerides (mmol/l)	0.18±0.02	0.64±0.2	1.26±0.50 [*]
Total Cholesterol (mmol/l)	1.50±0.05	18.10±2.66 [*]	16.82±1.72 [*]
LDL (mmol/l)	0.76±0.29	14.87±2.45 [*]	13.63±1.3 [*]
HDL (mmol/l)	0.60±0.03	5.70±0.35 [*]	5.12±0.40 [*]

All data are mean \pm SEM. ATH: pigs on atherogenic diet. DM+ATH: pigs with diabetes mellitus on atherogenic diet. Controls: healthy control pigs on a standard diet. LDL: Low density lipoprotein. HDL: High density lipoprotein. * $P < 0.05$ compared with Controls. # $P < 0.05$ compared with ATH pigs.

Early atherogenic diabetes mellitus leads to systemic microvascular damage

The microvascular morphology of the oral mucosal tissue in DM+ATH pigs was significantly disturbed as compared with the Controls (Fig. 1A). Indeed, the capillary tortuosity index was significantly increased in DM+ATH pigs (2.3 ± 0.2) as compared with ATH pigs (1.6 ± 0.1 , $p < 0.01$; Fig. 1B). Furthermore, capillary density was significantly lower in the DM+ATH (18.6 ± 1.3 capillaries/mm²) pigs as compared with the Controls (24.9 ± 0.8 capillaries/mm², $p < 0.01$; Fig. 1C). Representative videos of the SDF imaging are shown in the 'Supporting Information' section.

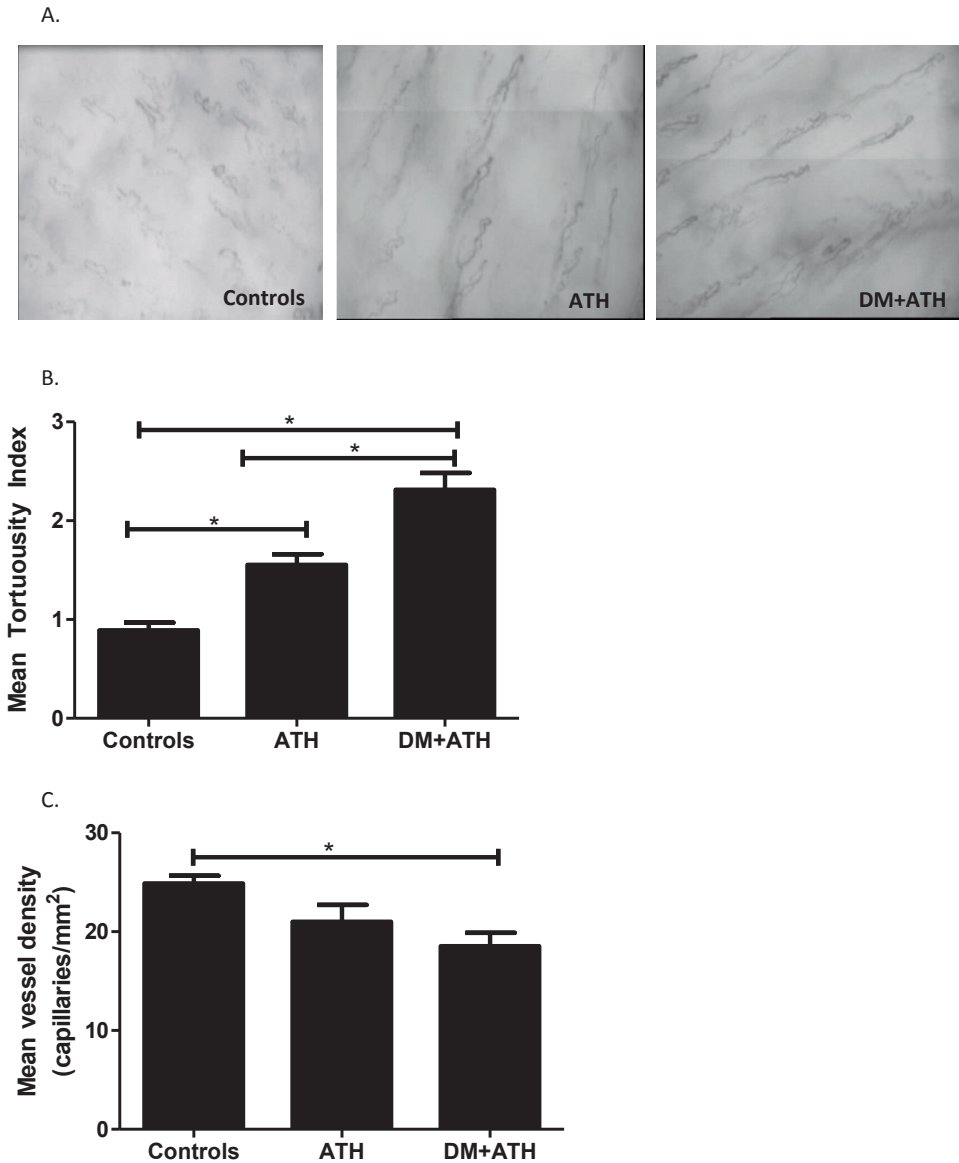


Figure 1. Early atherogenic DM leads to increased capillary tortuosity A. Sidestream darkfield images of the oral mucosa visualizing the microvascular capillaries of a representative pig in the Controls, ATH and DM+ATH group. B. Mean tortuosity index of microvascular capillaries in the Controls (n=7), ATH (n=5) and DM+ATH pigs (n=5). C. Mean vessel density (capillaries/mm²) in Controls (n=7), ATH (n=5) and DM+ATH (n=5) pigs. Data shown are mean±SEM. *P<0.05 compared to Controls or ATH pigs. Mean vessel density (capillaries/mm²) was calculated by evaluation of number of vessels per selected microcirculatory image. Subsequently, tortuosity of capillary loops was assessed according to a validated scoring system (0: no twists to 4: four or more twists) and the average of assessed capillary tortuosity was used to calculate mean tortuosity index per patient.

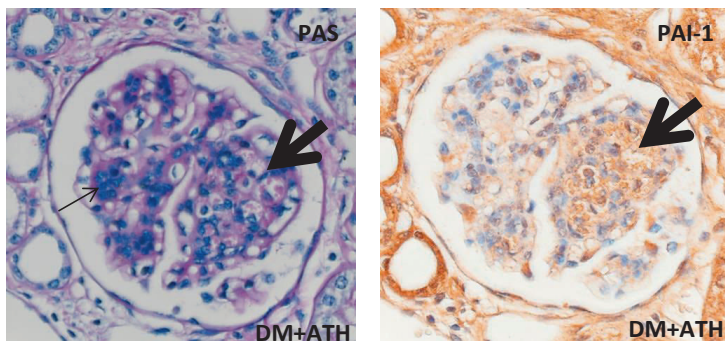
Renal damage after induction of atherogenic DM in pigs

Plasma creatinine levels were elevated in ATH pigs ($2.12 \pm 0.03 \mu\text{mol/L/kg}$) as compared with DM+ATH pigs ($1.60 \pm 0.13 \mu\text{mol/L/kg}$, $p < 0.01$) group. However, urinary albumin/creatinine ratio was not found to differ between the DM+ATH group ($0.045 \pm 0.0182 \text{ mg/mmol}$) and ATH pigs ($0.002 \pm 0.0007 \text{ mg/mmol}$, $p > 0.05$).

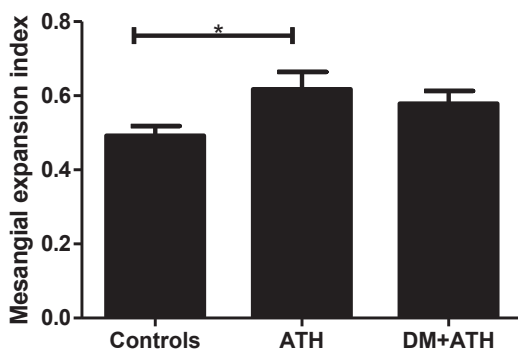
PAS-stained renal sections revealed marked tubular changes with foamy cytoplasm and hyalin droplets in all DM+ATH pigs and there were glomerular lesions consisting of mesangial expansion and podocyte lesions, also with foamy cytoplasm and hyaline droplets in four DM+ATH pigs (Fig. 2A). In contrast, but one ATH pig displayed similar lesions (Fig. 2A). Some glomeruli were found to have dilated capillaries containing numerous red blood cells, a phenomenon that is highly reminiscent of microangiopathic injury lesions that have been described to be the result of fibrinolytic/proteolytic activation system in combination with increased PAI-1 staining [25]. In keeping with this notion, we observed both co-localization and increased PAI-1 staining in the herein described lesions (Fig. 2A).

Next, we determined the mesangial expansion index in renal cross-sections. These studies showed significantly higher scores in the ATH pigs (0.62 ± 0.05 , $p = 0.03$) and a trend towards increased scores in the DM+ATH (0.58 ± 0.05 , $p = 0.066$) compared with the Controls (0.49 ± 0.03 ; Fig. 2B). Interestingly, the width of the GBM increased from 215 nM in a Controls animal to 252 and 279 nM in cases with mild and severe DN of the DM+ATH group, respectively. Moreover, lipid deposits were observed in kidneys of mild and severe DN pigs (Fig. 2C).

A.



B.



C.

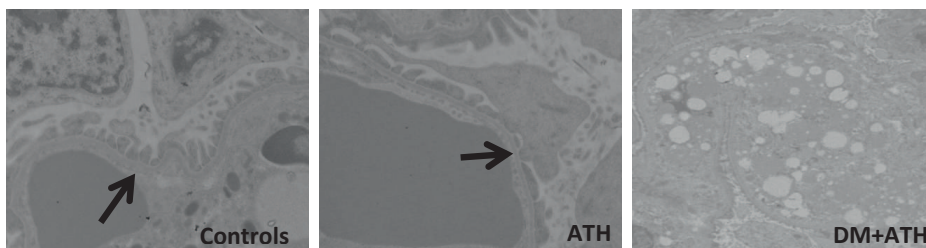


Figure 2. Early stages of atherogenic DM leads to renal damage. A: Representative illustration of PAS stained glomeruli from a DM+ATH pig, showing mesangial proliferation and matrix expansion with capillary loops lying around the mesangium as a corona, reminiscent of a beginning Kimmelstiel-Wilson nodule (left panel; thin black arrow). Dilated capillary loops with red cell fragments show intense PAI-1 staining on consecutive slides (right panel; thick black arrow). B: Mesangial expansion index in Controls (n=7), ATH (n=5) and DM+ATH (n=5) pigs. C: Electron microscopy images illustrating a normal GBM architecture (left panel; thick arrow) of the Controls pig. In ATH, there is slight effacement of the podocyte pedicles (middle panel; thick arrow). In DM+ATH, marked lipid deposits were found (right panel). Data are shown as mean ± SEM. *P<0.05 compared to Controls or ATH pigs. Magnification of A, x400 and C, x8000

Diabetes and atherogenic diet induces Angpt2/Angpt1dysbalance in pigs

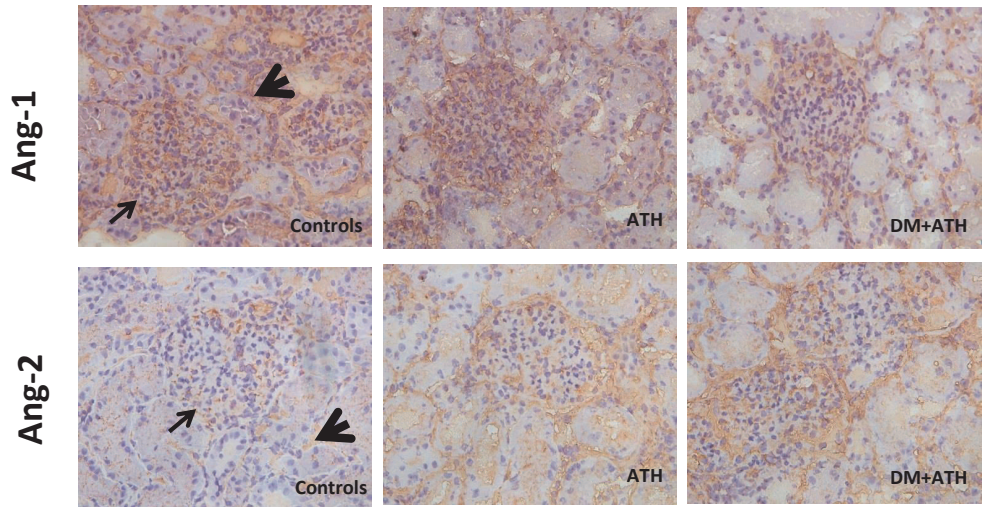
Serum Angpt-1 levels in the DM+ATH pigs were increased as compared to control pigs (26035 ± 1228 pg/ml versus 18061 ± 1228 pg/ml, $p < 0.01$). There were no significant differences in serum Ang-1 levels between DM+ATH and ATH pigs (19832 ± 1166 pg/ml, $p > 0.05$). Angpt-2 levels were not detectable in the circulation of the different groups.

With regard to Angpt1 staining in the kidneys, we observed positive Angpt1 staining in the glomeruli and in a capillary-like pattern between the tubuli of pigs in the Controls group (Fig. 3A). We found no difference in renal Angpt1 protein expression between ATH (78020 ± 12216 pixels/area) and DM+ATH (46763 ± 12360 pixels/area, $p > 0.05$) pigs, but Angpt1 expression was significantly higher in the Controls group (91788 ± 9777 pixels/area, $p < 0.05$; Fig. 3B). The Angpt1 mRNA levels in the kidney were significantly lower in the DM+ATH and ATH group compared with the Controls pigs (Fig. 3C). Double staining of Angpt1 and the pericyte marker desmin revealed predominantly expression of desmin in the glomeruli and Angpt1 expression in the same pattern as described above (Fig. 3D; left panel). However, no co-localization was observed, suggesting that other cells than pericytes might produce Angpt1 in the glomerulus. Angpt2 staining was predominantly present in glomeruli and tubuli and showed a significant increase in DM+ATH (54813 ± 3140 pixels/area) pigs compared to the Controls (22862 ± 3354 pixels/area, $p < 0.001$) and ATH (31005 ± 5011 pixels/area, $p < 0.01$) pigs (Fig. 3AB). Consequently, a higher Angpt2/ Angpt1 ratio was observed in DM+ATH (1.63 ± 0.43) pigs compared with Controls (0.28 ± 0.07 , $p < 0.001$) and ATH (0.43 ± 0.07 , $p < 0.01$) group (Fig. 3B). The Angpt2 mRNA levels in the kidney did not significantly differ between groups (Fig. 3C). Importantly, additional staining of vWF and Angpt2 revealed co-expression, suggesting that endothelial cells produce Angpt2 (Fig. 3D; middle and right panel).

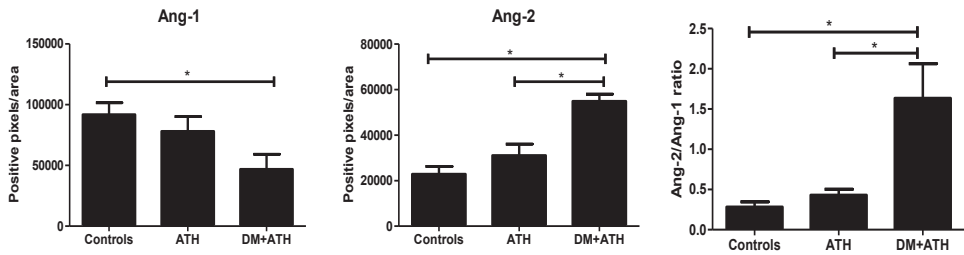
Staining of the endothelial marker vWF showed expression in the glomeruli and peritubular space, in the same pattern as Angpt1 (Fig. 3E). No significant differences were observed in vWF expression between the Controls (86611 ± 6163 pixels/area), ATH (84547 ± 9000 pixels/area) and DM+ATH pigs (102961 ± 13633 pixels/area) ($p > 0.05$).

VEGF staining revealed expression in podocytes, parietal epithelial cells and tubuli (most extensively) in all groups (Fig. 3F). There was no difference in VEGF-expression between the different groups.

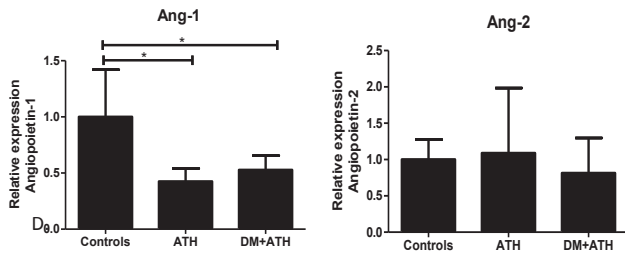
A.



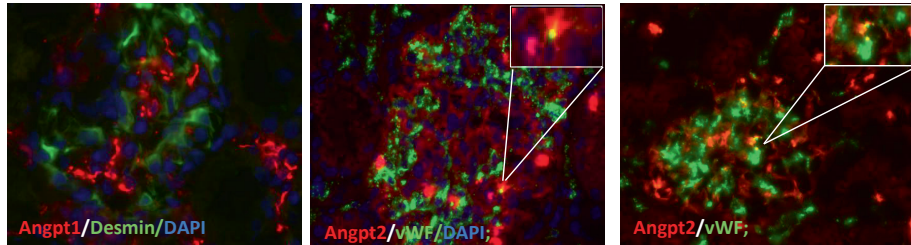
B.



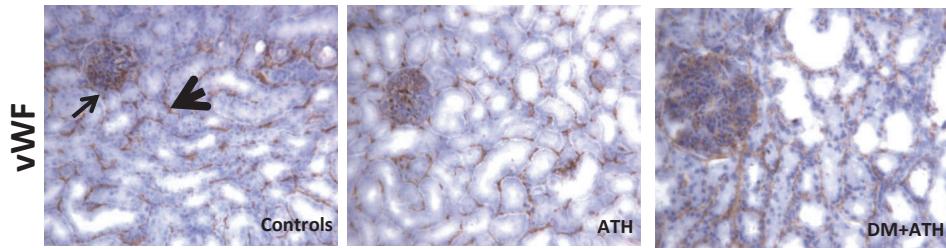
C.



D.



E.



F.

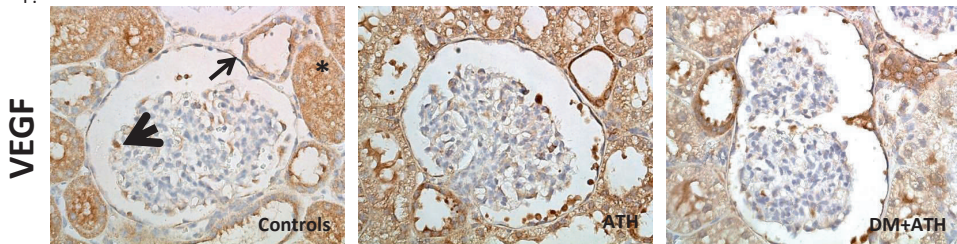


Figure 3. The Angpt2/Angpt1 balance is disturbed in atherogenic DM pigs. A. Representative illustrations of kidney sections stained with Angpt1 (upper panels; arrow: glomerulus; arrowhead: peritubular area) or Angpt2 (lower panels; arrow: glomerulus; arrowhead: tubular staining) in Controls, ATH, and DM+ATH pigs. B. Quantitative analysis of Angpt1, Angpt2 and Angpt2/Angpt1 ratio. C. Relative mRNA expression of Angpt1 and Angpt2. D. Immunofluorescent double staining of representative kidney sections for desmin (green)/Angpt1 (red; left panel) and vWF (green/Angpt2 red; middle/right panel). Insets: double positivity for vWF/Angpt2 staining in yellow. E. Representative illustrations of kidney sections stained with endothelial marker vWF (arrow: glomerulus; arrowhead: peritubular area) in Controls, ATH, and DM+ATH pigs. F. Representative images of kidney sections stained with VEGF in Controls, ATH, and DM+ATH pigs showing expression in podocytes (arrow head), parietal epithelial cells (thin arrow) and tubuli (asterisk). Data are shown as mean \pm SEM. * $P < 0.05$ compared to Controls or ATH pigs. Magnification of A, D, F x400 and E, x200.

Angpt2/Angpt1 dysbalance and creatinine levels are correlated with capillary tortuosity

Correlation analyses were performed between renal Angpt1, Angpt2, Angpt2/Angpt1 ratio, creatinine levels and albumin/creatinine ratio and oral mucosal capillary tortuosity and density indices. No correlation was found between capillary density index and renal angiotensin expression or urinary markers for renal function. However, a negative correlation was found between renal Angpt1 expression and microvascular tortuosity index ($r=-0.60$, $p=0.0100$; Fig. 4A). Moreover, we demonstrated a positive correlation between capillary tortuosity and Angpt2 staining ($r=0.70$, $p=0.0017$; Fig. 4B) and Angpt2/Angpt1 ratio ($r=0.80$, $p=0.0002$; Fig. 4C). No significant correlation was found between urinary albumin/creatinine ratio, creatinine levels and capillary tortuosity index.

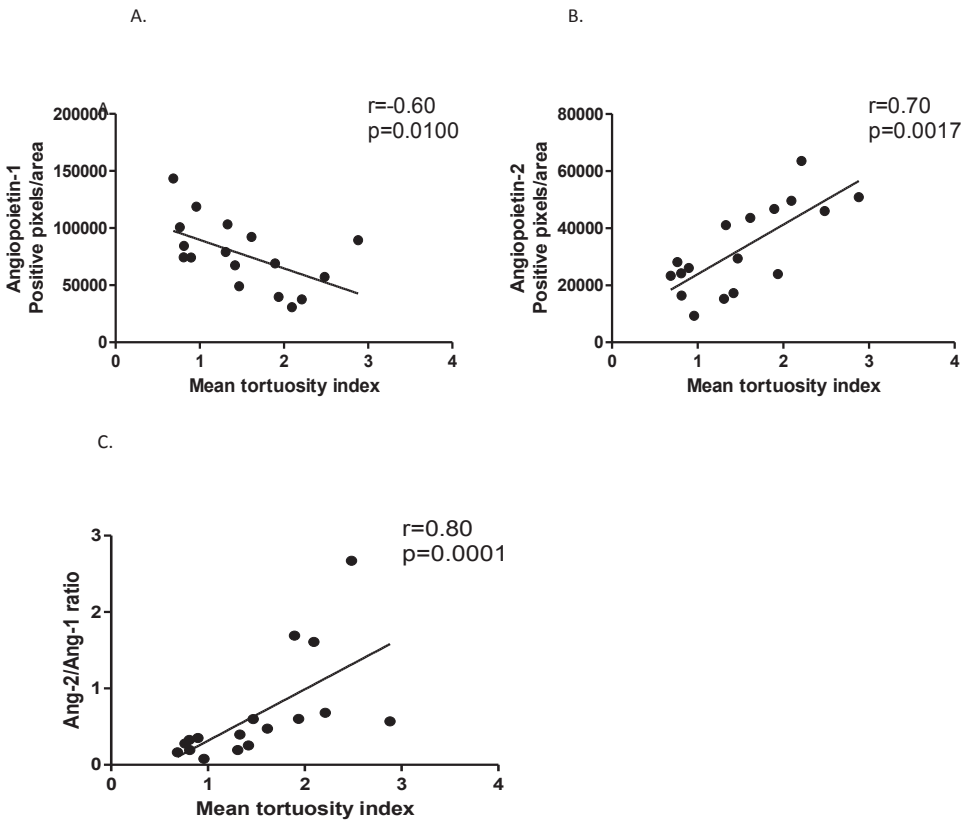


Figure 4. Correlation between capillary tortuosity and Angpt2/Angpt1 balance and creatinine levels. Scatter plot showing the correlation of renal protein expression of Angpt1(A), Angpt2 (B), Angpt2/Angpt1 ratio (C).

Discussion

In the present study, we show that the combination of an atherogenic diet and recent onset of DM leads to abnormalities in the systemic microvasculature, yielding SDF-detectable increases in capillary tortuosity and increased levels of serum Angpt1. Furthermore, we discovered that glomerular lesions develop during the early stages of DN and that the tight control of the Angpt2/Angpt1 balance is perturbed in the kidneys of diabetic atherogenic pigs.

Microvascular dysfunction is one of the most important causes of persistent diabetic complications. This is the result of disturbed hemodynamics and impaired endothelial function induced by metabolic alterations [26,27]. However, the early events involved in the pathogenesis of diabetic microvascular complications are not well understood, and are difficult to study in humans without the use of invasive techniques. SDF imaging allows for the easy, and rapid assessment of the presence of systemic microvascular derangements that could precede the development of diabetic macrovascular complications. In our study, we observed increased capillary tortuosity between the DM+ATH and ATH groups, already at ~15 months following DM induction. Using SDF imaging, we recently demonstrated increased capillary tortuosity in diabetes patients, and reversal of microvascular tortuosity after simultaneous pancreas-kidney transplantation [16]. Moreover, we have previously shown that increased capillary tortuosity in diabetic patients was associated with macrovascular disease [10]. In concordance with our observations, Sasongko et al demonstrated increased tortuosity in patients with diabetic retinopathy, suggesting that this may be an early sign of microvascular damage in DM [28,29]. However, these studies did not include patients with early stage DM and did not focus on the role of angiopoietins in microvascular alterations and renal injury in atherogenic DM.

In addition to increased microvascular tortuosity, we also observed increased serum levels of Angpt-1 in DM+ATH pigs compared with the control group. These data are in line with previous clinical studies in patients with moderate and severe non-proliferative diabetic retinopathy [30] and in patients with hypertension [31] that showed increased Angpt1 serum levels in these patients as well. While serum Angpt1 levels were increased in DM+ATH pigs, we found a decrease in Angpt1 protein and mRNA expression in kidneys of diabetic pigs compared to control groups. This observation suggests shedding of Angpt1 from renal vasculature into the circulation.

Interestingly, DM+ATH pigs were characterized by higher expression levels of Angpt2 protein as compared to the ATH group, resulting in a higher Angpt2/ Angpt1 ratio in the DM+ATH pigs. This is in agreement with Rizkalla and co-workers, who previously have shown that

both Angpt1 and Angpt2 protein levels are increased in the early phase of STZ-induced DM in rats [32]. However, disease progression was found to trigger a decrease in Angpt1 expression while Angpt2 continued to increase, a switch that both markedly alters but also disturbs the Angpt2/Angpt1 balance [32]. Although a difference in angiotensin expression between rats and pigs cannot be excluded, these findings suggest that angiotensins undergo time-dependent changes in expression at different stages of DM. Our identification that an increased urinary albumin/creatinine ratio is associated with a higher Angpt2/Angpt1 ratio (in DM+ATH pigs) is in keeping with recent studies that demonstrated an inability to express Angpt1 leads to extensive glomerular damage and proteinuria, indicating a protective role of Angpt1 [33]. These data suggest that angiotensins might play an important role in the pathophysiology of glomerular disease in DN.

Aside from angiotensins, numerous other mechanisms have been proposed to be causal for microvascular complications in DM, such as VEGF. Under pathological conditions, Angpt2 acts in concert with VEGF to induce inflammatory angiogenesis. By promoting pericyte dropout, Angpt2 will lead to destabilization between ECs and pericytes. In the presence of VEGF, Angpt2 can eventually lead to an active, sprouting state of ECs, but when VEGF is absent, Angpt2 promotes vessel regression [34–36]. Our immunohistochemical assessment of VEGF protein in the different groups revealed high expression levels in podocytes and parietal- and tubular epithelial cells, which is in keeping with literature [34,37–40]. However, in contrast to previous studies, we did not observe differences between the different groups.

An additional observation we made was the marked increase in PAI-1 expression in regions of microvascular injury. PAI-1, a protease and fibrinolysis inhibitor that is poorly expressed in healthy kidneys, which is a critical player in angiogenesis and vascular remodeling [41]. Our observation that glomerular and tubular expression of PAI-1 is increased in DM+ATH pigs is noteworthy due to the fact that: 1) PAI-1 was found to be prominently expressed in Kimmelstiel-Wilson nodules, in particular those with active microvascular damage [25]; 2) unilateral ureteral obstruction [42] and glomerulonephritis [43] have also been associated with increased expression of tubular PAI-1; and 3) endogenous PAI-1 deficiency protects diabetic mice from glomerular injury [44]. Collectively, these data support for a pathogenic role for PAI-1 in diabetic renal disease.

In the current study, there was a tendency towards increased mesangial expansion in the DM+ATH pigs, and significantly more mesangial expansion in kidneys of ATH pigs. The data confirm previous reports on pig studies which revealed that consumption of high-fat diet leads to the development of renal injury, characterized by mesangial expansion and increased plasma creatinine levels [45,46]. Moreover, rodent studies demonstrated that

hyperlipidemia exacerbates the development and progression of renal diseases, including DN [47,48]. Furthermore, our study also showed higher creatinine levels in the ATH group than the DM+ATH and Controls, which could be explained by the increased mesangial expansion observed in ATH pigs. The latter has been associated with obliteration of capillary lumen and decreased capillary perfusion in previous studies [49]. Furthermore, our study suggests that the combined hyperglycemia and hyperlipidemia in the DM +ATH pigs, induces a dysbalance in renal angiotensins that results in albuminuria and endothelial damage in the kidney. The potential contribution of tubular injury to albuminuria needs to be addressed in additional studies.

Some aspects of our porcine study require further discussion. First, it would have been interesting to study an additional group of pigs with only diabetes (i.e. without ATH) to explore the early effects of only hyperglycemia on the microvasculature. However, the clinically most relevant group of DN also reflects DM patients with some presence of atherosclerosis as well. Secondly, it could be argued that the differences in gender, age and weight between healthy control pigs (Controls) versus DM+ATH and ATH pigs may explain part of the difference in the observed capillary tortuosity between these groups. This is, however, unlikely as in a human study, age did not influence capillary tortuosity [16].

In conclusion, we present SDF imaging as a novel means of documenting capillary tortuosity, an event that is illustrative of renal injury in the setting of early DM and atherosclerosis. This technique enables one to non-invasively detect systemic microvascular damage. Furthermore, we also identified changes in the Angpt2/Angpt1 balance may represent initiating events of renal injury in early DM. We propose that the targeted intervention of angiotensins signaling could be an effective modality in minimizing microvascular damage that could serve as an early initiator of DN.

Acknowledgement

Eric van der Veer is greatly acknowledged for carefully reading the manuscript and providing constructive comments.

References

1. Cumbie BC, Hermayer KL (2007) Current concepts in targeted therapies for the pathophysiology of diabetic microvascular complications. *Vasc Health Risk Manag* 3: 823-832.
2. Tooke JE (1996) Microvasculature in diabetes. *Cardiovasc Res* 32: 764-771. 0008636396000910 [pii].
3. Feng D, Bursell SE, Clermont AC, Lipinska I, Aiello LP, Laffel L, King GL, Tofler GH (2000) von Willebrand factor and retinal circulation in early-stage retinopathy of type 1 diabetes. *Diabetes Care* 23: 1694-1698.
4. Targher G, Bertolini L, Zoppini G, Zenari L, Falezza G (2005) Increased plasma markers of inflammation and endothelial dysfunction and their association with microvascular complications in Type 1 diabetic patients without clinically manifest macroangiopathy. *Diabet Med* 22: 999-1004. DME1562 [pii];10.1111/j.1464-5491.2005.01562.x [doi].
5. Fiedler U, Augustin HG (2006) Angiopoietins: a link between angiogenesis and inflammation. *Trends Immunol* 27: 552-558. S1471-4906(06)00293-6 [pii];10.1016/j.it.2006.10.004 [doi].
6. Hammes HP, Lin J, Renner O, Shani M, Lundqvist A, Betsholtz C, Brownlee M, Deutsch U (2002) Pericytes and the pathogenesis of diabetic retinopathy. *Diabetes* 51: 3107-3112.
7. Tervaert TW, Mooyaart AL, Amann K, Cohen AH, Cook HT, Drachenberg CB, Ferrario F, Fogo AB, Haas M, de HE, Joh K, Noel LH, Radhakrishnan J, Seshan SV, Bajema IM, Bruijn JA (2010) Pathologic classification of diabetic nephropathy. *J Am Soc Nephrol* 21: 556-563. ASN.2010010010 [pii];10.1681/ASN.2010010010 [doi].
8. Edwards MS, Wilson DB, Craven TE, Stafford J, Fried LF, Wong TY, Klein R, Burke GL, Hansen KJ (2005) Associations between retinal microvascular abnormalities and declining renal function in the elderly population: the Cardiovascular Health Study. *Am J Kidney Dis* 46: 214-224. S0272-6386(05)00618-9 [pii];10.1053/j.ajkd.2005.05.005 [doi].
9. Goedhart PT, Khalilzada M, Bezemer R, Merza J, Ince C (2007) Sidestream Dark Field (SDF) imaging: a novel stroboscopic LED ring-based imaging modality for clinical assessment of the microcirculation. *Opt Express* 15: 15101-15114. 144629 [pii].
10. Djaberi R, Schuijf JD, de Koning EJ, Wijewickrama DC, Pereira AM, Smit JW, Kroft LJ, de RA, Bax JJ, Rabelink TJ, Jukema JW (2012) Non-invasive assessment of microcirculation by sidestream dark field imaging as a marker of coronary artery disease in diabetes. *Diab Vasc Dis Res*. 1479164112446302 [pii];10.1177/1479164112446302 [doi].
11. Kilkeny C, Browne WJ, Cuthill IC, Emerson M, Altman DG (2012) Improving bioscience research reporting: the ARRIVE guidelines for reporting animal research. *Osteoarthritis Cartilage* 20: 256-260. S1063-4584(12)00082-9 [pii];10.1016/j.joca.2012.02.010 [doi].
12. Gerrity RG, Natarajan R, Nadler JL, Kimsey T (2001) Diabetes-induced accelerated atherosclerosis in swine. *Diabetes* 50: 1654-1665.
13. van den Heuvel M, Sorop O, Koopmans SJ, Dekker R, de VR, van Beusekom HM, Eringa EC, Duncker DJ, Danser AH, van der Giessen WJ (2012) Coronary microvascular dysfunction in a porcine model of early atherosclerosis and diabetes. *Am J Physiol Heart Circ Physiol* 302: H85-H94. ajpheart.00311.2011 [pii];10.1152/ajpheart.00311.2011 [doi].
14. Koopmans SJ, Mroz Z, Dekker R, Corbijn H, Ackermans M, Sauerwein H (2006) Association of insulin resistance with hyperglycemia in streptozotocin-diabetic pigs: effects of metformin at isoenergetic feeding in a type 2-like diabetic pig model. *Metabolism* 55: 960-971. S0026-0495(06)00102-8 [pii];10.1016/j.metabol.2006.03.004 [doi].
15. Koopmans SJ, Dekker R, Ackermans MT, Sauerwein HP, Serlie MJ, van Beusekom HM, van den Heuvel M, van der Giessen WJ (2011) Dietary saturated fat/cholesterol, but not unsaturated fat or starch, induces C-reactive protein associated early atherosclerosis and ectopic fat deposition in diabetic pigs. *Cardiovasc Diabetol* 10: 64. 1475-2840-10-64 [pii];10.1186/1475-2840-10-64 [doi].

16. Khairoun M, de Koning EJ, van den Berg BM, Lievers E, de Boer HC, Schaapherder AF, Mallat MJ, Rotmans JI, van der Boog PJ, van Zonneveld AJ, de Fijter JW, Rabelink TJ, Reinders ME (2013) Microvascular damage in type 1 diabetic patients is reversed in the first year after simultaneous pancreas-kidney transplantation. *Am J Transplant* 13: 1272-1281. 10.1111/ajt.12182 [doi].
17. Khairoun M, van der Pol P, de Vries DK, Lievers E, Schlagwein N, de Boer HC, Bajema IM, Rotmans JI, van Zonneveld AJ, Rabelink TJ, van KC, Reinders ME (2013) Renal ischemia-reperfusion induces a dysbalance of angiopoietins, accompanied by proliferation of pericytes and fibrosis. *Am J Physiol Renal Physiol* 305: F901-F910. *ajprenal.00542.2012* [pii];10.1152/ajprenal.00542.2012 [doi].
18. David S, Kumpers P, Hellpap J, Horn R, Leitolf H, Haller H, Kielstein JT (2009) Angiopoietin 2 and cardiovascular disease in dialysis and kidney transplantation. *Am J Kidney Dis* 53: 770-778. S0272-6386(09)00027-4 [pii];10.1053/j.ajkd.2008.11.030 [doi].
19. David S, Kumpers P, Lukasz A, Fliser D, Martens-Lobenhoffer J, Bode-Boger SM, Kliem V, Haller H, Kielstein JT (2010) Circulating angiopoietin-2 levels increase with progress of chronic kidney disease. *Nephrol Dial Transplant* 25: 2571-2576. *gfg060* [pii];10.1093/ndt/gfq060 [doi].
20. Sugaru E, Sakai M, Horigome K, Tokunaga T, Kitoh M, Hume WE, Nagata R, Nakagawa T, Taiji M (2005) SMP-534 inhibits TGF-beta-induced ECM production in fibroblast cells and reduces mesangial matrix accumulation in experimental glomerulonephritis. *Am J Physiol Renal Physiol* 289: F998-1004. 00065.2005 [pii];10.1152/ajprenal.00065.2005 [doi].
21. Sugaru E, Nakagawa T, Ono-Kishino M, Nagamine J, Tokunaga T, Kitoh M, Hume WE, Nagata R, Taiji M (2006) SMP-534 ameliorates progression of glomerular fibrosis and urinary albumin in diabetic db/db mice. *Am J Physiol Renal Physiol* 290: F813-F820. 00357.2005 [pii];10.1152/ajprenal.00357.2005 [doi].
22. Trouw LA, Groeneveld TW, Seelen MA, Duijs JM, Bajema IM, Prins FA, Kishore U, Salant DJ, Verbeek JS, van KC, Daha MR (2004) Anti-C1q autoantibodies deposit in glomeruli but are only pathogenic in combination with glomerular C1q-containing immune complexes. *J Clin Invest* 114: 679-688. 10.1172/JCI21075 [doi].
23. van der Pol P, Schlagwein N, van Gijlswijk DJ, Berger SP, Roos A, Bajema IM, de Boer HC, de Fijter JW, Stahl GL, Daha MR, van KC (2012) Mannan-binding lectin mediates renal ischemia/reperfusion injury independent of complement activation. *Am J Transplant* 12: 877-887. 10.1111/j.1600-6143.2011.03887.x [doi].
24. van Ditzhuijzen NS, van den Heuvel M, Sorop O, van Duin RW, Krabbendam-Peters I, van HR, Ligthart JM, Witberg KT, Duncker DJ, Regar E, van Beusekom HM, van der Giessen WJ (2011) Invasive coronary imaging in animal models of atherosclerosis. *Neth Heart J* 19: 442-446. 10.1007/s12471-011-0187-0 [doi].
25. Paueksakon P, Revelo MP, Ma LJ, Marcantoni C, Fogo AB (2002) Microangiopathic injury and augmented PAI-1 in human diabetic nephropathy. *Kidney Int* 61: 2142-2148. *kid384* [pii];10.1046/j.1523-1755.2002.00384.x [doi].
26. Kalani M (2008) The importance of endothelin-1 for microvascular dysfunction in diabetes. *Vasc Health Risk Manag* 4: 1061-1068.
27. Kuryliszyn-Moskal A, Dubicki A, Zarzycki W, Zonnenberg A, Gorska M (2011) Microvascular abnormalities in capillaroscopy correlate with higher serum IL-18 and sE-selectin levels in patients with type 1 diabetes complicated by microangiopathy. *Folia Histochem Cytobiol* 49: 104-110.
28. Sasongko MB, Wong TY, Nguyen TT, Cheung CY, Shaw JE, Wang JJ (2011) Retinal vascular tortuosity in persons with diabetes and diabetic retinopathy. *Diabetologia* 54: 2409-2416. 10.1007/s00125-011-2200-y [doi].
29. Sasongko MB, Wong TY, Donaghue KC, Cheung N, Jenkins AJ, Benitez-Aguirre P, Wang JJ (2012) Retinal arteriolar tortuosity is associated with retinopathy and early kidney dysfunction in type 1 diabetes. *Am J Ophthalmol* 153: 176-183. S0002-9394(11)00476-4 [pii];10.1016/j.ajo.2011.06.005 [doi].

30. Patel JI, Hykin PG, Gregor ZJ, Boulton M, Cree IA (2005) Angiotensin concentrations in diabetic retinopathy. *Br J Ophthalmol* 89: 480-483. 89/4/480 [pii];10.1136/bjo.2004.049940 [doi].
31. Nadar SK, Blann A, Beevers DG, Lip GY (2005) Abnormal angiotensin II, angiotensin receptor Tie-2 and vascular endothelial growth factor levels in hypertension: relationship to target organ damage [a sub-study of the Anglo-Scandinavian Cardiac Outcomes Trial (ASCOT)]. *J Intern Med* 258: 336-343. JIM1550 [pii];10.1111/j.1365-2796.2005.01550.x [doi].
32. Rizkalla B, Forbes JM, Cao Z, Boner G, Cooper ME (2005) Temporal renal expression of angiogenic growth factors and their receptors in experimental diabetes: role of the renin-angiotensin system. *J Hypertens* 23: 153-164. 00004872-200501000-00026 [pii].
33. Jeansson M, Gawlik A, Anderson G, Li C, Kerjaschki D, Henkelman M, Quaggin SE (2011) Angiotensin-1 is essential in mouse vasculature during development and in response to injury. *J Clin Invest* 121: 2278-2289. 46322 [pii];10.1172/JCI46322 [doi].
34. Jain RK (2003) Molecular regulation of vessel maturation. *Nat Med* 9: 685-693. 10.1038/nm0603-685 [doi];nm0603-685 [pii].
35. Kim KL, Shin IS, Kim JM, Choi JH, Byun J, Jeon ES, Suh W, Kim DK (2006) Interaction between Tie receptors modulates angiogenic activity of angiotensin II in endothelial progenitor cells. *Cardiovasc Res* 72: 394-402. S0008-6363(06)00354-3 [pii];10.1016/j.cardiores.2006.08.002 [doi].
36. Lobov IB, Brooks PC, Lang RA (2002) Angiotensin II displays VEGF-dependent modulation of capillary structure and endothelial cell survival in vivo. *Proc Natl Acad Sci U S A* 99: 11205-11210. 10.1073/pnas.172161899 [doi];172161899 [pii].
37. Baelde HJ, Eikmans M, Doran PP, Lappin DW, de HE, Bruijn JA (2004) Gene expression profiling in glomeruli from human kidneys with diabetic nephropathy. *Am J Kidney Dis* 43: 636-650. S0272638604000083 [pii].
38. Baelde HJ, Eikmans M, Lappin DW, Doran PP, Hohenadel D, Brinkkoetter PT, van der Woude FJ, Waldherr R, Rabelink TJ, de HE, Bruijn JA (2007) Reduction of VEGF-A and CTGF expression in diabetic nephropathy is associated with podocyte loss. *Kidney Int* 71: 637-645. 5002101 [pii];10.1038/sj.ki.5002101 [doi].
39. Cooper ME, Vranes D, Youssef S, Stackel SA, Cox AJ, Rizkalla B, Casley DJ, Bach LA, Kelly DJ, Gilbert RE (1999) Increased renal expression of vascular endothelial growth factor (VEGF) and its receptor VEGFR-2 in experimental diabetes. *Diabetes* 48: 2229-2239.
40. Hohenstein B, Hausknecht B, Boehmer K, Riess R, Brekken RA, Hugo CP (2006) Local VEGF activity but not VEGF expression is tightly regulated during diabetic nephropathy in man. *Kidney Int* 69: 1654-1661. 5000294 [pii];10.1038/sj.ki.5000294 [doi].
41. Stefansson S, McMahon GA, Pettiler E, Lawrence DA (2003) Plasminogen activator inhibitor-1 in tumor growth, angiogenesis and vascular remodeling. *Curr Pharm Des* 9: 1545-1564.
42. Ishidoya S, Ogata Y, Fukuzaki A, Kaneto H, Takeda A, Orikasa S (2002) Plasminogen activator inhibitor-1 and tissue-type plasminogen activator are up-regulated during unilateral ureteral obstruction in adult rats. *J Urol* 167: 1503-1507. S0022-5347(05)65353-0 [pii].
43. Barnes JL, Mitchell RJ, Torres ES (1995) Expression of plasminogen activator-inhibitor-1 (PAI-1) during cellular remodeling in proliferative glomerulonephritis in the rat. *J Histochem Cytochem* 43: 895-905.
44. Lassila M, Fukami K, Jandeleit-Dahm K, Semple T, Carmeliet P, Cooper ME, Kitching AR (2007) Plasminogen activator inhibitor-1 production is pathogenetic in experimental murine diabetic renal disease. *Diabetologia* 50: 1315-1326. 10.1007/s00125-007-0652-x [doi].
45. Deji N, Kume S, Araki S, Soumura M, Sugimoto T, Isshiki K, Chin-Kanasaki M, Sakaguchi M, Koya D, Haneda M, Kashiwagi A, Uzu T (2009) Structural and functional changes in the kidneys of high-fat diet-induced obese mice. *Am J Physiol Renal Physiol* 296: F118-F126. 00110.2008 [pii];10.1152/ajprenal.00110.2008 [doi].

46. Taneja D, Thompson J, Wilson P, Brandewie K, Schaefer L, Mitchell B, Tannock LR (2010) Reversibility of renal injury with cholesterol lowering in hyperlipidemic diabetic mice. *J Lipid Res* 51: 1464-1470. jlr.M002972 [pii];10.1194/jlr.M002972 [doi].
47. Thompson J, Wilson P, Brandewie K, Taneja D, Schaefer L, Mitchell B, Tannock LR (2011) Renal accumulation of biglycan and lipid retention accelerates diabetic nephropathy. *Am J Pathol* 179: 1179-1187. S0002-9440(11)00515-3 [pii];10.1016/j.ajpath.2011.05.016 [doi].
48. Bonnet F, Cooper ME (2000) Potential influence of lipids in diabetic nephropathy: insights from experimental data and clinical studies. *Diabetes Metab* 26: 254-264. MDOI-DM-09-2000-26-4-1262-3036-101019-ART1 [pii].
49. Steffes MW, Osterby R, Chavers B, Mauer SM (1989) Mesangial expansion as a central mechanism for loss of kidney function in diabetic patients. *Diabetes* 38: 1077-1081.

Chapter 5

Microvascular damage in type 1 diabetic patients is reversed in the first year after simultaneous pancreas-kidney transplantation

Meriem. Khairoun, Eelco. J.P. de Koning, Bernard. M. van den Berg, E. Lievers,
Hetty. C. de Boer, Alexander. F.M. Schaapherder, Marko. J.K Mallat, Joris. I. Rotmans,
Paul. J.M van der Boog, Anton Jan van Zonneveld, Johan W. de Fijter, Ton J. Rabelink,
Marlies E.J. Reinders

Am J of Transplantation. 13; 1272-1281, 2013

Abstract

Background: Simultaneous pancreas-kidney transplantation (SPK) is an advanced treatment option for type 1 diabetes mellitus (DM) patients with microvascular disease including nephropathy. Sidestream darkfield (SDF) imaging has emerged as a noninvasive tool to visualize the human microcirculation. This study assessed the effect of SPK in diabetic nephropathy (DN) patients on microvascular alterations using SDF and correlated this with markers for endothelial dysfunction.

Methods: Microvascular morphology was visualized using SDF of the oral mucosa in DN (n=26) and SPK patients (n=38), healthy controls (n=20), DM1 patients (n=15, DM \geq 40ml/min) and DN patients with a kidney transplant (KTx, n=15). Furthermore, 21 DN patients were studied longitudinally up to 12 months after SPK. Circulating levels of angiotensin-1 (Ang-1), angiotensin-2 (Ang-2) and soluble thrombomodulin (sTM) were measured using ELISA.

Results: Capillary tortuosity in the DN (1.83 \pm 0.42) and DM \geq 40ml/min (1.55 \pm 0.1) group was increased and showed reversal after SPK (1.31 \pm 0.3, p<0.001), but not after KTx (1.64 \pm 0.1). sTM levels were increased in DN patients and reduced in SPK and KTx recipients (p<0.05), while the Ang-2/Ang-1 ratio was normalized after SPK and not after KTx alone (from 0.16 \pm 0.04 to 0.08 \pm 0.02, p<0.05). Interestingly, in the longitudinal study reversal of capillary tortuosity and decrease in Ang-2/Ang-1 ratio and sTM was observed within 12 months after SPK.

Conclusion: SPK is effective in reversing the systemic microvascular structural abnormalities in DN patients in the first year after transplantation.

Introduction

Diabetes mellitus (DM) is a severe metabolic disease that results in macrovascular as well as microvascular complications including retinopathy, nephropathy and neuropathy (1;2). The majority of these microvascular complications is associated with endothelial dysfunction, and upregulation of different angiogenic growth factors including angiopoietin-2 (Ang-2) (2;3) and soluble thrombomodulin (sTM) release in the circulation (4;5). Negative interference of Ang-2 with Ang-1 mediated Tie-2 signaling results in disruption of perivascular stromal cell–endothelial cell interaction, subsequent vessel destabilization and abnormal microvascular remodeling (6;7).

Simultaneous pancreas-kidney transplantation (SPK) has become an important option in the treatment of diabetic patients with nephropathy and seems to be superior to kidney transplantation alone (KTx), since SPK is associated with a better glycemic control as well as improved patient survival (8-10). It has been shown that SPK and pancreas transplantation alone effectively prevent the recurrence of diabetic nephropathy (DN) (11-15). However, in terms of stabilization or improvement of pre-existing neuropathy and retinopathy debate still continues on the benefit of SPK (16-20). Early non-invasive monitoring of the microvasculature may be of clinical value to assess progression of microvascular disease during diabetes and treatment efficacy after SPK. Sidestream darkfield (SDF) imaging has recently emerged as a non-invasive tool to visualize the human microcirculation and to assess microvascular remodeling (21). We have previously used this validated technique to compare the labial mucosal capillary tortuosity, as markers for microvascular disease, in diabetic patients with and without coronary artery disease (CAD) and healthy non-diabetic controls. Diabetic patients showed increased capillary tortuosity, especially in patients with CAD (22). However, to our knowledge no previous studies have used SDF imaging to monitor microvascular alterations before and after SPK.

In the present study, the effects of SPK on microvascular damage is assessed in a cross-sectional and longitudinal study using SDF imaging and correlated with markers for endothelial dysfunction. We hypothesized that SPK will reverse the microvascular damage in patients with diabetic nephropathy.

Material and Methods

Patients

All procedures were approved by the institutions Medical Ethical Committee. Written informed consent has been obtained from all the patients and healthy controls. A total of 114 persons (64 males and 50 females) were enrolled in this cross-sectional study after giving informed consent. Thirty-eight patients with simultaneous SPK were included (SPK group). Furthermore, we included 15 patients with a functioning kidney graft (KTx group), consisting of patients with a solitary kidney transplantation (n=13) and patients who received SPK and lost their pancreatic graft due to vascular thrombosis (n=2) at 2 and 4 days after transplantation. Biochemical markers for endothelial dysfunction including Ang-1, Ang-2 and sTM, together with mucosal capillary density and morphology were compared to 26 DM type 1 patients with nephropathy (DN group) on the waiting list for SPK and DM type 1 patients with an estimated glomerular filtration rate (eGFR) of ≥ 40 ml/min (n=15, DM ≥ 40 ml/min group). Patients with active infection, liver failure, active auto-immune disease, epilepsy or malignancy in the last 5 years (except patients treated for basal cell carcinoma that were in full remission) were excluded from the study. In addition, 21 patients from the DN group who underwent SPK were studied longitudinally for 12 months (SPKFU). In this group, SDF and the analysis of endothelial dysfunction markers Ang-1, Ang-2 and sTM were assessed at 1 (M1), 6 (M6) and 12 (M12) months after transplantation. Mean age and duration of diabetes were similar in follow-up patients compared to patients in DN-group and SPK-group. Twenty healthy and age matched volunteers served as the control group. None of the control subjects was taking medication.

All transplantations were performed at the Leiden University Medical Center (LUMC), the Netherlands. Organs for the SPK group came from brain-dead donors registered at the national donor registry. The procedure of SPK transplantation has been described previously (23). All SPK transplants were performed through a midline abdominal incision with both organs placed intraperitoneally. The kidney was placed in the left iliac fossa, with its vessels anastomosed to the common or external iliac vessels in an end-to-side fashion. The ureter urinary bladder anastomosis was performed using the Lich–Gregoir technique. Double-J stenting of the anastomosis was used. The portal vein of the pancreas graft was anastomosed end-to-side to the recipient's vena cava inferior or right iliac vessels. The superior mesenteric and splenic arteries were reconstructed using a donor iliac artery Y graft. In some cases, the pancreas graft was procured with the celiac trunk and superior mesenteric artery on the aorta patch in which no vascular reconstruction was needed. All pancreas grafts were anastomosed end-to-side to the common iliac artery of the recipient. In 22 of the 38 patients (58%) patients exocrine pancreatic juices were drained via the bladder, followed by enteric conversion and

the other patients had a direct enteric drainage. SPK patients used at least two types of immunosuppression. Type of induction immunosuppression during transplantation was dependent on date of transplantation. Patients transplanted before 2008 received induction with interleukin-2 receptor blocker daclizumab, (100 mg/day) on the day of transplantation and 10 days after transplantation, followed by triple therapy with prednisone (tapered to a dose of 10 mg by month 3), tacrolimus or cyclosporine and mycophenolate mofetil (MMF) (target area under the curve (AUC) 30-60 ng.h/ml). Cyclosporine and tacrolimus AUC were estimated using a population based, two-compartment pharmacokinetic model combined with limited sampling and Bayesian fitting (24-26). After each AUC assessment, dosage adjustments were made to achieve the predefined target AUC: Cyclosporine AUC: 5400 ng.h/ml within the first 6 wk, which corresponds with a mean average trough level of 225 ng/ml; after 6 wk, 3250 ng.h/ml, which corresponds to a mean average trough level of 125 ng/ml; tacrolimus AUC: 210 ng.h/ml within the first 6 wk, which corresponds to a mean average trough level of 12.5 ng/ml; after 6 wk, 125 ng.h/ml, which corresponds with a mean average trough level of 7.5 ng/ml. Patients transplanted after 2008 received induction therapy with anti-CD52 antibody alemtuzumab (15 mg/day, subcutaneously) for two days followed by glucocorticoid-free therapy with MMF and tacrolimus (n=12). In the SPKFU group, twenty patients received alemtuzumab as induction therapy and one patient received basiliximab (20 mg/day) at day 0 and 4.

Patients that received a KTx were transplanted in the following way: the iliac vessels were reached through a pararectal incision. The donor's renal vessels were anastomosed end-to-side to the common or external iliac vessels of the recipient. The ureter was anastomosed to the urinary bladder using the Lich–Gregoir technique. Double-J stenting for the vesico-ureteric anastomosis was used (27). Patients received daclizumab as induction therapy after solitary KTx (100 mg/day on the day of transplantation and 10 days after transplantation) followed by triple therapy with prednisone (tapered to a dose of 10 mg by 6 weeks), tacrolimus (AUC 210 ng.h/ml first 6 weeks, then 125 ng.h/ml) or cyclosporine (AUC 5400 ng.h/ml first 6 weeks then 3250 ng.h/ml) and MMF (AUC 30-60 ng.h/ml). Patients were treated routinely with oral val-ganciclovir prophylaxis for 3 months, except for a CMV negative donor recipient status.

Microcirculatory imaging

The SDF microscan (MicroVision Medical Inc., Wallingford, PA, U.S.A) was performed as described earlier with minor modifications (22). In short, all patients were measured in supine position in a temperature controlled room (22°C) by a trained observer. Oral mucosal microvasculature in the labial area was visualized with a 5x objective with a 0.2 NA providing a 325-fold magnification on screen and were sized 720 x 576 pixels (8 bit grey-scale). Ten video files (50 frames each) were obtained of capillary loops in labial mucosa from each quadrant of the lips and saved as Y800-AVI files using ICapture imaging software (The Imaging Source Europe GmbH, Bremen, Germany). The portable, handheld device was connected

to a computer and monitor via an analog to digital converter (Domino melody framegrabber, Euresys s.a., Angleur, Belgium). A concise review about the SDF imaging technique has been described previously (21).

Analysis of SDF measurements

Before analysis, the video files were anonymized so that the assessor was blinded to the subject's identity. Capillary loops were assessed by two individual assessors in a randomized, blind fashion. From the forty video files obtained of the microcirculation, the four technically best files were selected from each quadrant of the lip for analysis. Mean vessel density (capillaries/mm²) was calculated by observation of number of vessels per screen shot. Subsequently, tortuosity of capillary loops was assessed according to a validated scoring system described previously and the average of assessed capillary tortuosity was used to calculate mean tortuosity index per patient (22).

Laboratory assessment and endothelial structure evaluation

All persons enrolled in this study underwent routine venous blood sampling before the morning intake of immunosuppression. The following data were evaluated: creatinin, urea, HbA1c, glucose, hemoglobin and proteinuria in 24 hours urine. Glomerular filtration rate was calculated with creatinin concentration using the Modification of Diet in Renal Disease (MDRD) formula. Simultaneously, blood was collected for analysis of serum Ang-1, Ang-2 and sTM. Blood collection tubes were centrifuged for 10 minutes at 3000 rpm after which serum was stored in microcentrifuge tubes at -20°C until required for analysis. Ang-1, Ang-2 and sTM concentrations were measured by enzyme-linked immuno sorbent assay (ELISA) (R&D Systems, Minneapolis, MN, USA and Diaclone Research, Besançon, France) according to the manufacturer supplied protocol. The intra- and inter-assay coefficients of variation were 3.3% and 6.4% for Ang-1, 6.5% and 9.1% for Ang-2 levels and 3.9% and 9.8%, respectively, for sTM levels. Since the Ang-2/Ang-1 ratio, rather than the absolute levels of either cytokine has been considered to determine the functional status of the microvasculature, we calculated this ratio in the different groups (44; 45).

Statistical analyses

Continuous normally distributed data are presented as mean \pm standard error of the mean (SEM), unless stated otherwise. Differences between two groups in the cross-sectional study were analyzed using the unpaired two-sample T-test. When criteria for parametric testing were not met, median and interquartile range (IQR) are presented and tested with the Mann-Whitney test. Categorical variables were analyzed by a Chi-square test. In addition, multivariable linear regression was used to adjust for possible confounders. Comparisons of mean differences between the four time points in the longitudinal SPKFU study were performed using repeated measures ANOVA.

Correlations between interval variables were calculated using the Spearman rank correlation. Differences were considered statistically significant with $p < 0.05$. Data analysis was performed using SPSS version 17.0 (SPSS Inc, Chicago, IL) and GraphPad Prism, version 5.0 (GraphPad Prism Software Inc, San Diego, CA).

Results

Patient characteristics

Baseline subject characteristics of DN, $DM \geq 40$ ml/min, SPK and KTx groups in the cross-sectional study are presented in Table 1. There were no significant differences in patient characteristics between the DN and SPK group, with the exception of age, glucose and HbA1c levels, proteinuria and eGFR ($p < 0.05$). Compared to the $DM \geq 40$ ml/min patients, DN group had significantly higher systolic and diastolic blood pressure, decreased eGFR and proteinuria levels and higher HbA1c levels ($p < 0.05$). As expected, SPK showed improvement in renal function and normalization in blood glucose metabolism compared to DN and $DM \geq 40$ ml/min patients ($p < 0.05$). The median follow up period of patients after SPK was 45.0 months (I.Q.R 18.5-106.5) and after KTx 38.5 months (I.Q.R 8.5-73.5). Patients in the KTx group had significantly better renal function compared with DN patients and higher glucose and HbA1c levels compared with SPK patients.

More than 2 years after transplantation, three patients developed diabetes type II in the SPK group of which two were treated with oral antidiabetic medication and one patient with insulin. Fourteen of the 38 (37%) patients experienced acute rejection after SPK, which is similar to rejection rates reported in other studies after SPK (28). Of these, 10 patients had a renal biopsy proven interstitial acute rejection, one of these patients had also vascular rejection. Four patients were treated as rejection, without prior transplant biopsy. Seven patients were successfully treated with solumedrol, six patients with solumedrol and anti-thymocyte globulin (ATG) and one patient with ATG alone. In the KTx group, no patients developed rejection after transplantation.

Table 1: Patient characteristics of controls, diabetes mellitus Type 1 patients with an eGFR of ≥ 40 ml/min (DM ≥ 40 ml/min), diabetic nephropathy patients (DN), simultaneous pancreas kidney transplantation (SPK) and kidney transplantation (KTx) patients.

	Controls (N=20)	DM ≥ 40 ml/min (N=15)	DN (N=26)	SPK (N=38)	KTx (N=15)
Age (years)	44.8 $\pm 11^c$	54.6 ± 13	43.8 $\pm 6^c$	48.7 $\pm 9^{a,c}$	47.6 ± 10
Sex, male N (%)	10 (50%)	6 (40%)	18 (72%)	25 (66%)	6 (40%)
Smoking, N (%)	0 (0%)	2 (15%)	0 (0%)	3 (8%)	1 (7%)
Median time since transplantation (months) (IQR)	-	-	-	45.0 (18.5-106.5)	38.5 (8.5-73.5)*
Duration Diabetes (yrs)	-	35.5 ± 10	29.3 ± 8	27.9 ± 9	34.9 ± 9
BMI (kg/m ²)	25.3 ± 4	23.8 ± 3	25.2 ± 3	24.4 ± 4	25.0 ± 5
Dialysis, N (%)	-	0 (0%)	4 (5%)	0 (0%)	0 (0%)
Systolic BP (mmHg)	135 ± 18	130 ± 13	145 $\pm 20^c$	141 ± 25	138 ± 29
Diastolic BP (mmHg)	83 $\pm 9^c$	71 ± 8	86 $\pm 11^c$	82 $\pm 13^c$	81 $\pm 14^c$
eGFR (ml/min/1.73 m ²)	92.7 $\pm 16^{b,c,e}$	69.9 ± 24	23.9 $\pm 20^c$	52.7 $\pm 19^{a,c}$	62.0 $\pm 23^a$
Median proteinuria (g/24hr) (IQR)	-	0.3 (0.1-0.3)	0.7 (0.3-1.5) ^c	0.3 (0.2-0.8) ^a	0.2 (0.2-0.4) ^b
HbA1c (%)	-	7.1 ± 1	8.8 $\pm 2^c$	5.6 $\pm 1^{a,c}$	8.5 $\pm 1^{b,c}$
Glucose (mmol/L)	5.3 $\pm 1^{a,c,e}$	12.8 ± 5	13.3 ± 6	5.8 $\pm 3^{a,c}$	13 $\pm 7^d$
Hemoglobin (mmol/L)	8.7 $\pm 1^b$	8.2 ± 1	7.6 ± 1	8.1 ± 1	8.5 ± 1
Rejection after SPK or KTx, N (%)	-	-	-	14 (37%)	1 (7%)
Diabetes after SPK, N (%)	-	-	-	3 (8%)	-
Acetylsalicylic acid, N (%)	-	4 (27%)	4 (15%)	11 (29%)	3 (20%)
Anti-hypertensives, N (%)	-	-	-	-	-
ACE inhibitor	-	0 (0%)	16 (64%)	15 (40%)	7 (47%)
Diuretics	-	5 (33%)	13 (52%)	9 (24%) ^a	4 (27%)
β -blockers	-	0 (0%)	10 (40%) ^c	19 (50%) ^c	6 (40%) ^c
Calcium antagonists	-	2 (13%)	11 (44%) ^c	23 (61%) ^c	7 (47%) ^c
Angiotensin-II antagonists	-	3 (20%)	13 (52%) ^c	8 (21%) ^a	0 (0%) ^a
Statines, N (%)	-	8 (53%)	16 (60%)	27 (71%)	5 (33%) ^d
Steroid-free, Alemtuzumab induction, N (%)	-	-	-	12 (13%)	-
Immunosuppressive, N (%)	-	-	-	-	-
Cyclosporine	-	-	-	13 (34%)	1 (7%) ^d
Tacrolimus	-	-	-	25 (66%)	12 (80%)
Prednisone	-	-	-	27 (71%)	9 (60%)
Azathioprine	-	-	-	3 (8%)	0 (0%)
Everolimus	-	-	-	2 (5%)	0 (0%)
Sirolimus	-	-	-	0 (0%)	1 (7%)
Mycophenolate Mofetil	-	-	-	28 (74%)	14 (93%)

All data are mean \pm SD, unless otherwise specified. * The patients in this group who received SPK lost their pancreas graft after 2 and 4 days following transplantation (n=2).

^a p<0.05 vs DN group ^b p<0.05 vs DN and SPK group ^c p<0.05 vs DM ≥ 40 ml/min ^d p<0.05 vs SPK ^e p<0.05 vs KTx.

BMI, body mass index; BP, blood pressure; ACE, angiotensin converting enzyme; eGFR, estimated glomerular filtration rate; IQR, interquartile range; SPK, simultaneous pancreas kidney transplantation;

Table 2: Patient characteristics in SPKFU patients at 1 (M1), 6 (M6) and 12 (M12) months after SPK transplantation.

Characteristic	M1** (N=21)		M6 (N=21)		M12 (N=21)	
Age (yrs)	44.0	± 6	44.4	± 6	45.0	± 6
Sex, male N (%)	16	(76%)	-		-	
Smoking, N (%)	0		0		0	
BMI (kg/m ²)	23.8*	± 3	24.0	± 2	24.1	± 3*
Dialysis, N (%)	0		0		0	
Systolic BP (mmHg)	123	± 22	132	± 23	130	± 16
Diastolic BP (mmHg)	75	± 13	77	± 13	78	± 6
eGFR (ml/min/1,73 m ²)	56.5	± 23*	55.2	± 15*	54.1	± 10*
Median proteinuria (g/24hr) (IQR)	0.3	(0.3-1.2)	0.3	(0.2-1.0)	0.3	(0.1-0.7)
HbA1c (%)	6.7	± 2	5.3	± 0*	5.4	± 0*
Glucose (mmol/L)	6.2	± 1*	5.3	± 1*	5.7	± 1*
Hemoglobin (mmol/L)	6.6	± 1	7.4	± 1	7.9	± 1
Rejection after transplantation, N (%)	0		3	(14%)	2	(10%)
Diabetes after SPK, N (%)	1	(5%)	2	(10%)	0	
Acetylsalicylic acid, N (%)	3	(14%)	1	(5%)	4	(19%)
Anti-hypertensives, N (%)						
ACE inhibitor	2	(10%)	3	(14%)	4	(19%)
Diuretics	0	(0%)	1	(5%)	2	(10%)
β-blockers	7	(33%)	4	(19%)	4	(19%)
Calcium antagonists	4	(19%)	5	(24%)	8	(38%)
Angiotensin-II antagonists	0		0		0	
Statines, N (%)	2	(10%)	2	(10%)	3	(14%)
Steroid-free, Alemtuzumab induction, N (%)	20	(95%)	-		-	
Immunosuppressive, N (%)						
Tacrolimus	18	(86%)	17	(81%)	16	(76%)
Cyclosporine	2	(5%)	3	(14%)	3	(14%)
Prednisone	1	(5%)	6	(29%)	6	(29%)
Mycophenolate Mofetil	21	(100%)	20	(95%)	20	(95%)
Everolimus	1	(5%)	1	(5%)	2	(10%)

All data are mean ±SD, unless otherwise specified. * p<0.05 vs DN from Table 1. **Patients were recruited from the DN group (see Table 1 for patient characteristics). BMI, body mass index; BP, blood pressure; ACE, angiotensin converting enzyme; eGFR, estimated glomerular filtration rate; IQR, interquartile range; SPK, simultaneous pancreas kidney transplantation;

The clinical characteristics of the patients in the longitudinal SPKFU group are shown in Table 2. As expected, patients showed normalization of glucose levels (p=0.04) and eGFR (p=0.006) at 1 month after SPK. Since all the patients in the SPKFU group were transplanted after 2008, immunosuppressive therapy was initially glucocorticosteroid-free, with MMF and tacrolimus as maintenance therapy. Twelve months after SPK, two patients were converted to everolimus due to side effects of tacrolimus. In four patients treatment with prednisone was added at the time of conversion from tacrolimus to cyclosporine due to side effects caused by

tacrolimus (2 patients) or MMF (2 patients). In this group, five patients experienced interstitial rejection and one patient had also vascular rejection after transplantation. These patients were treated with prednisolone and ATG. Six month after SPK, 2 patient developed diabetes type II, which was treated with oral antidiabetic medication.

Reversibility in capillary tortuosity after SPK

There was no difference in the capillary density in the cross-sectional study between the DN (mean 19.88 ± 4.1 , SEM), $DM \geq 40$ ml/min (mean 19.03 ± 0.5 , SEM), SPK (mean 20.79 ± 3.1 , SEM), control (mean 21.34 ± 3.1 , SEM) and KTx (mean 19.14 ± 0.5 , SEM) group. However, the morphology of the capillaries in the DN and $DM \geq 40$ ml/min patients was significantly disturbed compared to the controls (Fig 1A). We observed significantly more capillary tortuosity in the DN patients (mean 1.83 ± 0.4 , SEM, $p < 0.001$) and $DM \geq 40$ ml/min patients (mean 1.55 ± 0.1 , SEM, $p < 0.0001$) compared to the controls (mean 1.15 ± 0.2 , SEM). After KTx (mean 1.64 ± 0.1 , SEM) there was no significant decrease in capillary tortuosity compared to DN ($p = 0.06$) and $DM \geq 40$ ml/min ($p = 0.3656$) group. However, interestingly, SPK (mean 1.31 ± 0.3 , SEM, $p < 0.001$) showed reversal in capillary tortuosity compared to DN and $DM \geq 40$ ml/min group (Fig 1B). The three patients who developed diabetes type II after SPK did not show more increased capillary tortuosity compared to the other patients in the SPK group.

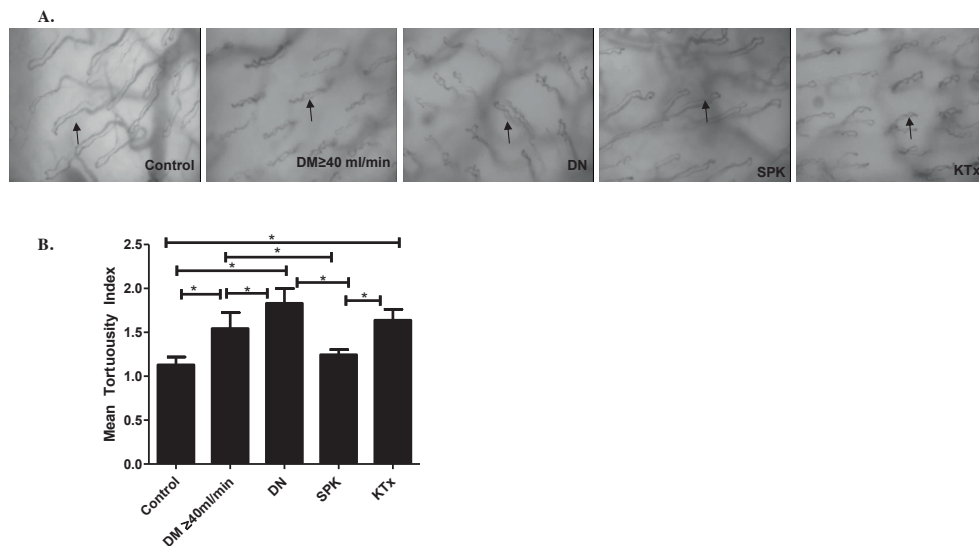
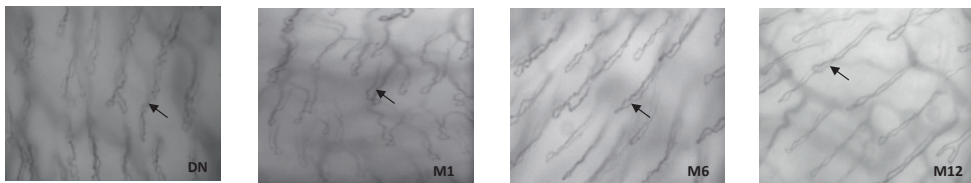


Figure 1. A. Sidestream darkfield images of the oral mucosa visualizing the microvascular capillaries of a representative patient in the control, $DM \geq 40$ ml/min, DN, SPK and KTx group. Black arrows: capillary loops. B. Mean tortuosity index of microvascular capillaries in the control ($n = 20$), $DM \geq 40$ ml/min ($n = 15$), DN ($n = 26$), SPK ($n = 38$) and KTx ($n = 15$) group. Data shown are mean \pm SEM. * $P < 0.05$.

Next, we investigated capillary density and morphology longitudinally in the SPKFU group before, 1, 6 and 12 months after SPK. No difference was observed in capillary density before and after SPK. Most importantly, SPK showed reversal of capillary tortuosity within 1 year after SPK, reaching significance at 6 and 12 months after transplantation (mean 1.52 ± 0.1 , SEM and 1.23 ± 0.0 versus DN 1.83 ± 0.4 , $p < 0.01$ and $p < 0.001$, respectively) (Fig 2AB). The differences remained significant in both the cross-sectional and SPKFU group after adjustment for age, sex, BMI body mass index (BMI), systolic and diastolic blood pressure and smoking.

A.



B.

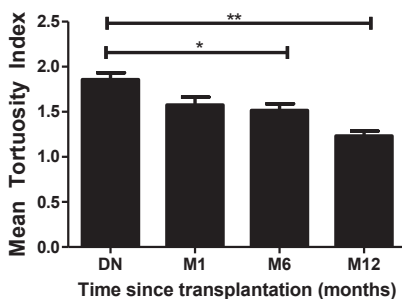


Figure 2. A. Sidestream dark field images of the oral mucosa visualizing the microvascular capillaries of a representative DN patient before (DN), 1 (M1), 6 (M6) and 12 (M12) months after SPK in the longitudinal SPKFU group. Black arrows: capillary loops. B. Longitudinal course of the mean tortuosity index of microvascular capillaries in DN patients before (DN, n=26), 1 (M1, n=21), 6 (M6, n=21) and 12 (M12, n=21) months after SPK in the SPKFU group. Data shown are mean \pm SEM. * $P < 0.01$, M6 compared to DN. ** $P < 0.001$, M12 compared to DN.

Correlation between tortuosity, Hb1Ac, renal function and previous rejection

Next, correlation analyses in the SPK patients was performed for the capillary density and tortuosity index with several factors that are known to influence the microvasculature, including time since transplantation, eGFR, HbA1c, proteinuria, and previous rejection. No correlation was found between capillary density and time since transplantation, eGFR, HbA1c, proteinuria and previous rejection. There was a significant correlation between tortuosity with eGFR ($r = -0.26$, $p = 0.005$), HbA1c levels ($r = 0.40$, $p < 0.0001$) and previous rejection ($p = 0.0160$). There was no association between tortuosity index and time since transplantation or proteinuria (data not shown).

Reversal to baseline of Ang-2/Ang-1 ratio after SPK

To evaluate the effects of SPK on the microvascular conditions, we also measured serum levels of sTM, Ang-1 and Ang-2 and calculated the Ang-2/Ang-1 ratio as markers for endothelial dysfunction. We detected a significant decrease in sTM levels in patients after SPK (mean 9.7 ± 1 ng/ml, SEM, $p=0.004$) and KTx (mean 6.3 ± 1 ng/ml, SEM, $p<0.0001$) compared to DN patients (mean 15.2 ± 1 ng/ml, SEM, $p=0.004$) (Fig 3A). In the SPKFU group, sTM levels started to decrease at 1 month (mean 13.35 ± 2.0 ng/ml, SEM) after transplantation and remained low after 6 months (mean 11.83 ± 1.6 ng/ml, SEM), reaching significance at 12 months (10.42 ± 1.2 ng/ml, SEM) as compared to before SPK (mean 15.2 ± 1 ng/ml, SEM, $p<0.01$) (Fig 3B). In addition, our results demonstrate normalization in Ang-2/Ang-1 ratio after SPK (mean 0.08 ± 0.02 , SEM) compared to the DN (mean 0.16 ± 0.04 , SEM, $p=0.04$) and $DM \geq 40$ ml/min patients (mean 0.16 ± 0.04 , SEM, $p=0.03$), but no significant decrease after KTx (mean 0.20 ± 0.04 , SEM, $p=0.6219$ and $p=0.5437$, respectively) (Fig 3C). In the longitudinal study, the Ang-2/Ang-1 ratio started to show a decrease at 6 months (mean 0.09 ± 0.03 , SEM) after SPK and remained decreased at 12 months (mean 0.09 ± 0.02 , SEM) following transplantation compared to before SPK (mean 0.16 ± 0.04 , SEM), however, statistical significance was not reached ($p=0.13$ and $p=0.14$, respectively) (data not shown).

Correlation of endothelial function markers with capillary tortuosity, renal function and HbA1c

Next, the correlation between the different endothelial dysfunction markers, capillary density and morphology, eGFR, HbA1c, previous rejection and time since transplantation was analyzed. No correlation between endothelial dysfunction markers and capillary density or tortuosity was found. Moreover, there was no correlation between time since transplantation, previous rejection and endothelial dysfunction markers. Increased Ang-2 and sTM levels correlated significantly with decreased eGFR ($r= -0.53$, $p<0.0001$ and $r=-0.28$, $p=0.0083$) and high Hb1Ac levels with increased Ang-2 ($r= 0.23$, $p=0.0319$). Interestingly, Ang-2/Ang-1 ratio correlated significantly with capillary tortuosity ($r=0.21$, $p=0.0348$), HbA1c ($r=0.32$, $p=0.0038$), eGFR ($r=-0.29$, $p=0.0460$) and proteinuria levels ($r=0.2640$, $p=0.0365$) (data not shown).

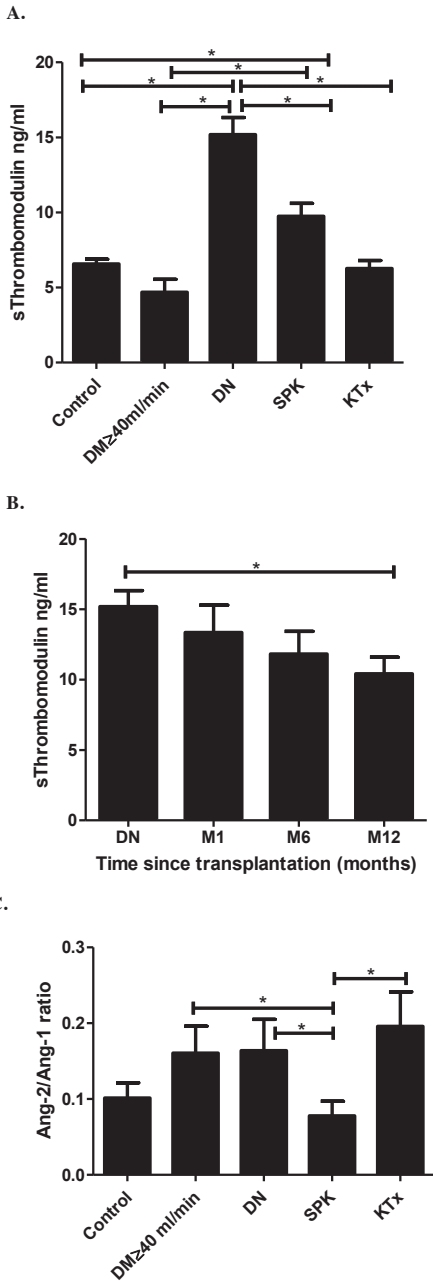


Figure 3. A. Soluble thrombomodulin serum levels in the control (n=20), DM≥40ml/min (n=15), DN (n=26), SPK (n=38) and KT_x (n=15) group. *P<0.05. B. Soluble thrombomodulin serum levels in DN patients before (DN), 1 (M1), 6 (M6) and 12 (M12) months after SPK in the SPKFU group. *P<0.05 compared to DN. C. Ang-2/ Ang-1 ratio in the control (n=20), DM≥40ml/min (n=15), DN (n=26), SPK (n=38) and KT_x (n=15) group. Data shown are mean±SEM. *P<0.05.

Discussion

This study shows increased microvascular tortuosity using SDF imaging, and a dysbalance in Ang-2/Ang-1 ratio in DM type 1 patients. Interestingly, we demonstrated reversal of capillary tortuosity and normalization of the Ang-2/Ang-1 ratio after SPK, but not after KTx alone. Furthermore, increased microvascular tortuosity correlated with increased Ang-2/Ang-1 ratio. Importantly, the longitudinal study demonstrated that both reversibility of microvascular damage and decrease in sTM and Ang-2/Ang-1 balance occurred in the first year after SPK. These findings suggest that SPK is effective in reversing systemic microvascular complications in DN patients early after transplantation. Assessment of capillary tortuosity, as marker for microvascular disease, using the non-invasive SDF imaging can be used to estimate the degree of microvascular derangements in DN patients before and after SPK.

Microvascular disease is one of the most important drivers of diabetic complications (29;30). Several mechanisms have been described for the pathogenesis of microvascular disorders in patients with diabetes mellitus. The capillaries in diabetic patients tend to be leaky and tortuous, lacking the hierarchical arrangement of arteries, capillaries and venules due to perivascular stromal cell loss (31-33). Hyperglycemia in particular can initiate disturbances in blood flow and afflict the interaction between perivascular stromal cells and microvascular endothelial cells. Hereby, the loss of perivascular stromal cells leads to loss of its primary functions, including autoregulation of the vessel integrity and compensatory mechanisms for the fluctuating hydrostatic pressure. Specifically, this impaired auto regulation of the microvasculature could result in disruption of the basement membrane and the failure to maintain the stability of the vessel wall against irregular longitudinal traction and transmural pressure leading to dilated and tortuous vessels (32-38). Ang-2 has been assumed to destabilize vessels by promoting the weakening of perivascular stromal - endothelial cell interaction (39;40).

The increased microvascular tortuosity in diabetes as observed in the present study concurs with previous data on microvascular alterations in diabetic patients as determined by skin capillaroscopy (41). Likewise, previous clinical observations using conventional capillaroscopy revealed that diabetic retinopathy appeared to be associated with increased tortuosity as well, suggesting that this might be an early sign of microvascular damage in diabetes (33). However, compared to conventional capillaroscopy, SDF imaging has the advantage to assess the microvasculature without injecting fluorescent dyes and it enables measurement of the superficial skin and mucous microcirculation in a noninvasive manner (21). We previously could demonstrate, using SDF measurements, that the presence of microvascular tortuosity is associated with macrovascular disease in diabetics (22). However, the extensiveness of microvascular abnormalities has not been measured in DN patients before and after SPK using SDF imaging and correlation with markers for endothelial dysfunction and clinical features has not been performed yet.

Previous clinical studies showed that 10 years of normoglycemia after pancreas transplantation ameliorated the glomerular and tubular lesions that characterize diabetic nephropathy in patients with long-term type 1 diabetes who did not receive renal grafts (42). Additional studies provided evidence for improvement of diabetic polyneuropathy after pancreatic transplantation as well (43;44). Although we observed reversal of microvascular tortuosity after SPK, this study did not explore the mechanisms behind these improvements.

Increased microvascular tortuosity in DN coincided with increased levels of sTM and a disturbed Ang-2/Ang-1 balance, which is in line with previous studies that have demonstrated a positive correlation with microvascular destabilization and these markers of endothelial dysfunction (45;46). Ang-2 is a competitive ligand for the same Tie-2 receptor as for Ang-1, with competing, antagonistic effects on angiogenesis and microvascular remodeling. Increased Ang-2/Ang-1 ratio has been shown to be associated with hyperglycemia, chronic kidney disease, acute coronary syndrome, sepsis and variety of diseases known for their common characteristic of endothelial dysfunction and microvascular inflammation (45;46). The Ang-2/ Ang-1 ratio showed only normalization after SPK, while it was still increased in the presence of diabetes and also was not affected by kidney transplantation alone. In addition, the Ang-2/Ang-1 ratio correlated to capillary tortuosity underscoring the systemic nature of microvascular destabilization in diabetes. (4;5;47-50). (51).

The strength of our study was the use of a noninvasive tool to visualize the microvasculature in a study of SPK and DN patients before and after transplantation. However, our study has also some limitations. In this studied cohort there were no patients who received a solitary kidney transplant that could be followed longitudinally. Therefore, future longitudinal studies should possibly also include such patients to further corroborate the potential contribution of reversal of diabetes on the microcirculation.

In conclusion, the present study revealed a disturbed microvascular morphology in DM type 1 patients and SPK resulted in reversal of systemic microvascular derangements and normalization of markers for endothelial dysfunction. The use of SDF imaging allows for easy non-invasive and sequential monitoring of microvascular disease in patients with diabetes.

Acknowledgments

This work was supported by a Veni grant from ZonMW to M.E.J.R.

References

- (1) Cumbie BC, Hermayer KL. Current concepts in targeted therapies for the pathophysiology of diabetic microvascular complications. *Vasc Health Risk Manag* 2007;3(6):823-32.
- (2) Tooke JE. Microvasculature in diabetes. *Cardiovasc Res* 1996 Oct;32(4):764-71.
- (3) Rabelink TJ, de Boer HC, van Zonneveld AJ. Endothelial activation and circulating markers of endothelial activation in kidney disease. *Nat Rev Nephrol* 2010 Jul;6(7):404-14.
- (4) Iwashima Y, Sato T, Watanabe K, Ooshima E, Hiraishi S, Ishii H, et al. Elevation of plasma thrombomodulin level in diabetic patients with early diabetic nephropathy. *Diabetes* 1990 Aug;39(8):983-8.
- (5) Oida K, Takai H, Maeda H, Takahashi S, Tamai T, Nakai T, et al. Plasma thrombomodulin concentration in diabetes mellitus. *Diabetes Res Clin Pract* 1990 Oct;10(2):193-6.
- (6) Fiedler U, Augustin HG. Angiopoietins: a link between angiogenesis and inflammation. *Trends Immunol* 2006 Dec;27(12):552-8.
- (7) Hammes HP, Lin J, Renner O, Shani M, Lundqvist A, Betsholtz C, et al. Pericytes and the pathogenesis of diabetic retinopathy. *Diabetes* 2002 Oct;51(10):3107-12.
- (8) Jukema JW, Smets YF, van der Pijl JW, Zwinderman AH, Vliegen HW, Ringers J, et al. Impact of simultaneous pancreas and kidney transplantation on progression of coronary atherosclerosis in patients with end-stage renal failure due to type 1 diabetes. *Diabetes Care* 2002 May;25(5):906-11.
- (9) Smets YF, Westendorp RG, van der Pijl JW, de Charro FT, Ringers J, de Fijter JW, et al. Effect of simultaneous pancreas-kidney transplantation on mortality of patients with type-1 diabetes mellitus and end-stage renal failure. *Lancet* 1999 Jun 5;353(9168):1915-9.
- (10) Sollinger HW, Odorico JS, Becker YT, D'Alessandro AM, Pirsch JD. One thousand simultaneous pancreas-kidney transplants at a single center with 22-year follow-up. *Ann Surg* 2009 Oct;250(4):618-30.
- (11) Becker BN, Brazy PC, Becker YT, Odorico JS, Pintar TJ, Collins BH, et al. Simultaneous pancreas-kidney transplantation reduces excess mortality in type 1 diabetic patients with end-stage renal disease. *Kidney Int* 2000 May;57(5):2129-35.
- (12) Bohman SO, Tyden G, Wilczek H, Lundgren G, Jaremko G, Gunnarsson R, et al. Prevention of kidney graft diabetic nephropathy by pancreas transplantation in man. *Diabetes* 1985 Mar;34(3):306-8.
- (13) Nyumura I, Honda K, Babazono T, Taneda S, Horita S, Teraoka S, et al. A long-term prevention of diabetic nephropathy in a patient with type 1 diabetes after simultaneous pancreas and kidney transplantation. *Clin Transplant* 2009 Aug;23 Suppl 20:54-7.
- (14) Tyden G, Bolinder J, Solders G, Brattstrom C, Tibell A, Groth CG. Improved survival in patients with insulin-dependent diabetes mellitus and end-stage diabetic nephropathy 10 years after combined pancreas and kidney transplantation. *Transplantation* 1999 Mar 15;67(5):645-8.
- (15) Wilczek HE, Jaremko G, Tyden G, Groth CG. Evolution of diabetic nephropathy in kidney grafts. Evidence that a simultaneously transplanted pancreas exerts a protective effect. *Transplantation* 1995 Jan 15;59(1):51-7.
- (16) Brekke IB, Ganes T, Syrdalen P, Egge K, Dyrbekk D, Flatmark A. Combined renal and pancreatic transplantation: effects on advanced diabetic neuropathy and retinopathy. *Life Support Syst* 1985;3 Suppl 1:680-4.
- (17) Mehra S, Tavakoli M, Kallinikos PA, Efron N, Boulton AJ, Augustine T, et al. Corneal confocal microscopy detects early nerve regeneration after pancreas transplantation in patients with type 1 diabetes. *Diabetes Care* 2007 Oct;30(10):2608-12.

- (18) Navarro X, Sutherland DE, Kennedy WR. Long-term effects of pancreatic transplantation on diabetic neuropathy. *Ann Neurol* 1997 Nov;42(5):727-36.
- (19) Pearce IA, Ilango B, Sells RA, Wong D. Stabilisation of diabetic retinopathy following simultaneous pancreas and kidney transplant. *Br J Ophthalmol* 2000 Jul;84(7):736-40.
- (20) Solders G, Wilczek H, Gunnarsson R, Tyden G, Persson A, Groth CG. Effects of combined pancreatic and renal transplantation on diabetic neuropathy: a two-year follow-up study. *Lancet* 1987 Nov 28;2(8570):1232-5.
- (21) Goedhart PT, Khalilzada M, Bezemer R, Merza J, Ince C. Sidestream Dark Field (SDF) imaging: a novel stroboscopic LED ring-based imaging modality for clinical assessment of the microcirculation. *Opt Express* 2007 Nov 12;15(23):15101-14.
- (22) Djaber R, Schuijff JD, de Koning EJ, Wijewickrama DC, Pereira AM, Smit JW, et al. Non-invasive assessment of microcirculation by sidestream dark field imaging as a marker of coronary artery disease in diabetes. *Diab Vasc Dis Res* 2012 May 23.
- (23) Marang-van de Mheen PJ, Nijhof HW, Khairoun M, Haasnoot A, van der Boog PJ, Baranski AG. Pancreas-kidney transplantations with primary bladder drainage followed by enteric conversion: graft survival and outcomes. *Transplantation* 2008 Feb 27;85(4):517-23.
- (24) Cremers SC, Scholten EM, Schoemaker RC, Lentjes EG, Vermeij P, Paul LC, et al. A compartmental pharmacokinetic model of cyclosporin and its predictive performance after Bayesian estimation in kidney and simultaneous pancreas-kidney transplant recipients. *Nephrol Dial Transplant* 2003 Jun;18(6):1201-8.
- (25) Scholten EM, Cremers SC, Schoemaker RC, Rowshani AT, van Kan EJ, den HJ, et al. AUC-guided dosing of tacrolimus prevents progressive systemic overexposure in renal transplant recipients. *Kidney Int* 2005 Jun;67(6):2440-7.
- (26) Rowshani AT, Scholten EM, Bemelman F, Eikmans M, Idu M, Roos-van Groningen MC, et al. No difference in degree of interstitial Sirius red-stained area in serial biopsies from area under concentration-over-time curves-guided cyclosporine versus tacrolimus-treated renal transplant recipients at one year. *J Am Soc Nephrol* 2006 Jan;17(1):305-12.
- (27) Khairoun M, Baranski AG, van der Boog PJ, Haasnoot A, Mallat MJ, Marang-van de Mheen PJ. Urological complications and their impact on survival after kidney transplantation from deceased cardiac death donors. *Transpl Int* 2009 Feb;22(2):192-7.
- (28) Malaise J, Arbogast H, Illner WD, Tarabichi A, Dieterle C, Landgraf R, et al. Simultaneous pancreas-kidney transplantation: analysis of rejection. *Transplant Proc* 2005 Jul;37(6):2856-8.
- (29) Cheung AT, Perez RV, Chen PC. Improvements in diabetic microangiopathy after successful simultaneous pancreas-kidney transplantation: a computer-assisted intravital microscopy study on the conjunctival microcirculation. *Transplantation* 1999 Oct 15;68(7):927-32.
- (30) Kuryliszyn-Moskal A, Dubicki A, Zarzycki W, Zonnenberg A, Gorska M. Microvascular abnormalities in capillaroscopy correlate with higher serum IL-18 and sE-selectin levels in patients with type 1 diabetes complicated by microangiopathy. *Folia Histochem Cytobiol* 2011;49(1):104-10.
- (31) Bergers G, Song S. The role of pericytes in blood-vessel formation and maintenance. *Neuro Oncol* 2005 Oct;7(4):452-64.
- (32) Boone MI, Farber ME, Jovanovic-Peterson L, Peterson CM. Increased retinal vascular tortuosity in gestational diabetes mellitus. *Ophthalmology* 1989 Feb;96(2):251-4.
- (33) Sasongko MB, Wong TY, Nguyen TT, Cheung CY, Shaw JE, Wang JJ. Retinal vascular tortuosity in persons with diabetes and diabetic retinopathy. *Diabetologia* 2011 May 29.
- (34) Dobrin PB, Schwarcz TH, Baker WH. Mechanisms of arterial and aneurysmal tortuosity. *Surgery* 1988 Sep;104(3):568-71.
- (35) Hanahan D. Signaling vascular morphogenesis and maintenance. *Science* 1997 Jul 4;277(5322):48-50.

- (36) Jackson ZS, Dajnowiec D, Gottlieb AI, Langille BL. Partial off-loading of longitudinal tension induces arterial tortuosity. *Arterioscler Thromb Vasc Biol* 2005 May;25(5):957-62.
- (37) Kohner EM, Patel V, Rassam SM. Role of blood flow and impaired autoregulation in the pathogenesis of diabetic retinopathy. *Diabetes* 1995 Jun;44(6):603-7.
- (38) Kristinsson JK, Gottfredsdottir MS, Stefansson E. Retinal vessel dilatation and elongation precedes diabetic macular oedema. *Br J Ophthalmol* 1997 Apr;81(4):274-8.
- (39) Cai J, Kehoe O, Smith GM, Hykin P, Boulton ME. The angiotensin/Tie-2 system regulates pericyte survival and recruitment in diabetic retinopathy. *Invest Ophthalmol Vis Sci* 2008 May;49(5):2163-71.
- (40) Hughes S, Gardiner T, Baxter L, Chan-Ling T. Changes in pericytes and smooth muscle cells in the kitten model of retinopathy of prematurity: implications for plus disease. *Invest Ophthalmol Vis Sci* 2007 Mar;48(3):1368-79.
- (41) Meyer MF, Pfohl M, Schatz H. [Assessment of diabetic alterations of microcirculation by means of capillaroscopy and laser-Doppler anemometry]. *Med Klin (Munich)* 2001 Feb 15;96(2):71-7.
- (42) Fioretto P, Steffes MW, Sutherland DE, Goetz FC, Mauer M. Reversal of lesions of diabetic nephropathy after pancreas transplantation. *N Engl J Med* 1998 Jul 9;339(2):69-75.
- (43) Kennedy WR, Navarro X, Goetz FC, Sutherland DE, Najarian JS. Effects of pancreatic transplantation on diabetic neuropathy. *N Engl J Med* 1990 Apr 12;322(15):1031-7.
- (44) Martinenghi S, Comi G, Galardi G, Di C, V, Pozza G, Secchi A. Amelioration of nerve conduction velocity following simultaneous kidney/pancreas transplantation is due to the glycaemic control provided by the pancreas. *Diabetologia* 1997 Sep;40(9):1110-2.
- (45) David S, John SG, Jefferies HJ, Sigrist MK, Kumpers P, Kielstein JT, et al. Angiotensin-2 levels predict mortality in CKD patients. *Nephrol Dial Transplant* 2012 May;27(5):1867-72.
- (46) Tuo QH, Zeng H, Stinnett A, Yu H, Aschner JL, Liao DF, et al. Critical role of angiotensin/Tie-2 in hyperglycemic exacerbation of myocardial infarction and impaired angiogenesis. *Am J Physiol Heart Circ Physiol* 2008 Jun;294(6):H2547-H2557.
- (47) David S, Kumpers P, Hellpap J, Horn R, Leitolf H, Haller H, et al. Angiotensin 2 and cardiovascular disease in dialysis and kidney transplantation. *Am J Kidney Dis* 2009 May;53(5):770-8.
- (48) David S, Kumpers P, Lukasz A, Fliser D, Martens-Lobenhoffer J, Bode-Boger SM, et al. Circulating angiotensin-2 levels increase with progress of chronic kidney disease. *Nephrol Dial Transplant* 2010 Aug;25(8):2571-6.
- (49) Keven K, Elmaci S, Sengul S, Akar N, Egin Y, Genc V, et al. Soluble endothelial cell protein C receptor and thrombomodulin levels after renal transplantation. *Int Urol Nephrol* 2010 Dec;42(4):1093-8.
- (50) Lip PL, Chatterjee S, Caine GJ, Hope-Ross M, Gibson J, Blann AD, et al. Plasma vascular endothelial growth factor, angiotensin-2, and soluble angiotensin receptor tie-2 in diabetic retinopathy: effects of laser photocoagulation and angiotensin receptor blockade. *Br J Ophthalmol* 2004 Dec;88(12):1543-6.
- (51) Patel JI, Hykin PG, Gregor ZJ, Boulton M, Cree IA. Angiotensin concentrations in diabetic retinopathy. *Br J Ophthalmol* 2005 Apr;89(4):480-3.

Chapter 6

Improvement of microvascular damage after living donor kidney-transplantation

M. Khairoun, B.M. van den Berg, R. Timal, E. Lievers, D.K de Vries, J.I. Rotmans,
M.J.K. Mallat, A.P.J. de Vries, J.W. de Fijter, A.J. van Zonneveld, T.J. Rabelink,
M.E.J. Reinders.

In preparation

Abstract

Background: Chronic kidney disease (CKD) is associated with endothelial damage and microvascular destabilization. Recently, sidestream dark-field (SDF) imaging has emerged as a noninvasive tool to visualize the microcirculation. In this study, we investigated whether CKD is associated with systemic microvascular damage using SDF imaging. In addition, the effects of kidney transplantation (KTx) on microvascular alterations was studied.

Methods: Mean capillary density and microvascular morphology were visualized with SDF imaging of the oral mucosa. Twenty-eight CKD patients were studied longitudinally before (CKD), 1, 6 and 12 months after living donor KTx. Furthermore, circulating levels of growth factors that control microvascular structure, including Angiopoietin-2 (Ang-2) and soluble Thrombomodulin (sTM) were measured using ELISA.

Results: We found increased capillary tortuosity in CKD patients compared to controls and reversibility starting at 6 months after KTx (respectively mean 1.9 ± 0 , SEM and 1.6 ± 0 , $p < 0.05$). In line with these findings, endothelial destabilization markers Ang-2 (4084 ± 612 pg/ml) and sTM (19 ± 6 ng/ml) were increased in CKD patients and showed an improvement starting at 1 month after KTx (2263 ± 316 pg/ml and 6.1 ± 1 ng/ml respectively, $p < 0.05$).

Conclusion: The microcirculation, as assessed by SDF, was disturbed in CKD patients compared to controls. Interestingly, KTx resulted in an improvement of microvascular tortuosity and normalization of angiogenic growth factors. Our findings indicate a clinical implication of SDF imaging to assess microvascular alterations in CKD patients before and after KTx.

Introduction

Progressive renal disease is characterized by a loss of the microvasculature, which is associated with the development of glomerular and tubulointerstitial scarring. The development of tubulointerstitial fibrosis is characteristic of chronic kidney disease (CKD) of diverse etiologies, and inhibition of its progression has been proposed to be of major importance in the preservation of renal function. In both experimental animal models and in humans, it has been shown that a significant loss of peritubular capillaries as well as defective capillary repair, triggers development of fibrotic changes and ultimately scar formation with progressive renal dysfunction (1;2). Besides renal microvascular abnormalities, patients with CKD demonstrate abnormalities which may represent manifestations of ongoing systemic microvascular damage, including a dysbalance of angiogenic factors and an increased incidence of atherosclerosis (3).

The microvasculature is relatively inaccessible to direct examination. Therefore investigators have concentrated on various surrogate markers of endothelial function which include the measurement of specific plasma markers including, circulating endothelial cells (CECs), angiopoietin-1 (Ang-1), Angiopoietin-2 (Ang-2) and soluble Thrombomodulin (sTM) (4-8). Competitive inhibition of Ang-2 to the Tie-2 receptor, destabilizes quiescent endothelium and leads to altered endothelial/pericyte interaction with subsequently abnormal microvascular remodeling (9-11). Different studies have assessed the expression of these factors in CKD and after kidney transplantation (KTx). Indeed, elevated circulating levels of Ang-2 and sTM were observed in CKD patients, which normalized after kidney transplantation (5;7).

An additional method for the assessment of endothelial function in CKD patients includes monitoring of the systemic microcirculation. Recently, SDF imaging has been used to visualize the human circulation (10;12). Using this non-invasive technique, we could previously demonstrate that patients with diabetes mellitus (DM) had significantly more microvascular damage compared to healthy controls and simultaneous pancreas-kidney transplantation (SPK) resulted in restoration of microvascular damage (10). However, there are no studies using SDF imaging in CKD patients, to monitor microvascular alterations before and after KTx. The aim of our study was to use this validated SDF imaging technique to compare the labial mucosal capillary tortuosity, as markers for microvascular disease, in patients with CKD. In addition, we investigated whether KTx improves the microvasculature, in a prospective longitudinal study up to 1 year after transplantation. Furthermore, we assessed whether microvascular alterations were associated with increase in endothelial dysfunction markers. We hypothesize that CKD patients have a disturbed systemic microvasculature and that KTx will reverse microvascular damage.

Material and Methods

Patients

All procedures were approved by the institutions Medical Ethical Committee. Written informed consent was obtained from all the patients and healthy controls. A total of 48 persons (30 males and 18 females) were enrolled in the current longitudinal study after giving informed consent. We included 28 CKD patients with different dialysis modalities who were receiving a living donor KTx including 11 patients on hemodialysis (HD), 4 peritoneal dialysis (PD) patients and 13 preemptive kidney transplant recipients. Biochemical markers for endothelial dysfunction including Ang-2 and sTM, together with mucosal capillary density and morphology were compared to healthy and age matched volunteers who served as control group. None of the control subjects was taking medication. Patients with active infection, liver failure, active auto-immune disease, epilepsy or malignancy in the last 5 years (except patients treated for basal cell carcinoma that were in full remission) were excluded from the study. SDF measurements and the analysis of endothelial dysfunction markers were assessed prior to transplantation (CKD), and 1 (M1), 6 (M6) and 12 (M12) months after transplantation.

Transplantation aspects

All kidney transplantations were performed at the Leiden University Medical Center (LUMC) between 2010 and 2012 in the Netherlands. Kidney transplantation was performed as described previously (10). Patients were treated with basiliximab as induction therapy (20 mg on the day of transplantation and 4 days after transplantation) followed by triple therapy with prednisone (tapered to a dose of 10 mg by 6 weeks), tacrolimus (area under the curve (AUC) 210 ng.h/ml first 6 weeks, then 125 ng.h/ml) or cyclosporine (AUC 5400 ng.h/ml first 6 weeks then 3250 ng.h/ml) and mycophenolate mofetil (MMF) (AUC 30-60 ng.h/ml). Patients were treated routinely with oral valganciclovir prophylaxis for 3 months, except for cytomegalovirus (CMV) negative recipients receiving a CMV-negative graft.

Microcirculatory imaging and analysis of SDF measurements

The SDF microscan (MicroVision Medical Inc., Wallingford, PA, U.S.A) and analyses were performed as described earlier (10;13).

Laboratory assessment and endothelial structure evaluation

All persons enrolled in this study underwent routine venous blood sampling before the morning intake of immunosuppression. The following data were evaluated: creatinin, urea, HbA1c, glucose, hemoglobin and proteinuria in 24 hours urine. Glomerular filtration rate (eGFR) was calculated with creatinin concentration using the Modification of Diet in Renal Disease (MDRD) formula. Simultaneously, blood was collected for analysis of serum Ang-2

and sTM. Blood collection tubes were centrifuged for 10 minutes at 3000 rpm after which serum was stored in microcentrifuge tubes at -20°C until required for analysis. Ang-2 and sTM concentrations were measured by enzyme-linked immuno sorbent assay (ELISA) (R&D Systems, Minneapolis, MN, USA and Diaclone Research, Besançon, France) according to the manufacturer supplied protocol. The intra- and inter-assay coefficients of variation were 6.5% and 9.1% for Ang-2 levels and 3.9% and 9.8%, respectively, for sTM levels.

Statistical analyses

Continuous normally distributed data are presented as mean \pm SEM, unless stated otherwise. Comparisons of mean differences between the four time points in the longitudinal study were performed using repeated measures ANOVA. Correlations between interval variables were calculated using the Spearman rank correlation. Differences between 2 groups were analyzed using the unpaired two-sample T-test. When criteria for parametric testing were not met, median and interquartile range (IQR) are presented and tested with the Mann-Whitney test. Categorical variables were analyzed by a Chi-square test. In addition, multivariable linear regression was used to adjust for possible confounders. Differences were considered statistically significant with $p < 0.05$. Data analysis was performed using SPSS version 17.0 (SPSS Inc, Chicago, IL) and GraphPad Prism, version 5.0 (GraphPad Prism Software Inc, San Diego, CA).

Results

Patient characteristics

Baseline characteristics are shown in Table 1. There were no significant differences between CKD patients and healthy controls, with exception for eGFR and hematocrit levels ($p < 0.05$). As expected, KTx showed improvement of eGFR and proteinuria ($p < 0.05$). After transplantation, 2 patients experienced interstitial rejection treated with methylprednisolone. In total 4 patients developed diabetes type II (1 patient at M1; 3 patients at M6) treated with oral antidiabetics or insulin. In 3 patients diabetes mellitus was resolved at 12 months after transplantation. HbA1c levels were not significantly different after KTx compared to before transplantation ($p > 0.05$).

Table 1: Patient characteristics of controls and chronic kidney disease patients before (CKD), 1 month (M1), 6 months (M6) and 12 months (M12) after kidney transplantation.

Patients characteristics	Controls (N=20)	CKD (N=28)	M1 (N=28)	M6 (N=28)	M12 (N=28)
Age (years)	44.8 ±1	47.1 ±14	47.3 ±14	47.8 ±14	48.8 ±14
Sex, male N (%)	10 (50%)	20 (71%)	-	-	-
Smoking, N (%)	0 (0%)	3 (11%)	-	-	-
Primary kidney disease, N (%)	-	-	-	-	-
Glomerulonephritis		7 (25%)			
Focal segmental glomerulosclerosis		5 (18%)			
Urologic		2 (7%)			
Polycystic kidney disease		7 (25%)			
Hypertension		2 (7%)			
Unknown		4 (14%)			
Other		1 (4%)			
BMI (kg/m ²)	25.3 ±4	26.4 ±4	25.9 ±4	26.9 ±4	27.0 ±4
Dialysis, N (%)	-		0 (0%)	0 (0%)	0 (0%)
HD		11 (40%)			
PD		4 (14%)			
Preemptive		13 (46%)			
Median dialysis duration (years)	-	1.0 (1.0-2.0)	-	-	-
Systolic BP (mmHg)	135 ±18	138 ±15	131 ±18	131 ±12	134 ±1
Diastolic BP (mmHg)	83 ±9	84 ±12	78 ±7	79 ±7	81 ±8
eGFR (ml/min/1.73 m ²)	92 ±16	8.8 ±4*	51.7 ±15**	53.5 ±13**	54.3 ±14**
Median proteinuria (g/24hr) (IQR)	-	1.5 (0.8-2.4)	0.2 (0.2-0.3)#	0.2 (0.2-0.4)#	0.2 (0.2-0.3)#
HbA1c (%)	-	5.2 ±0	5.3 ±1	5.5 ±1	5.6 ±1
Glucose (mmol/L)	5.3 ±1	5.3 ±1	6.0 ±2	5.7 ±1	5.8 ±2
Hematocrit (L/L)	0.4 ±0	0.4 ±0	0.4 ±0	0.4 ±0	0.4 ±0
Anti-hypertensives, N (%)	-				
ACE inhibitor		13 (46%)	3 (11%)	6 (21%)	8 (29%)
Diuretics		18 (64%)	1 (4%)	5 (18%)	4 (14%)
β-blockers		10 (36%)	12 (43%)	9 (32%)	7 (25%)
Calcium antagonists		12 (43%)	21 (75%)	20 (71%)	16 (57%)
Angiotensin-II antagonists		10 (36%)	2 (7%)	3 (11%)	7 (25%)
Statines, N (%)	-	13 (46%)	4 (14%)	10 (36%)	10 (36%)
Acetylsalicylic acid, N (%)	-	6 (21%)	3 (10%)	2 (7%)	2 (7%)
Immunosuppressive, N (%)	-	-			
Cyclosporine			3 (11%)	6 (21%)	4 (14%)
Tacrolimus			24 (86%)	19 (68%)	19 (68%)
Prednisone			28 (100%)	28 (100%)	28 (100%)
Everolimus			1 (3%)	3 (11%)	5 (18%)
Mycophenolate mofetil			27 (96%)	26 (93%)	24 (86%)
Donor characteristics	-		-	-	-
Age (years)		56.0 ±13			
Sex, male N (%)		10 (36%)			
Warm ischemia time (minutes)		29.5 ±8			

All data are mean ±SD, unless otherwise specified. * p<0.05 vs controls. # p<0.05 vs CKD. BMI, body mass index; BP, blood pressure; ACE, angiotensin converting enzyme; eGFR, estimated glomerular filtration rate; IQR, interquartile range;

CKD patients have increased capillary tortuosity and angiogenic factors compared with controls

Our study demonstrated a markedly disturbed microvasculature with increased capillary tortuosity in CKD patients (mean 1.9 ± 0 , SEM) compared with healthy controls (mean 1.6 ± 0 , SEM, $p < 0.05$) (Fig 1A). Dialysis modalities did not influence capillary tortuosity. Mean vessel density was not significantly different between CKD (mean 19.9 ± 1 , SEM) and controls (mean 21.4 ± 1 , SEM, $p > 0.05$).

Consistently, Ang-2 and sTM levels were elevated in CKD patients (mean 4084 ± 612 pg/ml and 19 ± 6 ng/ml, SEM, respectively) compared with healthy controls (mean 2291 ± 326 pg/ml and 6.6 ± 0 ng/ml, SEM, $p < 0.05$ and $p < 0.0001$, respectively) (Fig 1B-C).

The difference in capillary tortuosity, Ang-2 and sTM between controls and CKD patients remained significant after adjustment for age, sex, body mass index (BMI), blood pressure and glucose levels.

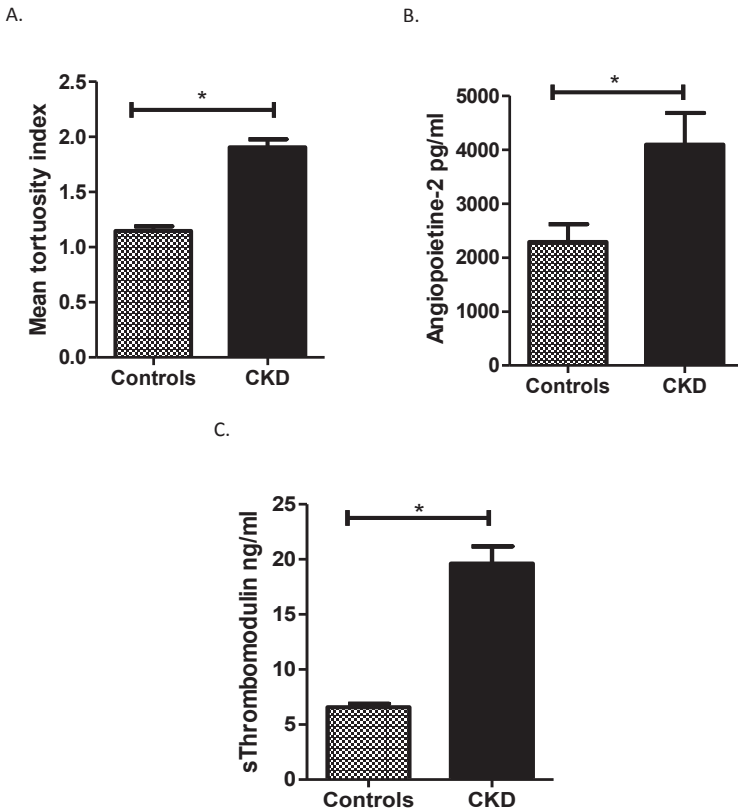


Figure 1. A. Mean tortuosity index of microvascular capillaries in the control and CKD group. Serum levels of Angiotensin-2 (B) and Soluble thrombomodulin (C) levels in CKD patients and healthy controls. Data shown are mean \pm SEM. * $P < 0.05$ compared to controls.

Kidney transplantation leads to reversal of microvascular tortuosity and decrease in circulating levels of Ang-2 and sTM

After KTx a significant decrease in capillary tortuosity was observed as early as 6 months (mean 1.6 ± 0 , SEM, $p < 0.001$) following transplantation (Fig 2A). Mean vessel density did not show significant changes between the different time points after KTx (Fig 2B).

In line with the observed decrease of capillary tortuosity after KTx, Ang-2 levels showed a significant decrease already at 1 month (mean 2263 ± 316 pg/ml, SEM, $p < 0.05$) after KTx and remained decreased up to 1 year (mean 2080 ± 281 pg/ml, SEM, $p < 0.01$) after transplantation (Fig 2C). sTM levels started to decrease at 1 month after transplantation (mean 6 ± 1 ng/ml, SEM, $p < 0.001$) compared with before KTx (Fig 2D). After correction for age, sex, BMI, blood pressure, glucose levels and smoking the differences remained significant for capillary tortuosity, Ang-2 and sTM.

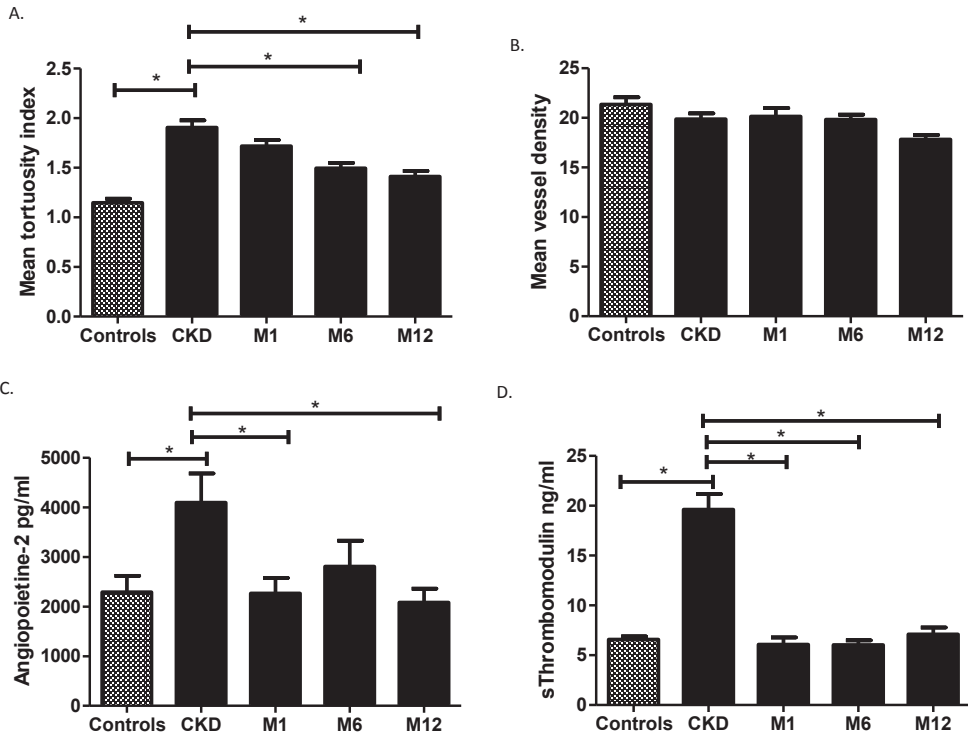
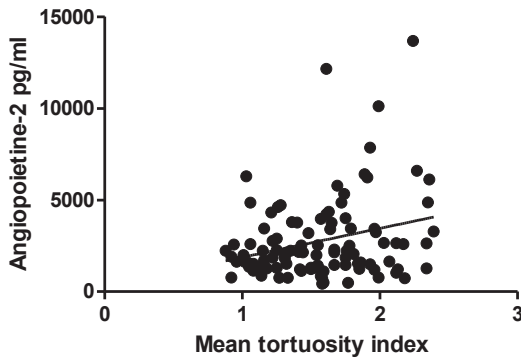


Figure 2. A. Longitudinal course of mean tortuosity index (A) and vessel density (B) before (CKD), 1 (M1), 6 (M6) and 12 (M12) months after KTx. Longitudinal course of serum levels Angiopoietin-2 (C) and soluble thrombomodulin (D). Data shown are mean \pm SEM. * $P < 0.05$.

Correlation analyses

Spearman's correlation analyses were performed between Ang-2, sTM serum levels and capillary tortuosity, glucose levels, calcineurin inhibitor use (CNI) and proteinuria. The Ang-2 ($r=0.1893$, $p=0.05$; Fig 3A), sTM ($r=0.2917$, $p=0.0014$) and proteinuria ($r=0.3036$, $p=0.0025$) were positively correlated with microvascular tortuosity. In addition, a negative correlation was observed between eGFR, tortuosity ($r=-0.5762$, $p<0.0001$; Fig 3B), Ang-2 ($r=-0.2352$, $p=0.0114$) and sTM ($r=-0.4959$, $p<0.0001$). Moreover, sTM correlated positively with proteinuria levels ($r=0.4188$, $p<0.001$) and no correlation between Ang-2 with proteinuria was observed. No correlation was found between the different markers and tortuosity with glucose levels and CNI use.

A.



B.

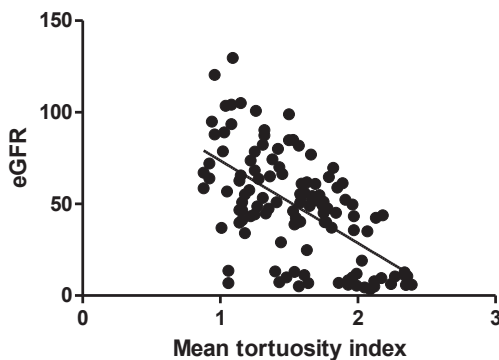


Figure 3. A. Scatter plots with correlation analyses between Angiotensin-2 (A) and eGFR (B) and mean tortuosity index.

Discussion

The present study demonstrated increased capillary tortuosity in CKD patients using SDF imaging, and elevated levels of markers for endothelial destabilization Ang-2 and sTM. Interestingly, KTx showed reversal of microvascular damage and normalization of Ang-2 and sTM levels, within 1 year after transplantation. Furthermore, we found a correlation between capillary tortuosity and Ang-2 and sTM. These data suggest that KTx is effective in reversing microvascular damage early after transplantation. Early non-invasive monitoring of the microvasculature may be of great clinical value to assess progression and treatment efficacy of microvascular disease in CKD patients before and after KTx.

A major contributor to microvascular damage in CKD patients is the accumulation of uremic toxins, which leads to changes in renal EC structure and function that favor microvascular injury, which may play a role as a trigger for the inflammatory response (14). Microvascular destabilization induces local areas of interstitial hypoxia and is associated with a dysbalance of angiogenic growth factors (9;11). Increased expression or release of Ang-2 after EC injury has been shown to destabilize capillaries and to increase inflammation and vessel leakage, by promoting the weakening of pericyte-EC interaction (9). Activation of pericytes will lead to differentiation of pericytes into collagen producing myofibroblasts and detachment from ECs (1;15-17). This process is accompanied by failure of reparative angiogenesis and consequently formation of unstable and tortuous vessels (1;10).

In the current study a significantly disturbed systemic microvasculature was observed in patients with CKD compared to healthy controls using SDF imaging. Using this imaging technique, we could previously demonstrate increased capillary tortuosity in patients with diabetic nephropathy (10). To date, there are no studies investigating the systemic changes or abnormalities in non-diabetic CKD patients before and after KTx using SDF imaging and correlated this with angiogenic growth factors and renal function. In a study of Snoeijs et al, SDF imaging was used to study the human renal microcirculation after KTx by direct visualization of cortical peritubular capillaries. In this study, ischemic acute kidney injury was associated with reduced cortical microvascular blood flow (12). Moreover, Edwards et al. showed an association between retinal microvascular alterations and renal dysfunction (3). In our recent study in diabetic nephropathy patients, KTx alone did not result in reversal of capillary tortuosity and angiogenic growth factors (10). Previous studies have demonstrated that improvement in glucose control with pancreas transplantation, performed simultaneously or after KTx, is the most important therapeutic approach of microvascular disease in diabetes mellitus patients (18;19). These findings suggest, in concordance with our previous study, that in diabetic nephropathy patients, normalization of renal function alone is not sufficient to

restore microvascular damage, but glycemic control is also necessary (10). However, In this study, KTx resulted in reversal of microvascular tortuosity within 1 year after transplantation and renal function correlated significantly with capillary tortuosity. Thus, in non-diabetic CKD patients, normalization of uremic state is able to improve microvascular damage evident in these patients.

Another interesting finding is that the observed increase in capillary tortuosity coincided with increase in Ang-2 and sTM levels in CKD and showed the same course after KTx. Moreover, there was also a correlation between Ang-2, sTM and capillary tortuosity. Our data suggest that these factors might participate in the pathogenesis of microvascular tortuosity in CKD. This is consistent with previous reports which demonstrated an association between microvascular damage and these angiogenic markers (4;6;10;29). Consistent with our observation, David et al demonstrated increased Ang-2 levels in serum of CKD patients and normalization after KTx (5). Recently, we reported on the relation between endothelial activation and increased renal expression of Ang-2 in rats subjected to renal ischemia reperfusion injury (I/R), which was accompanied by proliferation of pericytes, endothelial cell loss and development of fibrosis (16). Moreover, de Vries et al demonstrated Ang-2 release in the circulation from human kidneys grafts shortly after reperfusion (30).

In conclusion, this study demonstrates systemic microvascular damage in CKD patients, reflected by increased capillary tortuosity and angiogenic growth factors. Kidney transplantation resulted in reversal of capillary tortuosity and normalization of angiogenic growth factor levels. Given the central role of microvascular damage in CKD, therapies aiming at restoring the renal microvasculature might be an effective strategy to prevent profibrotic responses in CKD. Our findings indicate a clinical implication of SDF imaging to assess microvascular alterations after in CKD patients before and after KTx.

Acknowledgments

This work was supported by a Veni grant from ZonMW to M.E.J.R.

References

- (1) Long DA, Norman JT, Fine LG. Restoring the renal microvasculature to treat chronic kidney disease. *Nat Rev Nephrol* 2012 April;8(4):244-50.
- (2) Rabelink TJ, Wijewickrama DC, de Koning EJ. Peritubular endothelium: the Achilles heel of the kidney? *Kidney Int* 2007 October;72(8):926-30.
- (3) Edwards MS, Wilson DB, Craven TE, Stafford J, Fried LF, Wong TY et al. Associations between retinal microvascular abnormalities and declining renal function in the elderly population: the Cardiovascular Health Study. *Am J Kidney Dis* 2005 August;46(2):214-24.
- (4) David S, Kumpers P, Lukasz A, Kielstein JT, Haller H, Fliser D. Circulating angiotensin-2 in essential hypertension: relation to atherosclerosis, vascular inflammation, and treatment with olmesartan/pravastatin. *J Hypertens* 2009 August;27(8):1641-7.
- (5) David S, Kumpers P, Hellpap J, Horn R, Leitolf H, Haller H et al. Angiotensin 2 and cardiovascular disease in dialysis and kidney transplantation. *Am J Kidney Dis* 2009 May;53(5):770-8.
- (6) David S, Kumpers P, Lukasz A, Fliser D, Martens-Lobenhoffer J, Bode-Boger SM et al. Circulating angiotensin-2 levels increase with progress of chronic kidney disease. *Nephrol Dial Transplant* 2010 August;25(8):2571-6.
- (7) Keven K, Elmaci S, Sengul S, Akar N, Egin Y, Genc V et al. Soluble endothelial cell protein C receptor and thrombomodulin levels after renal transplantation. *Int Urol Nephrol* 2010 December;42(4):1093-8.
- (8) Kumpers P, Hellpap J, David S, Horn R, Leitolf H, Haller H et al. Circulating angiotensin-2 is a marker and potential mediator of endothelial cell detachment in ANCA-associated vasculitis with renal involvement. *Nephrol Dial Transplant* 2009 June;24(6):1845-50.
- (9) Fiedler U, Augustin HG. Angiotensins: a link between angiogenesis and inflammation. *Trends Immunol* 2006 December;27(12):552-8.
- (10) Khairoun M, de Koning EJ, van den Berg BM, Liewers E, de Boer HC, Schaapherder AF et al. Microvascular damage in type 1 diabetic patients is reversed in the first year after simultaneous pancreas-kidney transplantation. *Am J Transplant* 2013 May;13(5):1272-81.
- (11) Woolf AS, Gnudi L, Long DA. Roles of angiotensins in kidney development and disease. *J Am Soc Nephrol* 2009 February;20(2):239-44.
- (12) Snoeijs MG, Vink H, Voesten N, Christiaans MH, Daemen JW, Peppelenbosch AG et al. Acute ischemic injury to the renal microvasculature in human kidney transplantation. *Am J Physiol Renal Physiol* 2010 November;299(5):F1134-F1140.
- (13) Djaberri R, Schuijff JD, de Koning EJ, Wijewickrama DC, Pereira AM, Smit JW et al. Non-invasive assessment of microcirculation by sidestream dark field imaging as a marker of coronary artery disease in diabetes. *Diab Vasc Dis Res* 2013 March;10(2):123-34.
- (14) Schiffrin EL, Lipman ML, Mann JF. Chronic kidney disease: effects on the cardiovascular system. *Circulation* 2007 July 3;116(1):85-97.
- (15) Humphreys BD, Lin SL, Kobayashi A, Hudson TE, Nowlin BT, Bonventre JV et al. Fate tracing reveals the pericyte and not epithelial origin of myofibroblasts in kidney fibrosis. *Am J Pathol* 2010 January;176(1):85-97.
- (16) Khairoun M, van der Pol P, de Vries DK, Liewers E, Schlagwein N, de Boer HC et al. Renal ischemia-reperfusion induces a dysbalance of angiotensins, accompanied by proliferation of pericytes and fibrosis. *Am J Physiol Renal Physiol* 2013 September 15;305(6):F901-F910.
- (17) Lin SL, Kisseleva T, Brenner DA, Duffield JS. Pericytes and perivascular fibroblasts are the primary source of collagen-producing cells in obstructive fibrosis of the kidney. *Am J Pathol* 2008 December;173(6):1617-27.

- (18) Fioretto P, Steffes MW, Sutherland DE, Goetz FC, Mauer M. Reversal of lesions of diabetic nephropathy after pancreas transplantation. *N Engl J Med* 1998 July 9;339(2):69-75.
- (19) Fioretto P, Mauer M. Effects of pancreas transplantation on the prevention and reversal of diabetic nephropathy. *Contrib Nephrol* 2011;170:237-46.
- (20) Chade AR, Zhu X, Lavi R, Krier JD, Pislaru S, Simari RD et al. Endothelial progenitor cells restore renal function in chronic experimental renovascular disease. *Circulation* 2009 February 3;119(4):547-57.
- (21) Lerman LO, Chade AR. Angiogenesis in the kidney: a new therapeutic target? *Curr Opin Nephrol Hypertens* 2009 March;18(2):160-5.
- (22) Chade AR. VEGF: Potential therapy for renal regeneration. *F1000 Med Rep* 2012;4:1.
- (23) Jung YJ, Kim DH, Lee AS, Lee S, Kang KP, Lee SY et al. Peritubular capillary preservation with COMP-angiopoietin-1 decreases ischemia-reperfusion-induced acute kidney injury. *Am J Physiol Renal Physiol* 2009 October;297(4):F952-F960.
- (24) Kim W, Moon SO, Lee SY, Jang KY, Cho CH, Koh GY et al. COMP-angiopoietin-1 ameliorates renal fibrosis in a unilateral ureteral obstruction model. *J Am Soc Nephrol* 2006 September;17(9):2474-83.
- (25) Chen B, Bo CJ, Jia RP, Liu H, Wu R, Wu J et al. The renoprotective effect of bone marrow-derived endothelial progenitor cell transplantation on acute ischemia-reperfusion injury in rats. *Transplant Proc* 2013 June;45(5):2034-9.
- (26) Hohenstein B, Kuo MC, Addabbo F, Yasuda K, Ratiiff B, Schwarzenberger C et al. Enhanced progenitor cell recruitment and endothelial repair after selective endothelial injury of the mouse kidney. *Am J Physiol Renal Physiol* 2010 June;298(6):F1504-F1514.
- (27) Patschan D, Plotkin M, Goligorsky MS. Therapeutic use of stem and endothelial progenitor cells in acute renal injury: ca ira. *Curr Opin Pharmacol* 2006 April;6(2):176-83.
- (28) Zerbini G, Piemonti L, Maestroni A, Dell'Antonio G, Bianchi G. Stem cells and the kidney: a new therapeutic tool? *J Am Soc Nephrol* 2006 April;17(4 Suppl 2):S123-S126.
- (29) Chang FC, Lai TS, Chiang CK, Chen YM, Wu MS, Chu TS et al. Angiopoietin-2 is associated with albuminuria and microinflammation in chronic kidney disease. *PLoS One* 2013;8(3):e54668.
- (30) de Vries DK, Khairoun M, Lindeman JH, Bajema IM, de HE, Roest M et al. Renal ischemia-reperfusion induces release of angiopoietin-2 from human grafts of living and deceased donors. *Transplantation* 2013 August 15;96(3):282-9.

Chapter 7

Acute rejection of kidney transplants is associated with a dysbalance in angiopoietins and a sustained increase in systemic microvascular tortuosity

Meriem Khairoun, Gürbey Ocak, Joris I. Rotmans, Aiko P.J. de Vries,
Bernard M. van den Berg, Alexander F. Schaapherder, Ellen Lievers, Marko J.K. Mallat,
Dorottya K de Vries, Johan W. de Fijter, Anton Jan van Zonneveld, Ton J. Rabelink,
Marlies E.J. Reinders

Submitted

Abstract

Background: Microvascular endothelial cells (ECs) are very susceptible to injury, including episodes of acute rejection (AR). Whether AR after renal transplantation is associated with sustained systemic microvascular damage is unknown.

Methods: Using SDF imaging, microvascular alterations in AR patients (n=13) were compared with transplant recipients with stable renal function (n=25). In addition, 11 patients were studied longitudinally at 1, 6 and 12 months after rejection. Angiotensin-1 (Ang-1), Angiotensin-2 (Ang-2), Vascular Endothelial Growth Factor-A (VEGF-A) and soluble Thrombomodulin (sTM) levels were measured.

Results: Capillary tortuosity was significantly increased in patients with AR (1.74 ± 0.5) compared with the stable group (1.41 ± 0.13 , $p < 0.05$). Furthermore, the Ang-2/Ang-1 ratio (0.09 ± 0.02 vs 0.05 ± 0.01), VEGF-A (567 ± 188 vs 202 ± 27 pg/ml) and sTM (19667 ± 1809 vs 9667 ± 921 pg/ml) plasma levels were significantly higher in patients with AR compared with stable patients (all $p < 0.05$). Interestingly, patients with AR showed persisting increased capillary tortuosity ($p < 0.05$) and a disturbed Ang-2/Ang-1 balance up to 1 year after AR. VEGF-A and sTM levels remained significantly elevated up to 1 and 6 months after AR ($p < 0.05$), but returned to baseline at 12 months.

Conclusion: AR is associated with increased systemic microvascular tortuosity up to 1 year after rejection, which is associated with elevated levels of angiogenic growth factors. SDF imaging might be a useful tool to assess the degree of microvascular damage in these patients.

Introduction

Endothelial cells (ECs) line the lumina of all blood vessels and form the interface between the blood and tissue. In the context of kidney transplantation, ECs are very susceptible to injury during episodes of allograft rejection. ECs get activated in response to cytokines and growth factors that are produced as part of the alloimmune response (1-6). These activated ECs express adhesion molecules, release cytokines, chemokines and growth factors that mediate recruitment of recipient leukocytes (4;7). This will result in perpetual EC damage and promotion of angiogenesis within the allograft (1;3;4). This process is mediated by different pro-inflammatory and angiogenic growth factors, most notably Vascular Endothelial Growth Factor (VEGF) and Angiopoietin-2 (Ang-2), which play a central role in the angiogenic and inflammatory responses (1-3;6;8-10). The upregulation of Ang-2 destabilizes the endothelial cell lining and promotes the dissociation of pericytes from ECs, which results in the formation of abnormal capillary networks and abnormal blood flow. Local areas of interstitial hypoxia trigger fibrotic and inflammatory changes and ultimately lead to the development of interstitial fibrosis and tubular atrophy (IFTA) (1;2;4;9;11;12).

The endothelium is relatively inaccessible to direct examination. Therefore, investigators have concentrated on various surrogate markers of endothelial function which includes measurement of specific plasma markers including angiopoietins, VEGF and serum soluble Trombomodulin (sTM) (13-16). In allograft rejection different studies showed elevated circulating levels of VEGF and sTM in patients after solid organ transplantation, suggesting (systemic) endothelial cell activation (1;13;17-23).

An additional method for the assessment of endothelial function includes monitoring of the microvasculature. Recently, sidestream darkfield (SDF) imaging has emerged as a non-invasive tool to visualize the human microcirculation and to assess microvascular remodeling (24). We have previously validated this technique and used it to investigate the labial mucosal capillary tortuosity, as marker for systemic microvascular disease in diabetes mellitus type I (DM) patients before and after simultaneous pancreas kidney transplantation (SPK) (24;25). Diabetic patients showed increased capillary tortuosity compared to healthy non-diabetic controls and SPK resulted in reversal of microvascular damage within 1 year after transplantation (24).

To our knowledge no previous studies have studied whether inflammatory changes in the transplanted organ can impact on the systemic microcirculation. In the present study, we therefore assessed whether AR is associated with systemic microvascular damage in a cross-sectional study using SDF imaging and correlated this with markers for endothelial function. In addition, we investigated the long-term effects of AR on the systemic microvasculature in a longitudinal study up to 1 year after rejection.

Material and Methods

Study population

All procedures were approved by the institutions Medical Ethical Committee. Informed consent was obtained from all the patients. A total of 38 patients (24 males and 14 females) were enrolled in the cross-sectional study after given informed consent. Thirteen patients were included because of a decrease in renal function and biopsy proven acute cellular rejection (AR group). Of these patients, 11 had interstitial acute rejection, and the two other patients had vascular rejection. Ten patients were treated with methylprednisolone, one patients with anti-thymocyte globulin (ATG), one patient with methylprednisolone followed by alemtuzumab treatment and one patients with methylprednisolone followed by ATG. Of the 13 AR patients, 1 had donor specific antibodies against HLA class I antigens and none of the patients had positive HLA class II antibodies. Biochemical markers for endothelial function including, Ang-1, Ang-2, sTM and VEGF-A, together with mucosal capillary density and morphology were compared to 25 kidney transplant recipients with stable renal function (eGFR of 30 ml/min or more, stable group). In addition, analyses were performed in 10 patients from the stable renal function group with an eGFR similar to the AR patients, to differentiate between the effects of renal function and rejection on microvascular parameters. Patients with SPK, active infection, liver failure, active auto-immune disease, epilepsy or malignancy in the last 5 years (except patients treated for basal cell carcinoma who were in full remission) were excluded from the study. The patients in the AR group were also studied prospectively in a longitudinally study at 1 (M1, n=13), 6 (M6, n=13) and 12 months (M12, n=11, two patients discontinued their participation) after rejection. All measurements were performed before patients received treatment for AR. None of the 38 patients had signs of infection at the time of the measurements.

Transplantation aspects

All patients underwent solitary kidney transplantation at the Leiden University Medical Center (LUMC) between 2003 and 2012. Kidney transplantation was performed as described previously (24).

Patients were treated with prednisone (tapered to a dose of 10 mg by 6 weeks and a dose of 7.5 mg by 3 months), cyclosporine (targeted to an area under the curve (AUC) 5400 ng.h/ml first 6 weeks then 3250 ng.h/ml) or tacrolimus (AUC 210 ng.h/ml first 6 weeks, then 125 ng.h/ml) and mycophenolate mofetil (MMF) (AUC 30-60 ng.h/ml). In case of side effects patients were converted to everolimus (AUC 120-150 ng.h/ml). All patients received induction treatment with basiliximab (40 mg at day 0 and 4) or daclizumab (100 mg/day on the day of transplantation and 10 days after transplantation). Patients were treated routinely with oral valganciclovir prophylaxis for 3 months, except for cytomegalovirus (CMV) negative recipients receiving a CMV-negative graft.

Laboratory and urinary assessments

All persons enrolled in this study underwent routine venous blood sampling that was collected before the morning intake of immunosuppression to assess creatinine, urea, HbA1c, glucose and hemoglobin. Proteinuria was measured in collected 24-hours urine. The eGFR was calculated with plasma creatinine concentration using the Modification of Diet in Renal Disease (MDRD) formula. At the same time, blood sampling for routine laboratory measurements, blood was collected for analysis of serum Ang-1, Ang-2, VEGF-A and sTM concentrations. Both Ang-1 and Ang-2 were measured by ELISA (R&D Systems, Minneapolis, MN, USA) according to the manufacturer supplied protocol. Likewise, VEGF-A and sTM (Gen-Probe Diaclone Research, Besançon, France) levels were assessed. Since the Ang-2/Ang-1 rather than the absolute levels of either cytokine has been considered to determine the functional status of the microvasculature (9;10;14), this ratio was calculated for the different groups and time points.

Microcirculatory imaging

The SDF microscan (MicroVision Medical Inc., Wallingford, PA, U.S.A) was performed as described previously (24;25). Before analysis, the video files were anonymized so that the assessor was blinded to the subject's identity. Capillary loops were assessed by two individual assessors in a randomized, blind fashion. From the forty video files obtained of the microcirculation in each subject, four technically best files were selected from each lip quadrant for analysis. Mean vessel density (capillaries/mm²) was calculated by counting the number of vessels per screen shot. Subsequently, tortuosity of capillary loops was assessed using a validated scoring system described previously and the average of assessed capillary tortuosity was used to calculate mean tortuosity index per patient (25).

Statistical analyses

Continuous normally distributed data are presented as mean \pm SEM, unless stated otherwise. Differences between two groups in the cross-sectional study were analysed using the unpaired two-sample T-test. When criteria for parametric testing were not met, median and interquartile range (IQR) are presented and tested with the Mann-Whitney test. For categorical variables cross-tables were used and analysed with the chi-square test. In addition, multivariable linear regression was used to adjust for possible confounders. Comparisons of mean differences between the different time points in the longitudinal study were performed using ANOVA analysis.

Correlations between interval variables were calculated using the Spearman rank correlation coefficient. Differences were considered statistically significant with $p < 0.05$. Data analysis was performed using SPSS version 17.0 (SPSS Inc, Chicago, IL) and GraphPad Prism, version 5.0 (GraphPad Prism Software Inc, San Diego, CA).

Results

Characteristics of transplant recipients with stable renal function and patients with AR

Baseline subject characteristics are presented in Table 1. Renal function of the patients with stable allograft function (47.2 ± 13 ml/min/1.73 mm²) was better compared to AR patients (38.1 ± 13 ml/min/1.73 mm², $p < 0.05$). In order to elucidate if renal function itself affect capillary tortuosity and levels of angiogenic growth factors, we selected a subgroup of 10 patients with stable renal allograft function with comparable allograft function (36.7 ± 6 ml/min/1.73 mm²) as patients with AR (38.1 ± 13 ml/min/1.73 mm², $p > 0.05$) group. Patients in this subgroup had comparable age (52.6 ± 14 years), body mass index (BMI) (25.2 ± 4 kg/m²), systolic (131 ± 12 mmHg) and diastolic (84 ± 12 mmHg) blood pressure as AR patients (52.7 ± 10 years, 24.3 ± 3 kg/m², 142 ± 19 and 83 ± 13 mmHg, respectively, $p > 0.05$). Patients with AR (8.3 ± 3 mmol/L) had increased glucose levels compared to stable patients (6.0 ± 2 mmol/L) and also compared to the subset of 10 stable patients (5.6 ± 2 mmol/L, both $p < 0.05$). In the AR group, 2 patients were treated for type II diabetes (both with insulin) which was not significantly different from the stable group ($n=4$, 3 patient treated with insulin and 1 with oral anti-diabetics). In addition, 4 patients with AR and 4 stable patients stopped MMF due to side effects. In 1 patient from the stable group, tacrolimus was replaced by everolimus because of side effects.

In the longitudinal study (Table 1) patients showed significant decreased renal function during all time points after AR compared to stable patients. Glucose levels were increased during AR and showed a significant decrease at 1 and 12 ($p < 0.05$) months following rejection. Moreover, one patient developed new-onset diabetes after treatment with methylprednisolone and was treated with oral anti-diabetics. In four patients MMF was discontinued before rejection, due to side effects. In 2 patients treatment with tacrolimus was added, because of rejection under dual therapy with prednisone and MMF. In 1 patient tacrolimus was given instead of cyclosporine because of rejection.

Patients with AR have increased capillary tortuosity compared to stable patients

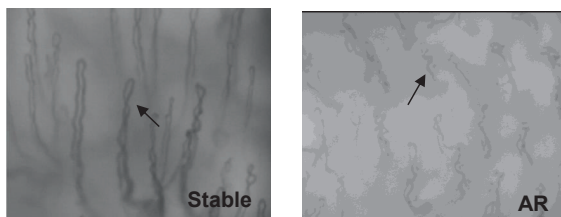
Patients with AR (1.70 ± 0.1 , $p < 0.01$) showed significantly increased capillary tortuosity compared to stable patients (mean 1.41 ± 0.06) (Fig 1AB), also after adjustment for age, sex, BMI, blood pressure, glucose levels and smoking. Capillary tortuosity in the subset of 10 stable patients with eGFR of 36.7 ml/min/1.73 mm² (1.40 ± 0.13) was comparable with capillary tortuosity of the remaining patients with a stable allograft function with eGFR of 54.6 ± 13 ml/min/1.73 mm² (1.41 ± 0.06). Capillary density showed no significant difference between the stable renal function group and patients with AR ($p = \text{NS}$, data not shown).

Table 1: Patients characteristics of acute rejection patients during AR, one (M1), six (M6) and twelve (M12) months after rejection compared with stable renal transplant recipients

Patients characteristics	Stable renal transplant (N=25)	D0 (N=13)	M1 (N=13)	M6 (N=13)	M12 (N=11)
Age (years)	53.2 ± 13	51.7 ± 10	51.8 ± 10	52.4 ± 10	52.7 ± 10
Sex, male N (%)	15 (60%)	9 (69%)			
Smoking, N (%)	3 (12%)	1 (8%)	1 (8%)	1 (8%)	0
Median time since transplantation (months) (IQR)	5 (1-19)	12 (3-22)			
Primary kidney disease, N (%)					
Glomerulonephritis	8 (32%)	0	0	0	0
Diabetes Mellitus	3 (12%)	1 (8%)	1 (8%)	1 (8%)	1 (8%)
Pyelonephritis or interstitial nephritis	1 (4%)	2 (15%)	2 (15%)	2 (15%)	2 (15%)
Focal segmental glomerulosclerosis	3 (12%)	0	0	0	0
Urologic	1 (4%)	1 (8%)	1 (8%)	1 (8%)	1 (8%)
Polycystic kidney disease	4 (16%)	4 (31%)	4 (31%)	4 (31%)	4 (31%)
Hypertension	2 (8%)	2 (15%)	2 (15%)	2 (15%)	2 (15%)
Unknown	2 (8%)	2 (15%)	2 (15%)	2 (15%)	2 (15%)
Other	1 (4%)	1 (8%)	1 (8%)	1 (8%)	1 (8%)
BMI (kg/m ²)	25.8 ± 4	24.3 ± 3	24.3 ± 3	23.8 ± 4	25.2 ± 4
Dialysis, N (%)	4 (16%)	0	0	0	0
Systolic BP (mmHg)	137 ± 20	142 ± 19	132 ± 10	132 ± 16	127 ± 19
Diastolic BP (mmHg)	82 ± 9	83 ± 13	77 ± 9	79 ± 12	72 ± 10
eGFR (ml/min/1.73 m ²)	47.2 ± 13	38.1 ± 13 [#]	35.4 ± 15 [#]	40.2 ± 16 [#]	36.0 ± 18 [#]
Median proteinuria (g/24hr) (IQR)	0.2 (0.2-0.4)	0.4 (0.3-1.0) [#]	0.3 (0.2-0.7)	0.2 (0.2-0.3)	0.3 (0.1-0.3)
Glucose (mmol/L)	6.0 ± 2	8.3 ± 3 [#]	5.7 ± 2 [*]	6.3 ± 3	5.9 ± 1 [*]
Hemoglobin (mmol/L)	7.9 ± 1	7.6 ± 1	7.3 ± 1	7.7 ± 1	7.7 ± 1
Hematocrit (L/L)	0.40 ± 0.06	0.38 ± 0.04	0.36 ± 0.05	0.39 ± 0.05	0.39 ± 0.05
Anti-hypertensives, N (%)					
ACE inhibitor	5 (20%)	2 (15%)	3 (23%)	3 (23%)	2 (18%)
Diuretics	6 (24%)	3 (23%)	4 (31%)	2 (15%)	1 (9%)
β-blockers	11 (44%)	6 (46%)	7 (54%)	7 (54%)	6 (55%)
Calcium antagonists	14 (56%)	8 (62%)	9 (69%)	6 (46%)	6 (55%)
Angiotensin-II antagonists	1 (4%)	3 (23%)	3 (23%)	2 (15%)	3 (27%)
Statines, N (%)	9 (36%)	5 (39%)	6 (46%)	7 (54%)	7 (64%)
Immunosuppressive, N (%)					
Cyclosporine	3 (12%)	3 (23%)	3 (23%)	2 (15%)	0
Tacrolimus	19 (76%)	7 (54%)	8 (62%)	10 (77%)	9 (81%)
Prednisone	24 (96%)	13 (100%)	13 (100%)	13 (100%)	11 (100%)
Everolimus	2 (8%)	1 (8%)	0	0	1 (9%)
Mycophenolate Mofetil	21 (84%)	9 (69%)	9 (69%)	10 (77%)	7 (64%)
Donor characteristics					
Age (years)	52.3 ± 9	46.4 ± 11			
Sex, male N (%)	8 (32%)	4 (31%)			
Donortype, deceased donors, N (%)	5 (20%)	5 (39%)			

All data are mean ±SD, unless otherwise specified. [#]p<0.05 compared to stable patients. ^{*}P<0.05 compared to AR. BMI, body mass index;BP, blood pressure ACE,angiotensin converting enzyme; eGFR, estimated glomerular filtration rate; IQR, interquartile range.

A.



B.

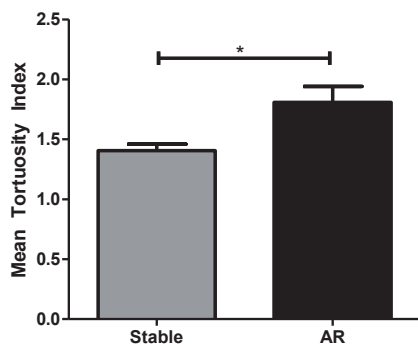


Figure 1. A. Sidestream darkfield images of the oral mucosa visualizing the microvascular capillaries of a representative patient in stable and AR group. Black arrows: capillary loops. **B.** Mean tortuosity index of microvascular capillaries in the stable (n=25) and AR (n=13) group. Data shown are mean±SEM. *P<0.05 compared to stable group.

During the follow-up period after AR, capillary tortuosity remained increased at 1 month (1.72 ± 0.1 , $p < 0.01$), 6 (1.71 ± 0.4 , $p < 0.05$) and 12 months (1.74 ± 0.1 , $p < 0.001$) following AR compared to patients with a stable renal function (1.41 ± 0.06) (Fig 2AB).

Ang-2/Ang-1 ratio, VEGF-A and sTM levels are increased in AR patients

To evaluate the effects of AR on the expression of angiogenic factors, we calculated the Ang-2/Ang-1 ratio and measured serum levels of VEGF-A and sTM. The Ang-2/Ang-1 ratio was significantly increased in AR group (0.09 ± 0.02) compared with stable renal transplant recipients (0.05 ± 0.01 , $p = 0.01$) (Fig 3A). In line with these observations, VEGF-A serum levels were increased in AR patients (567 ± 188 pg/ml, $p = 0.02$) compared to stable recipients (202 ± 27 pg/ml) (Fig 3B).

In addition, elevated sTM serum levels were detected in AR group (19667 ± 1809 pg/ml) group compared with stable patients (9667 ± 921 pg/ml, $p < 0.0001$) (Fig 3C). The differences remained significant after adjustment for age, sex, BMI, blood pressure, glucose levels and smoking ($p < 0.05$).

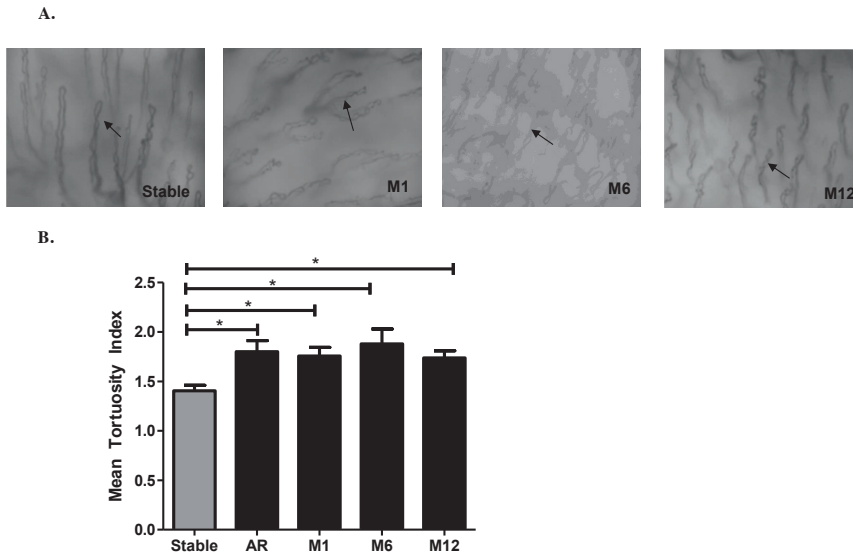


Figure 2. A. Sidestream dark field images of the oral mucosa visualizing the microvascular capillaries of a representative stable kidney transplant patient, one (M1), six (M6) and twelve (M12) months after rejection in the longitudinal rejection study. Black arrows: capillary loops.

B. Longitudinal course of the mean tortuosity index of microvascular capillaries in the stable group (n=25) and at one (M1, n=13), six (M6, n=13) and twelve (M12, n=11) months after rejection. Data shown are mean±SEM. * P<0.05 compared to stable group.

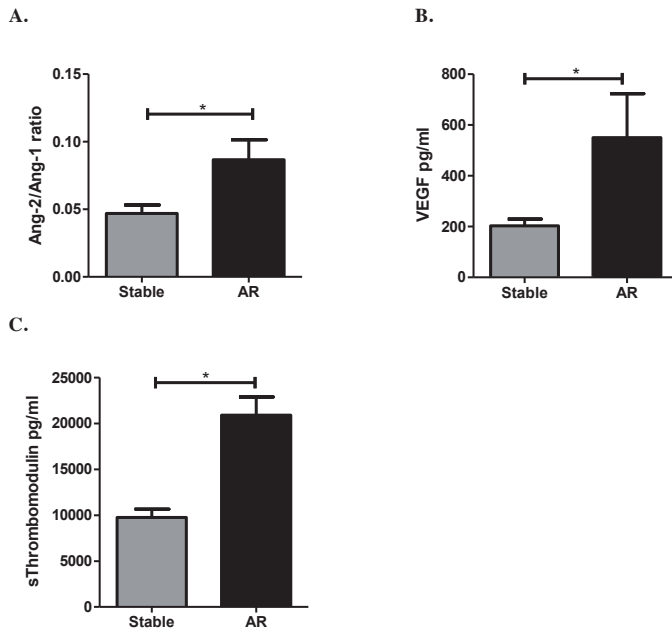


Figure 3: Ang-2/Ang-1 ratio (A), VEGF-A (B) and soluble thrombomodulin (C) serum levels (pg/ml) in stable (n=25) and AR (n=13) group. Data shown are mean±SEM. *P<0.05.

Ang-2/Ang-1 ratio remained increased and VEGF-A and sTM serum levels decreased in the first year after acute rejection

During follow up, the Ang-2/Ang-1 ratio remained elevated at 1 month (0.07 ± 0.02 , $p=0.35$), 6 months (0.06 ± 0.02 , $p=0.44$) and 12 months (0.07 ± 0.02 , $p=0.36$) after AR compared with stable renal transplant recipients (0.05 ± 0.01) however, statistical significance was not reached (Fig 4A). Furthermore, VEGF-A serum levels remained significantly increased up to 1 month after rejection (465 ± 109 pg/ml) compared with stable renal transplant recipients (202 ± 27 pg/ml, $p=0.03$) and started to show a decrease at 6 (368 ± 150 pg/ml, $p=0.23$) and 12 months (257 ± 95 pg/ml, $p=0.42$) compared with period during AR (Fig 4B). Mean sTM serum levels were significantly higher at 1 (20083 ± 3468 pg/ml, $p=0.02$) and 6 months (14927 ± 2330 pg/ml, $p=0.02$) after rejection compared to stable patients. At 12 months after rejection, sTM serum levels showed a significant decrease (10875 ± 1549 pg/ml, $p<0.05$) compared to during AR (19667 ± 1809 pg/ml) (Fig 4C). The differences remained significant after correction for age, sex, BMI, blood pressure, glucose levels and smoking.

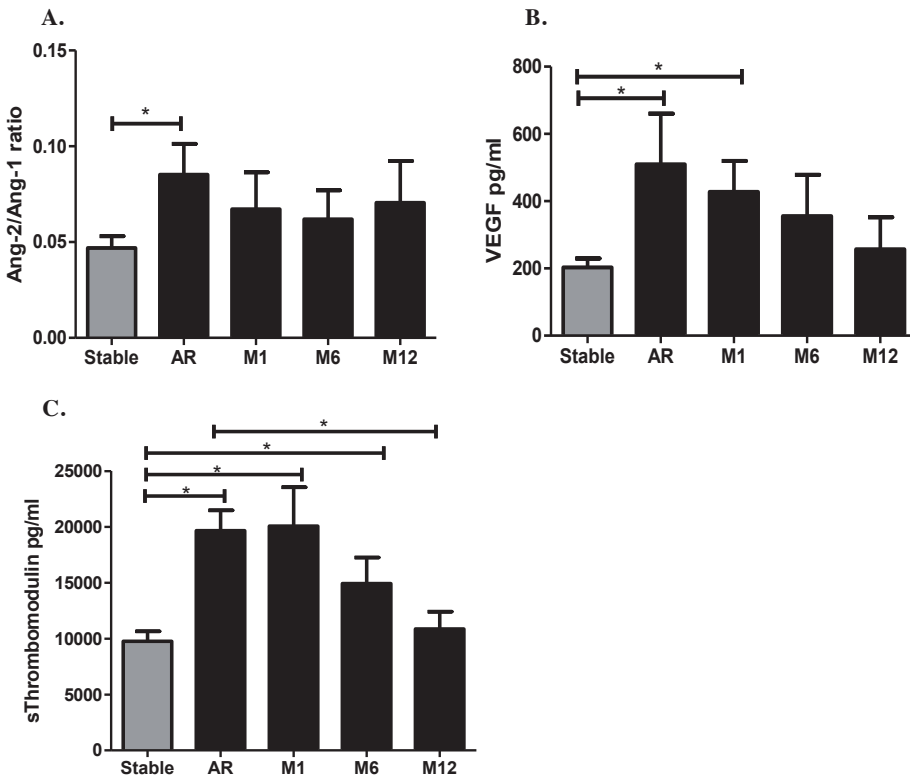


Figure 4: Longitudinal course of Ang-2/Ang-1 ratio (A), serum VEGF-A (B) and soluble thrombomodulin (pg/ml) (C) levels at one (M1, n=13), six (M6, n=13) and twelve (M12, n=11) months after rejection compared with stable group. Data shown are mean±SEM.

*P<0.05.

Serum levels of VEGF-A and sTM correlate with capillary tortuosity, eGFR and proteinuria

Next, the correlation between Ang-2/Ang-1 ratio, VEGF-A, sTM serum levels and capillary tortuosity, time since transplantation, eGFR, glucose levels, calcineurin inhibitors use (CNI) and proteinuria was assessed. sTM levels correlated positively with capillary tortuosity ($r=0.43$, $p<0.0010$), proteinuria ($r=0.58$, $p<0.001$) and glucose levels ($r=0.44$, $p<0.0001$). Moreover, there was a negative correlation with Ang-2/Ang-1 ratio, VEGF-A, sTM and eGFR ($r=-0.43$, $p<0.001$, $r=-0.38$, $p=0.01$, $r=-0.48$, $p<0.001$, respectively).

Discussion

In the present study, we demonstrate that the systemic microvasculature, assessed by SDF imaging, is markedly disturbed in patients with AR compared with stable renal transplant recipients. This coincides with an increased Ang-2/Ang-1 ratio as well as increased VEGF-A and sTM serum levels in the circulation. Interestingly, capillary tortuosity remained increased up to 1 year after rejection in patients in the longitudinal study. The current findings suggest that AR alter the systemic microvasculature chronically, and that SDF imaging might be a useful tool to assess the degree of microvascular damage in these patients.

To date, there are only a few studies that have used SDF for assessment of microvascular alterations after solid organ transplantation. In our previous study, it was demonstrated that capillary tortuosity is reversed in the first year after SPK in DM patients, which was also associated with a normalization of the Ang-2/Ang-1 balance and sTM levels. Interestingly, in this study DM patients who received a solitary kidney transplantation did not demonstrate reversibility of increased capillary tortuosity (24). These findings support the hypothesis that with SPK, i.e. beta cell function and renal failure reversal and not renal function alone is required to restore systemic microvascular tortuosity (24). In the current study, an increased systemic microvascular tortuosity was observed in patients after AR using SDF imaging. Interestingly, in the longitudinal rejection study this increased capillary tortuosity remained for up to 1 year after the rejection episode, suggesting that rejection can induce a sustained injury of the endothelium. Graft biopsies performed in patients after treatment of allograft rejection episodes revealed persistence of infiltrates in the graft (5;26;27). Interestingly the presence of monocytes/ macrophages and CD3⁺T cell infiltrates was strongly associated with the induced expression of VEGF in rejecting human cardiac allografts and VEGF is likely a key intermediary between sustained cell-mediated immune inflammation and the associated angiogenesis reaction (5;6). Alternatively, loss of kidney function after rejection may be responsible for the observed sustained systemic microvascular damage. Indeed, Edwards et al showed a significant association between retinal microvascular abnormalities and renal

function deterioration (28). To differentiate between AR and loss of renal function as a cause for the sustained change in microvascular parameters we did a case-control analysis in subjects with stable renal function that was matched for the renal function after 1 year in the AR group. Capillary tortuosity of this subset of patients was similar to the other patients with a stable renal function, making loss of renal function as an explanation less likely.

An interesting observation in our study is that the observed increased microvascular tortuosity coincided with a disturbed Ang-2/Ang-1 ratio and with increased levels of sTM and VEGF-A. This is in line with previous studies that have demonstrated a positive correlation between microvascular destabilization and such markers of endothelial dysfunction (14-16;18;24). Ang-1 is a competitive ligand for the same Tie-2 receptor as for Ang-2, with competing, antagonistic effects on angiogenesis and microvascular remodeling (10;14). It has been reported that Ang-2 displays VEGF dependent modulation of the microvascular structure, suggesting that these factors may act in concert to induce the observed microvascular damage (29). A disturbed Ang-2/Ang-1 balance and increased sTM levels, have been reported in patients with chronic kidney disease, with normalization after renal transplantation (14;16). Similarly, sTM levels have been reported to be higher during rejection after liver transplantation (23). Moreover, during chronic cardiac allograft rejection, Ang-1 expression was decreased, while Ang-2 was upregulated in the microvascular ECs of rejecting cardiac allografts (30). In our study a disturbed Ang-2/Ang-1 balance in AR patients was observed compared with stable renal transplant recipients and remained increased up to 1 year following rejection.

Several studies have reported on the pivotal role of VEGF-A in the development of endothelial dysfunction in acute and chronic rejection (4;31). High serum and urine levels of VEGF-A were found in patients with cardiac and renal allograft rejection, which return to baseline levels after successful treatment of the rejection (22;32). Increased serum VEGF-A levels were also found in our study in patients with AR, which remained significantly increased up to 1 month after rejection and had almost normalized at 1 year following rejection.

In conclusion, the current study demonstrates systemic microvascular damage in AR patients. Simultaneous increase of angiogenic growth factors and capillary tortuosity suggests that these factors might participate in the pathogenesis of microvascular damage during rejection. Since EC activation results in impaired survival of allografts, therapies aimed at maintaining microvascular integrity may have beneficial effects on long-term graft survival after rejection episodes. Monitoring of the microcirculation by SDF imaging may be a novel non-invasive approach for the detection of early microvascular damage during allograft rejection.

Acknowledgments

We want to acknowledge and thank Rients de Boer and Rohit Timal for participating in the data collection and SDF measurements.

Grants

This work was supported by a Veni grant from ZonMW (01086089) to M.E.J. Reinders.

References

- (1) Bruneau S, Woda CB, Daly KP, Boneschansker L, Jain NG, Kochupurakkal N, et al. Key Features of the Intragraft Microenvironment that Determine Long-Term Survival Following Transplantation. *Front Immunol* 2012;3:54.
- (2) Contreras AG, Briscoe DM. Every allograft needs a silver lining. *J Clin Invest* 2007 Dec;117(12):3645-8.
- (3) Denton MD, Davis SF, Baum MA, Melter M, Reinders ME, Exeni A, et al. The role of the graft endothelium in transplant rejection: evidence that endothelial activation may serve as a clinical marker for the development of chronic rejection. *Pediatr Transplant* 2000 Nov;4(4):252-60.
- (4) Reinders ME, Rabelink TJ, Briscoe DM. Angiogenesis and endothelial cell repair in renal disease and allograft rejection. *J Am Soc Nephrol* 2006 Apr;17(4):932-42.
- (5) Reinders ME, Fang JC, Wong W, Ganz P, Briscoe DM. Expression patterns of vascular endothelial growth factor in human cardiac allografts: association with rejection. *Transplantation* 2003 Jul 15;76(1):224-30.
- (6) Reinders ME, Sho M, Izawa A, Wang P, Mukhopadhyay D, Koss KE, et al. Proinflammatory functions of vascular endothelial growth factor in alloimmunity. *J Clin Invest* 2003 Dec;112(11):1655-65.
- (7) Dormond O, Dufour M, Seto T, Bruneau S, Briscoe DM. Targeting the intragraft microenvironment and the development of chronic allograft rejection. *Hum Immunol* 2012 Dec;73(12):1261-8.
- (8) Cautero N, Gelmini R, Villa E, Bagni A, Merighi A, Masetti M, et al. Orthogonal polarization spectral imaging: a new tool in morphologic surveillance in intestinal transplant recipients. *Transplant Proc* 2002 May;34(3):922-3.
- (9) Fagiani E, Christofori G. Angiopoietins in angiogenesis. *Cancer Lett* 2013 Jan 1;328(1):18-26.
- (10) Tuo QH, Zeng H, Stinnett A, Yu H, Aschner JL, Liao DF, et al. Critical role of angiopoietins/Tie-2 in hyperglycemic exacerbation of myocardial infarction and impaired angiogenesis. *Am J Physiol Heart Circ Physiol* 2008 Jun;294(6):H2547-H2557.
- (11) Long DA, Norman JT, Fine LG. Restoring the renal microvasculature to treat chronic kidney disease. *Nat Rev Nephrol* 2012 Apr;8(4):244-50.
- (12) Steegh FM, Gelens MA, Nieman FH, van Hooff JP, Cleutjens JP, van Suylen RJ, et al. Early loss of peritubular capillaries after kidney transplantation. *J Am Soc Nephrol* 2011 Jun;22(6):1024-9.
- (13) Aharinejad S, Krenn K, Zuckermann A, Schafer R, Gmeiner M, Thomas A, et al. Serum matrix metalloproteinase-1 and vascular endothelial growth factor--a predict cardiac allograft rejection. *Am J Transplant* 2009 Jan;9(1):149-59.
- (14) David S, Kumpers P, Hellpap J, Horn R, Leitolf H, Haller H, et al. Angiopoietin 2 and cardiovascular disease in dialysis and kidney transplantation. *Am J Kidney Dis* 2009 May;53(5):770-8.
- (15) David S, Kumpers P, Lukasz A, Fliser D, Martens-Lobenhoffer J, Bode-Boger SM, et al. Circulating angiopoietin-2 levels increase with progress of chronic kidney disease. *Nephrol Dial Transplant* 2010 Aug;25(8):2571-6.
- (16) Keven K, Elmaci S, Sengul S, Akar N, Egin Y, Genc V, et al. Soluble endothelial cell protein C receptor and thrombomodulin levels after renal transplantation. *Int Urol Nephrol* 2010 Dec;42(4):1093-8.
- (17) Cao G, Lu Y, Gao R, Xin Y, Teng D, Wang J, et al. Expression of fractalkine, CX3CR1, and vascular endothelial growth factor in human chronic renal allograft rejection. *Transplant Proc* 2006 Sep;38(7):1998-2000.
- (18) Daly KP, Seifert ME, Chandraker A, Zurakowski D, Nohria A, Givertz MM, et al. VEGF-C, VEGF-A and related angiogenesis factors as biomarkers of allograft vasculopathy in cardiac transplant recipients. *J Heart Lung Transplant* 2013 Jan;32(1):120-8.

- (19) Malmstrom NK, Kallio EA, Rintala JM, Nykanen AI, Raisanen-Sokolowski AK, Paavonen T, et al. Vascular endothelial growth factor in chronic rat allograft nephropathy. *Transpl Immunol* 2008 May;19(2):136-44.
- (20) Ozdemir BH, Ozdemir FN, Haberal N, Emiroglu R, Demirhan B, Haberal M. Vascular endothelial growth factor expression and cyclosporine toxicity in renal allograft rejection. *Am J Transplant* 2005 Apr;5(4 Pt 1):766-74.
- (21) Peng W, Chen J, Jiang Y, Shou Z, Chen Y, Wang H. Prediction of subclinical renal allograft rejection by vascular endothelial growth factor in serum and urine. *J Nephrol* 2008 Jul;21(4):535-42.
- (22) Peng W, Chen J, Jiang Y, Shou Z, Chen Y, Wang H. Acute renal allograft rejection is associated with increased levels of vascular endothelial growth factor in the urine. *Nephrology (Carlton)* 2008 Feb;13(1):73-9.
- (23) Wen CG, Luo SK, He XS, Li J, Liu M, Zou WY, et al. [Values of soluble thrombomodulin and von Willebrand factor judging reject reaction in liver transplantation]. *Zhonghua Gan Zang Bing Za Zhi* 2003 May;11(5):295-7.
- (24) Khairoun M, de Koning EJ, van den Berg BM, Lievers E, de Boer HC, Schaapherder AF, et al. Microvascular Damage in Type 1 Diabetic Patients Is Reversed in the First Year After Simultaneous Pancreas-Kidney Transplantation. *Am J Transplant* 2013 Feb 22.
- (25) Djaberri R, Schuijf JD, de Koning EJ, Wijewickrama DC, Pereira AM, Smit JW, et al. Non-invasive assessment of microcirculation by sidestream dark field imaging as a marker of coronary artery disease in diabetes. *Diab Vasc Dis Res* 2012 May 23.
- (26) Gaber LW, Moore LW, Gaber AO, Tesi RJ, Meyer J, Schroeder TJ. Correlation of histology to clinical rejection reversal: a thymoglobulin multicenter trial report. *Kidney Int* 1999 Jun;55(6):2415-22.
- (27) Rush DN, Karpinski ME, Nickerson P, Dancea S, Birk P, Jeffery JR. Does subclinical rejection contribute to chronic rejection in renal transplant patients? *Clin Transplant* 1999 Dec;13(6):441-6.
- (28) Edwards MS, Wilson DB, Craven TE, Stafford J, Fried LF, Wong TY, et al. Associations between retinal microvascular abnormalities and declining renal function in the elderly population: the Cardiovascular Health Study. *Am J Kidney Dis* 2005 Aug;46(2):214-24.
- (29) Lobov IB, Brooks PC, Lang RA. Angiopoietin-2 displays VEGF-dependent modulation of capillary structure and endothelial cell survival in vivo. *Proc Natl Acad Sci U S A* 2002 Aug 20;99(17):11205-10.
- (30) Nykanen AI, Tikkanen JM, Krebs R, Keranen MA, Sihvola RK, Sandelin H, et al. Angiogenic growth factors in cardiac allograft rejection. *Transplantation* 2006 Jul 15;82(1 Suppl):S22-S24.
- (31) Pilmore HL, Eris JM, Painter DM, Bishop GA, McCaughan GW. Vascular endothelial growth factor expression in human chronic renal allograft rejection. *Transplantation* 1999 Mar 27;67(6):929-33.
- (32) Abramson LP, Pahl E, Huang L, Stellmach V, Rodgers S, Mavroudis C, et al. Serum vascular endothelial growth factor as a surveillance marker for cellular rejection in pediatric cardiac transplantation. *Transplantation* 2002 Jan 15;73(1):153-6.

Chapter 8

General summary and future perspective

Summary

Endothelial injury and repair are most important concepts for our understanding of renal disease and allograft injury. The concept that injury to the endothelium may precede renal fibrosis strongly suggests that interventions to maintain vascular integrity are of major importance for renal function. Understanding the mechanisms of microvascular dysfunction in renal disease and after transplantation might be helpful to determine future targets for therapeutic interventions.

Renal I/R injury is an important clinical problem and an inevitable consequence of organ transplantation, and a major determinant of patient and graft survival. So far, many contributors to I/R injury are incompletely understood. It has become increasingly recognized that microvascular EC damage and aberrant capillary repair are one of the earliest events following I/R injury, that precede and drive the profibrotic changes of the kidney parenchyma. In this context, potential causes of vascular damage are disturbances in EC-pericyte interactions, regulated by angiogenic growth factors (including the angiopoietins) involved in the maintenance of vascular integrity. In **Chapter 2**, we studied the effect of renal I/R on dynamics of angiopoietin expression and its association with microvascular remodeling, pericytes and fibrosis development up to 9 weeks after renal I/R injury in a rat model. We demonstrate loss of peritubular capillary ECs at early timepoints after renal I/R injury, which coincided with a dysbalance in Ang-2/Ang-1, proliferation of pericytes and development of renal interstitial fibrosis. Importantly, our study shows reversal of the Ang-2/Ang-1 balance to baseline at 9 weeks after renal I/R, which was accompanied by restoration of ECs and pericytes. These findings support the hypothesis that angiopoietins and pericytes play an important role in renal microvascular remodeling.

Although these experimental data suggest a functional role of angiopoietins in microvascular ECs damage in renal I/R injury, their involvement in human renal I/R injury had not been investigated yet and was the aim of our subsequent study. We hypothesized that the inflammatory cascade of human clinical I/R injury is initiated by endothelial activation and consequent Ang-2 release. In **chapter 3**, this hypothesis was studied in clinical kidney transplantation (both LD and DD) using an unique method of arteriovenous measurements over the reperfused kidney. Paired arterial and renal venous blood samples were collected at consecutive time-points during early reperfusion. In this study, Ang-2 release from both LD and DD kidneys shortly after reperfusion was observed, indicating injury to ECs, which could release Ang-2 from Weibel–Palade bodies upon activation. This was accompanied by a loss of ECs, reflected by decrease in CD34 and vWF protein expression, and diminished Ang-1 protein and mRNA expression. Our findings suggests that angiopoietins may play an important role in renal microvascular remodeling during I/R injury.

In **chapter 4**, we continued our studies on local capillary damage in kidneys during early stage of DM. Microvascular abnormalities in the kidneys are common histopathologic findings in DN. In human DN, morphological changes in capillaries, such as elongation and an increase in the number of glomerular capillaries, are demonstrated. Furthermore, alterations in the expression of VEGF-A and angiopoietins have been implicated in the progression of DN. Using an established streptozotocin-induced model of diabetes and atherogenesis, we investigated whether the early stages of DM combined with atherogenesis are associated with systemic microvascular disease. In addition, we assessed the earliest events in DM induced renal damage, focusing on microvascular alterations and angiopoietins in pigs with a follow-up period up to 15 months after induction of DM. We show that early atherogenic DM leads to systemic microvascular abnormalities, reflected by increased capillary tortuosity as assessed by SDF imaging. Furthermore, development of glomerular lesions representative of early stages of DN and a dysbalance of Ang-2/Ang-1 expression in the kidneys of diabetic atherogenic pigs in the early stage were observed, which coincided with increased urinary albumin/creatinine ratio. The dysbalance of Ang-2/Ang-1 was correlated with increased capillary tortuosity, suggesting a relationship between increased systemic microvascular tortuosity and altered expression of renal Ang-2/Ang-1 balance, in favor of the proinflammatory marker Ang-2. Collectively, these observations suggest that systemic microvascular damage and Ang-2/Ang-1 dysbalance may represent initiating events of renal injury in early DM combined with atherogenesis.

In the following studies we assessed systemic microvascular damage in DN patients and patients with CKD (non-diabetic). In **chapter 5**, the effects of SPK on microvascular damage in DM type 1 patients, with and without DN, were assessed in a cross-sectional and longitudinal study using SDF imaging. Furthermore, systemic capillary tortuosity was correlated with markers for endothelial dysfunction. Consistent with previous reports, this study shows increased capillary tortuosity using SDF imaging in DM type 1 patients compared with healthy controls. This was accompanied by a dysbalance in Ang-2/Ang-1 ratio and increased levels of sTM. Interestingly, reversal of capillary tortuosity and normalization of the Ang-2/Ang-1 ratio was found after SPK, but not after KTx alone suggesting that both beta cell function and renal failure reversal, and not renal function alone is required to restore systemic microvascular damage early after transplantation. Furthermore, increased microvascular tortuosity correlated with increased Ang-2/Ang-1 ratio. In our longitudinal study both reversibility of microvascular damage and a decrease in sTM and Ang-2/Ang-1 balance occurred in the first year after SPK. Angiopoietins might play a role alongside other angiogenic pathways in the pathophysiology of microvascular derangements observed in DM patients. Assessment of capillary tortuosity, as marker for microvascular disease using the noninvasive SDF imaging and measurements of serum levels of angiopoietins, could be useful tools to estimate the degree of microvascular derangements in DM patients before and after SPK.

In **chapter 6** SDF analysis and measurements of endothelial dysfunction markers were performed in non-diabetic CKD patients and compared with healthy controls. Our first observation in this study is that CKD patients have a markedly disturbed microvasculature with increased tortuosity and enhanced levels of Ang-2 and sTM compared to healthy controls. Thus besides increased capillary tortuosity in DN patients, as shown in chapter 5, non-diabetic CKD patients also have systemic microvascular damage. Moreover, in the longitudinally study the effects of KTx were investigated on the observed microvascular derangements. Interestingly, KTx results in restoration of tortuosity and normalization in Ang-2 and sTM levels within 6 months after transplantation. Thus, normalization of renal function in non-diabetic CKD patients is able to improve microvascular damage evident in these patients.

Finally, microvascular alterations were studied in renal recipients during and after allograft rejection, as described in **chapter 7**. It is known that repetitive insults of AR target ECs and lead to capillary destabilization, however, whether AR after KTx is associated with sustained systemic microvascular damage had not been studied so far. We found a markedly disturbed systemic microvasculature, assessed by SDF imaging, in patients with AR compared with stable renal transplant recipients. In line, increased Ang-2/Ang-1 ratio as well as increased VEGF-A and sTM serum levels were observed in the circulation. Surprisingly, capillary tortuosity remained increased up to 1 year after rejection in patients in the longitudinal study. Since EC activation results in impaired survival of allografts, therapies aimed at maintaining microvascular integrity may have beneficial effects on long-term graft survival after rejection episodes. Monitoring of the microcirculation by SDF imaging may be a novel non-invasive approach for the detection of early microvascular damage during allograft rejection.

In conclusion, the results of this thesis demonstrate an important role for endothelial injury and repair in renal disease and after transplantation. Both renal I/R and DM induced systemic capillary damage reflected by increased capillary tortuosity by SDF imaging and a dysbalance in angiopoietins. In addition, patients with renal disease and allograft rejection after renal transplantation also had systemic microvascular derangements. Transplantation was effective in reversing the systemic microvascular alterations. Since angiopoietins are considered important microvascular regulators, future research including studies with a therapeutic intervention would be required to prove a causal relationship between the functions of angiopoietins and pericytes and its role in EC stabilization and repair. Modulation of the Ang-2/Ang-1 balance may have therapeutic potential for microvascular stabilization in renal disease. Complementary use of SDF imaging to measure microvascular tortuosity and the assessment of endothelial dysfunction markers may be useful diagnostic tool for monitoring the microvasculature before and after transplantation.

Chapter 9

Nederlandse samenvatting

Acknowledgment

Curriculum vitae

Publication list

Nederlandse samenvatting

In de ontwikkeling van nierziekten en afstotingsreactie na niertransplantatie, spelen endotheel schade en herstel en de ontwikkeling van nierfibrose (bindweefselvorming) een belangrijke rol. Endotheel cellen (EC) vormen de binnenste laag van onze bloedvaten in de nieren. Het concept dat het begin van nierfibrose zou kunnen ontstaan door beschadiging aan EC, suggereert dat interventies om vasculaire integriteit in stand te houden essentieel zijn voor het behoud van nierfunctie. Door beter te begrijpen welke mechanismen betrokken zijn bij EC schade tijdens nierziekten en na niertransplantatie, is het wellicht mogelijk om hierop in te grijpen en therapeutische interventies te ontwikkelen. In dit proefschrift is onderzocht welke factoren van belang zijn in het proces van EC schade en herstel in chronische nierfalen (CKD), diabetes mellitus (DM) type 1, Ischemie/Reperfusie schade (I/R schade) en na transplantatie.

I/R schade van de nier ontstaat na transplantatie en is een belangrijke voorspeller voor nierfalen na een niertransplantatie. Tot dusver is niet geheel bekend welke mechanismen bijdragen aan I/R schade. Steeds meer studies wijzen in de richting van EC schade en een gestoord capillair herstel als vroege mechanismen die betrokken zijn bij I/R schade. De microvasculaire EC schade die optreedt is geassocieerd met profibrotische veranderingen van het nierweefsel. Het begin van deze microvasculaire schade zou kunnen ontstaan doordat EC niet meer op normale wijze signaleren naar pericyten (de steuncellen van de bloedvaten). Deze interactie tussen pericyten en EC wordt gereguleerd door verschillende angiogene factoren, waaronder angiopoietine-1 (beschermend/anti-inflammatoir) en angiopoietine-2 (pro-inflammatoir). In **hoofdstuk 2**, werd gebruik gemaakt van een rat model waar I/R schade van de nieren geïnduceerd werd en 9 weken daarna vervolgd is. In deze periode werd op verschillende tijdstippen het effect van nier I/R schade op veranderingen in angiopoietines expressie bestudeerd. Daarnaast werd de associatie met microvasculaire remodelling, pericyten expressie en ontwikkeling van nierfibrose bestudeerd. Uit deze studie bleek dat verlies van peritubulaire capillaire EC vroeg na I/R schade in de nier gepaard ging met een gestoorde Ang-2/Ang-1 balans, toename in pericyten en ontwikkeling van interstitiële fibrose. Negen weken na inductie van I/R schade trad er een verbetering op in de Ang-2/Ang-1 balans welk gepaard ging met herstel in aantal EC en pericyten. Deze data ondersteunen de hypothese dat angiopoietines en pericyten een belangrijke rol spelen in de microvasculaire EC schade en in het herstel van de nierschade.

Hoewel deze experimentele bevindingen een functionele rol suggereren van angiopoietines in EC schade in de nieren, is er weinig bekend of de rol van angiopoietines bij humane I/R schade in de nieren. Onze hypothese was dat de inflammatoire cascade in humane nier I/R schade geïnitieerd wordt door EC activatie en daaropvolgend angiopoietine-2 (Ang-2)

afgifte. In **hoofdstuk 3**, werd deze hypothese bestudeerd in klinische niertransplantatie (zowel levende als overleden donoren), door gebruik te maken van arterioveneuze metingen over de gereperfundeerde nier. Gepaarde arteriële en veneuze bloedsamples uit de nieren werden verzameld opeenvolgende tijdstippen gedurende de vroege fase van reperfusie. Deze studie liet zien dat nieren van zowel levende als overleden donoren Ang-2 afgeven. Dit ging gepaard met verlies van ECs in de nieren, wat bleek uit daling in CD34 en vWF expressie en verminderde angiopoietine-1 (Ang-1) eiwit en mRNA expressie. Onze bevindingen suggereren dat angiopoietines en pericyten een belangrijke rol spelen in microvasculaire remodeling tijdens I/R schade in de nier.

In **hoofdstuk 4**, werd onze studie naar lokale vasculaire EC schade voortgezet in vroege DM. Microvasculaire afwijkingen in de nieren zijn veel voorkomende histopathologische bevindingen bij diabetische nephropathie (DN). In humane DN worden morfologische veranderingen in capillairen gevonden, zoals elongatie en toename in aantal glomerulaire capillairen. Veranderingen in angiogene factoren zoals VEGF-A en angiopoietines zouden betrokken zijn bij de progressie van DN. Door gebruik te maken van een streptozotocine geïnduceerd diabetes model in varkens met een atherogeen dieet, is onderzocht of het vroege stadium van DM geassocieerd is met systemische microvasculaire schade. Daarnaast is onderzocht welke vroege factoren betrokken zijn bij de ontwikkeling van diabetische nefropathie. Hiervoor werd een varkensmodel gebruikt met een follow-up periode van 15 maanden na inductie van DM. Deze studie liet zien dat vroege atherogene DM leidt tot systemische microvasculaire afwijkingen, weerspiegeld door toegenomen capillaire kronkeligheid gemeten met de niet-invasieve sidestream darkfield techniek (SDF). Daarnaast werden er glomerulaire afwijkingen gevonden passend bij vroege DN en een dysbalans in angiopoietines in de nieren van diabetische atherogene varkens. Dit ging gepaard met een verhoogde urine albumine/creatinine ratio. De dysbalans in angiopoietines was geassocieerd met toegenomen capillaire kronkeligheid. Dit suggereert een relatie tussen toegenomen systemische microvasculaire kronkeligheid en veranderde expressie van angiopoietines in de nieren. Samenvattend wijzen deze bevindingen erop dat systemische microvasculaire schade en angiopoietine dysbalans de eerste gebeurtenissen zijn in het initiëren van nierschade in de vroege fase van DN.

In de vorige hoofdstukken lag de focus vooral op microvasculaire schade in de nieren na I/R schade en DM type 1. Om te onderzoeken of deze beschadigingen aan het endotheel zich ook systemisch manifesteren hebben wij de microcirculatie in beeld gebracht met SDF techniek in DN en CKD patiënten (niet-diabeten).

In **hoofdstuk 5**, werden de effecten van gecombineerde nier-pancreas transplantatie op microvasculaire schade in DM type 1 patiënten, met en zonder DN, bestudeerd in cross-sectionele en longitudinale studies. Daarnaast werd systemische capillaire kronkeligheid gecorreleerd met markers voor endotheelschade in het bloed, inclusief soluble thrombomoduline (sTM) en Ang-2/Ang-1. Vergelijkbaar met andere studies, liett deze studie toegenomen capillaire kronkeligheid zien in DM type 1 patiënten ten opzichte van gezonde controles. Dit ging gepaard met Ang-2/Ang-1 dysbalans en een toename in sTM. Een interessante bevinding van deze studie is dat er een verbetering werd gezien van capillaire kronkeligheid en normalisatie van Ang-2/Ang-1 balans na nier-pancreas transplantatie, maar niet na niertransplantatie alleen. Dit suggereert dat zowel β -cel functie als herstel van nierfunctie noodzakelijk zijn om systemische microvasculaire schade te verbeteren na transplantatie. Tevens werd er een correlatie gevonden tussen microvasculaire kronkeligheid en toegenomen Ang-2/Ang-1 ratio. In de longitudinale studie werden reversibiliteit van zowel microvasculaire schade als afname in sTM en Ang-2/Ang-1 dysbalans waargenomen binnen het eerste jaar na nier-pancreas transplantatie. Beoordeling van de mate van capillaire kronkeligheid, als marker voor microvasculaire schade, door gebruik te maken van de SDF techniek en angiopoetine waarden in het serum, zouden belangrijke hulpmiddelen kunnen zijn om de mate van microvasculaire verstoringen in DM patiënten in te schatten voor en na nier-pancreas transplantatie.

Naast onze bevindingen in nier-pancreas transplantatie patiënten, werden in **hoofdstuk 6** de resultaten van SDF metingen en endotheel dysfunctie marker bepalingen vergeleken in niet-diabetische CKD patiënten en gezonde controles. Daarnaast werd het effect van niertransplantatie bestudeerd. Onze eerste bevinding was dat niet diabetische CKD patiënten een gestoorde systemische microvasculatuur hebben met toegenomen kronkeligheid en verhoogde Ang-2 en sTM waarden in het serum in vergelijking met gezonde vrijwilligers. Dus naast toegenomen capillaire kronkeligheid in DN patiënten, zoals besproken in hoofdstuk 5, lieten niet-diabetische CKD patiënten ook systemische microvasculaire schade zien. De groep CKD patiënten werd vervolgens gedurende 12 maanden na niertransplantatie vervolgd om het effect van transplantatie op microvasculaire veranderen te onderzoeken. Interessant is dat niertransplantatie leidt tot verbetering van microvasculaire kronkeligheid en normalisatie in Ang-2 en sTM binnen 6 maanden na transplantatie. Dus, herstel van uremie in niet-diabetische CKD patiënten leidt in deze patiënten tot verbetering van de microvasculaire schade.

Tot slot werden in **hoofdstuk 7** microvasculaire veranderingen bestudeerd in niertransplantatie patiënten na acute rejectie (AR). Het is bekend dat herhaalde episodes van AR de EC beschadigen en tot destabilisatie van peritubulaire capillairen in de nieren. Echter, of AR na

niertransplantatie geassocieerd is met systemische microvasculaire schade is nog niet eerder onderzocht. Uit onze studie bleek dat AR tot gestoorde systemische microvasculaire schade leidt met toegenomen capillaire kronkeligheid, in vergelijking met stabiele niertransplantatie patiënten. De capillaire kronkeligheid bleef aanhouden tot 1 jaar na AR. Daarnaast was er een stijging in circulerende Ang-2/Ang-1 ratio, VEGF-A en sTM. Deze angiogene factoren, zouden een rol kunnen spelen in de pathogenese van microvasculaire schade tijdens inflammatoire processen en acute rejectie in de nieren. Sinds EC activatie/schade de kans op overleving van het transplantaat beïnvloedt, zouden therapeutische interventies gericht op behoud van microvasculaire integriteit een gunstig effect kunnen hebben op de lange termijn transplantaat overleving na AR. Monitoring van de microcirculatie middels SDF techniek zou een nieuwe niet-invasieve methode kunnen zijn om in een vroeg stadium microvasculaire schade te detecteren tijdens AR.

Concluderend lieten de resultaten van dit proefschrift zien dat EC schade en herstel een belangrijke rol spelen in nierziekten en na transplantatie. Zowel nier I/R schade als DM induceerden systemische microvasculaire schade wat blijkt uit in toegenomen capillaire kronkeligheid, gemeten met SDF techniek, en een dysbalans in angiopoietines. Tevens vertoonden patiënten met nierziekten en rejectie na niertransplantatie systemische microvasculaire afwijkingen. Transplantatie liet herstel zien van systemische microvasculaire verstoringen in diabetische en niet-diabetische CKD patiënten. De resultaten in dit proefschrift suggereren dat angiopoietines belangrijke factoren zijn in het reguleren van microvasculaire homeostase. Toekomstig onderzoek gericht op therapeutische interventies is noodzakelijk om een oorzakelijk verband aan te tonen tussen de rol van angiopoietines en pericyten in EC stabilisatie en herstel. Agentia om de Ang-2/Ang-1 balans te moduleren zouden een gunstig effect kunnen hebben als therapeutisch middel voor microvasculaire stabilisatie in nierziekten. Het gebruik van SDF techniek en markers voor endotheel dysfunctie zouden als diagnostisch middel gebruikt kunnen worden voor en na transplantatie.

Acknowledgement

The work presented in this thesis would not have been possible without the help and support of many people. First of all I would especially like to thank all the patients and volunteers that participated in our studies.

I would sincerely like to thank my promotor Professor Ton Rabelink for the opportunity to work on this project. Dear Ton, thank you for encouraging my research and for allowing me to grow as a research scientist. Your advice and help have been priceless. Despite your busy schedules, you have always made time to guide me during this PhD-project.

Also, I would gratefully like to thank my co-promotor Dr. Marlies Reinders for her guidance during this PhD project. Dear Marlies, thank you for your invaluable supervision, help and patience during this project. I learned a lot from you. I admire your passion for your work and the ambition to realize this project with me. Despite your busy schedules your door was always open to me when needed.

I also want to thank my second promoter Professor Anton-Jan van Zonneveld. Dear Anton-Jan, been a member of your vascular group was a pleasure for me. It was a unique experience working at your laboratory and learning all the basics of fundamental science. Thank you for your valuable discussions during the lab meetings. I admire your enthusiasm for science and the way you motivate people around you.

Also I would like to express my gratitude to Professor Cees van Kooten. Dear Cees, thank you for your valuable inputs and contributions to my projects.

Dear colleagues and students at the laboratory of department of Nephrology thank you for all the support during different steps of this thesis. Thank you for your warm welcome at the laboratory and for your help and conversations we had about non-work related topics. I would especially like to thank Ellen Lievers and Nicole Schlagwein for their valuable help with the experiments and laboratory work. This thesis would not have been possible without your help, patience teaching me the laboratory skills and your support. Also many thanks to all the other technicians for their help. I would also thank Kim Zuidwijk for her help during the start of my PhD-project.

I am also thankful to all the co-authors and collaborators in this thesis. It was a pleasant working with you and meeting you.

Next, I would further like to thank my roommates, Ethan, Rianne, Françoise, Karin, Maaïke and Pieter, thank you for the nice time, listening and advice when needed.

I would like to thank the nephrologists, fellow-nephrologist and nurse practitioners, especially Jeannet Bisschop, for their help with inclusion of patients. Also thanks to the secretaries Marianne Lobbezoo and Arnelle Kallan-van Loenen for their administrative and supportive help when needed during this PhD-project.

I am also thankful to my current supervisors at the Diakonessenhuis in Utrecht, Dr. A.F. Muller and Dr. T.J.M. Tobe. Dear Alex and Tom, thank you for providing me the time and space to complete this thesis in the last period. Also many thanks to my co-residents at the department of Internal medicine for their support.

Next, I would like to thank my family and friends. I would deeply like to thank my parents, Rahma Bekkouri and Abdelmajid Khairoun, for their endless love, support and helping me through this period of my life. Thank you for the interest and opportunities you gave me and the sacrifice you made and for helping me taking care for our daughter Safiye. Without your support I would not be able to finish this thesis and stand here on this day. I owe my special thanks to my sisters Hajar, Hanae, Sarah and my brother Othman Khairoun for their support. Also many thanks to my grandmother, uncles and aunts, especially my aunt Fatima Bekkouri.

A special gratitude to my parents in law, dear baba Mustafa Ocak and anne Gönül Bakan, I would like to thank you for being there for me when I needed you and for your unconditional support. I appreciate your help with taking care of our daughter Safiye, while I was working on this thesis. Dear Nursena and Fatih Ocak thank you for your support and encouragement.

Finally, I would like to sincerely thank my beloved husband, friend and colleague Gürbey Ocak. Thank you for going with me during this journey, for your support and belief in me. I am grateful to have you by my side. Dear Safiye, my dearest daughter, thank you for being there for me and making me laugh every day.

Curriculum vitae

De auteur van dit proefschrift werd geboren in 1982 te Tanger in Marokko. In 1989 emigreerde zij naar Nederland en volgde ze haar basisschool en middelbare school in Zoetermeer. In 2001 behaalde zij haar VWO diploma aan het Meander College en is zij aan de opleiding geneeskunde begonnen aan de universiteit van Leiden. Tijdens haar studie was zij al vroeg betrokken bij meerdere onderzoeksprojecten binnen verschillende afdelingen als student-assistent, waarvan een onderzoek naar urologische complicaties bij ontvangers van non-heart beating type III nieren onder leiding van Dr. A. Baranski (transplantatie heekunde) en Dr. P.J. Marang- vd Mheen (medische besliskunde) in het Leids Universitair Medisch Centrum (LUMC) wat resulteerde in een publicatie. In 2007 heeft zij haar semi-arts stage gedaan op de afdeling nierziekten/niertransplantatie (LUMC) waar haar interesse voor onderzoek binnen de transplantatie geneeskunde is ontstaan. In 2008 behaalde zij haar arts-examen en is zij aan dit promotieonderzoek begonnen onder supervisie van Prof. Dr. T.J Rabelink en Dr. M.E.J Reinders. Data uit proefschrift zijn op verschillende nationale en internationale congressen gepresenteerd. Vanaf mei 2013 is zij in opleiding tot internist onder leiding van Dr. A.F Muller in het Diaconessenziekenhuis in Utrecht.

Curriculum vitae (English)

The author of this thesis was born on 1982 in Tanger, Morocco. In 1989 she immigrated to the Netherlands and continued her primary and secondary education in Zoetermeer. In 2001 she completed her VWO (secondary) education and started to study medicine at the university of Leiden. During her study she participated at different research projects at different department of the LUMC, of which one study under supervision of Dr. A. Baranski (transplant surgery) and Dr. P.J.Marang-vd Mheen (medical decision making) at the Leiden University Medical Center (LUMC) about urological complications and their impact on survival after kidney transplantation from deceased cardiac death donors, which resulted in a publication. In 2007 she performed her final clinical elective training at the department of nephrology/kidney transplantation (LUMC) where her clinical and research interest began for transplantation field. In 2008 she graduated from medical school and started the current PhD project under supervision of Prof. T.J. Rabelink and Dr. M.E.J. Reinders. Data from this thesis are presented at different national and international conferences. From May 2013 she started her specialist training for internal medicine at the Diaconessenhospital in Utrecht, under supervision of Dr. A.F. Muller.

Publicationlist

Marang-van de Mheen PJ, Nijhof HW, **Khairoun M**, Haasnoot A, van der Boog PJ, Baranski AG. Pancreas-kidney transplantations with primary bladder drainage followed by enteric conversion: graft survival and outcomes. *Transplantation*. 2008 Feb 27;85(4):517-23.

Khairoun M, Baranski AG, van der Boog PJ, Haasnoot A, Mallat MJ, Marang-van de Mheen PJ. Urological complications and their impact on survival after kidney transplantation from deceased cardiac death donors. *Transpl Int*. 2009 Feb;22(2):192-7.

Reinders ME, Roemeling-van Rhijn M, **Khairoun M**, Lievers E, de Vries DK, Schaapherder AF, Wong SW, Zwaginga JJ, Duijs JM, van Zonneveld AJ, Hoogduijn MJ, Fibbe WE, de Fijter JW, van Kooten C, Rabelink TJ, Roelofs H. Bone marrow-derived mesenchymal stromal cells from patients with end-stage renal disease are suitable for autologous therapy. *Cytotherapy*. 2013 Jun;15(6):663-72.

Khairoun M, de Koning EJ, van den Berg BM, Lievers E, de Boer HC, Schaapherder AF, Mallat MJ, Rotmans JI, van der Boog PJ, van Zonneveld AJ, de Fijter JW, Rabelink TJ, Reinders ME. Microvascular damage in type 1 diabetic patients is reversed in the first year after simultaneous pancreas-kidney transplantation. *Am J Transplant*. 2013 May;13(5):1272-81.

Khairoun M, van der Pol P, de Vries DK, Lievers E, Schlagwein N, de Boer HC, Bajema IM, Rotmans JI, van Zonneveld AJ, Rabelink TJ, van Kooten C, Reinders ME. Renal ischemia-reperfusion induces a dysbalance of angiotensins, accompanied by proliferation of pericytes and fibrosis. *Am J Physiol Renal Physiol*. 2013 Sep 15;305(6):F901-10

de Vries DK, **Khairoun M**, Lindeman JH, Bajema IM, de Heer E, Roest M, van Zonneveld AJ, van Kooten C, Rabelink TJ, Schaapherder AF, Reinders ME. Renal ischemia-reperfusion induces release of angiotensin-2 from human grafts of living and deceased donors. *Transplantation*. 2013 Aug 15;96(3):282-9.

Dane MJ, **Khairoun M**, Lee DH, van den Berg BM, Eskens BJ, Boels MG, van Teeffelen JW, Rops AL, van der Vlag J, van Zonneveld AJ, Reinders ME, Vink H, Rabelink TJ. Association of kidney function with changes in the endothelial surface layer. *Clin J Am Soc Nephrol*. 2014 Apr;9(4):698-704.

Bijkerk R, van Solingen C, de Boer HC, van der Pol P, **Khairoun M**, de Bruin RG, van Oeveren-Rietdijk AM, Lievers E, Schlagwein N, van Gijlswijk DJ, Roeten MK, Neshati Z, de Vries AA, Rodijk M, Pike-Overzet K, van den Berg YW, van der Veer EP, Versteeg HH, Reinders ME, Staal FJ, van Kooten C, Rabelink TJ, van Zonneveld AJ. Hematopoietic microRNA-126 protects against renal ischemia/reperfusion injury by promoting vascular integrity. *J Am Soc Nephrol*. 2014 Aug;25(8):1710-22

Roemeling-van Rhijn M, **Khairoun M**, Korevaar SS, Lievers E, Leuning DG, Ijzermans JN, Betjes MG, Genever PG, van Kooten C, de Fijter HJ, Rabelink TJ, Baan CC, Weimar W, Roelofs H, Hoogduijn MJ, Reinders ME. Human Bone Marrow- and Adipose Tissue-derived Mesenchymal Stromal Cells are Immunosuppressive In vitro and in a Humanized Allograft Rejection Model. *J Stem Cell Res Ther*. 2013 Nov 25;Suppl 6(1):20780.

